REPUBLIC OF TURKEY
YILDIZ TECHNICAL UNIVERSITY
GRADUATE SCHOOL OF SCIENCE AND ENGINEERING

PARAMETER OPTIMIZATION FOR FABRICATION OF TITANIUM DIOXIDE NANOPARTICLE REINFORCED PUA MATRIX PHOTOCATALYTIC COMPOSITES TO IMPROVE WEAR RESISTANCE

Metehan DEMİRKOL

MASTER OF SCIENCE THESIS
Department of Mechanical Engineering
Manufacturing Program

Supervisor
Assoc. Prof. Bedri Onur KÜÇÜKYILDIRIM

January, 2023

REPUBLIC OF TURKEY

YILDIZ TECHNICAL UNIVERSITY

GRADUATE SCHOOL OF SCIENCE AND ENGINEERING

PARAMETER OPTIMIZATION FOR FABRICATION OF TITANIUM DIOXIDE NANOPARTICLE REINFORCED PUA MATRIX PHOTOCATALYTIC COMPOSITES TO IMPROVE WEAR RESISTANCE

A thesis submitted by Metehan DEMİRKOL in partial fulfillment of the requirements for the degree of MASTER OF SCIENCE is approved by the committee on 19.01.2023 in Department of Mechanical Engineering, Manufacturing Program.

Assoc. Prof. Dr. Bedri Onur KÜÇÜKYILDIRIM
Yildiz Technical University
Supervisor

Approved By the Examining Committee

Assoc. Prof. Bedri Onur KÜÇÜKYILDIRIM,
Supervisor
Yildiz Technical University _____

Assoc. Prof. Tolga MERT, Member _____
Yildiz Technical University

Assoc. Prof. Egemen SULUKAN, Member _____
National Defence University

I hereby declare that I have obtained the required legal permissions during data collection and exploitation procedures, that I have made the in-text citations and cited the references properly, that I haven't falsified and/or fabricated research data and results of the study and that I have abided by the principles of the scientific research and ethics during my Thesis Study under the title of Parameter Optimization for Fabrication of Titanium Dioxide Nanoparticle Reinforced PUA Matrix Photocatalytic Composites to Improve Wear Resistance supervised by my supervisor, Assoc. Prof. Dr. Bedri Onur KÜÇÜKYILDIRIM. In the case of a discovery of false statement, I am to acknowledge any legal consequence.

Metehan DEMİRKOL

Dedicated to my family

and my closest companions

ACKNOWLEDGEMENTS

This thesis study is one of the co-works dedicated in development of nanocomposites and their manufacturing processes, and realized in Yıldız Technical University (YTU), which will be a guiding light for others that want to walk through that path. Such an achievement does not belong to one individual, but also the people, who have their utmost support and contribution.

First of all, I would like to express my deepest and sincere gratitude to my thesis advisor, my mentor, Dr. Bedri Onur KÜÇÜKYILDIRIM, who has been guiding me, not just throughout my academic career, but also in my life, being just as an older brother of mine. I would also want to express my sincere respects to our Professor, Dr. Ayşegül AKDOĞAN EKER for her lasting guidance and immense knowledge and experience of all.

I would like to thank every past and current member of YTU – Advanced Materials Research Group, who contributed in any phase of this thesis study, and also its precursor studies related with. In particular, I would like to thank Marziyeh “Ava” Heydarpoor, who is currently continuing her academic career as a master science student in Politechnico di Milano.

Most importantly, as my very supporters since the very beginning, I would like to thank my mother Ayşegül and my father Azmi, for their never-ending efforts, compassion and company. I could not achieve such a self-realization without their existence; therefore, I remain grateful throughout my entire life.

Metehan DEMİRKOL

TABLE OF CONTENTS

LIST OF SYMBOLS

°C	Degree celcius
g/cm^3	Gram per centimeter cube
J/m	Joule per meter
MPa	Megapascal
m	Meter
m^2/g	Meter square per gram
mm	Millimeter
mPa	Millipascal
$CaAl_2O_4$	Monocalcium aluminate
nm	Nanometer
N	Newton
ppm	Parts per million
TiO_2	Titanium dioxide
wt %	Weight percentage

LIST OF ABBREVIATIONS

AM	Additive Manufacturing
ASTM	American Society for Testing and Materials
CAD	Computer-aided Design
CMC	Ceramic Matrix Composite
CoF	Coefficient of Friction
DLP	Digital Light Processing
FCC	Face-centered Cubic
FDM	Fused Deposition Modeling
HIP	Hot Isostatic Pressing
LCD	Liquid Crystal Display
LOM	Laminated Object Manufacturing
MMC	Metal Matrix Composite
PMC	Polymer Matrix Composite
PMMA	Polymethyl methacrylate
PUA	Polyurethane acrylate
SEM	Scanning Electron Microscopy
SLA	Stereolithography apparatus
SN	Signal-to-noise
STL	Standard Tessellation Language
UMW	Ultrasonic Metal Welding
UV	Ultraviolet
XRD	X-ray Diffraction

LIST OF FIGURES

LIST OF TABLES

ABSTRACT

Parameter Optimization for Fabrication of Titanium Dioxide Nanoparticle Reinforced PUA Matrix Photocatalytic Composites to Improve Wear Resistance

Metehan DEMİRKOL

Department of Mechanical Engineering

Master of Science Thesis

Supervisor: Assoc. Prof. Dr. Bedri Onur KÜÇÜKYILDIRIM

Throughout the course of the technological development, breakthrough events occurring in manufacturing technologies has become major factors for realization of new technological advances. One of these developments in manufacturing technologies, such as additive manufacturing (AM), has presented utmost flexibility and versatility in fabrication needs. Such improvements come with some downsides, that parts manufactured by AM mostly lack mechanical improvements normally obtainable by conventional manufacturing methods. Overcoming these downsides has become one of the challenges in this field of study, and as an effective solution for such problems has been presented as usage of composite materials for AM applications.

Some materials of different composition and morphology has been studied as potential reinforcement materials according to the expected field of application. Among these materials, titanium dioxide nanoparticles have attracted interest of researchers due to their high strength, photocatalytic properties and biocompatibility. Still, their application on additive-manufactured composite parts

is not enough, since their synergy between manufacturing parameters has not been taken into account.

Aim of this study is to present the relation between varying amount of reinforcement and manufacturing parameters, and obtaining titanium dioxide reinforced nanocomposites that has high anti-friction and anti-wear properties, by optimizing the parameters that affect these properties. For the parameter optimization, a L9 Taguchi design of experiment (DoE) was prepared with three repetitions for each parameter combination, where the factors were chosen as reinforcement amount, layer thickness and UV exposure time. Accordingly, nanoresins with varying amount of reinforcement materials were prepared by probe sonication, to obtain homogeneously dispersed solutions. Prepared nanoresins were utilized in a digital light processing (DLP) type 3-D printer with the fabrication parameters defined at the DoE. Printed specimens were subjected to ball-on-disk tests to observe their friction characteristics. Wear tracks were imaged by scanning electron microscopy to observe their wear characteristics. Friction coefficient and specific wear rate values for each specimen were recorded and used as outputs of Taguchi DoE, which were also used to obtain relation between experimental inputs and outputs, thus optimized set of parameters. To validate this set of parameters, a validation test was also conducted. Both friction and wear properties were evaluated together with theoretical foundations.

By realizing such a thesis study, addtively manufactured composite parts can be obtainable in an optimized way, and presented set of experimental procedures will be applicable for all related future studies. This study is also a source of information in terms of presentation of theoretical bases related with manufacturing of such composite parts and utilization of these parts in sliding friction systems.

Keywords: Titanium dioxide nanoparticles, nanocomposite, wear.

ÖZET

Titanyum Dioksit Nanopartikül Takviyeli PUA Matrisli Fotokatalitik Kompozitlerin Aşınma Dayanımını Artırmaya Yönelik Üretim Parametrelerinin Optimizasyonu

Metehan DEMİRKOL

Makine Mühendisliği Anabilim Dalı

Yüksek Lisans Tezi

Danışman: Doç. Dr. Bedri Onur KÜÇÜKYILDIRIM

Teknolojik gelişmeler boyunca imalat teknolojilerinde meydana gelen çığır açan olaylar, yeni teknolojik ilerlemelerin gerçekleştirilmesinde önemli rol oynamıştır. İmalat teknolojilerindeki söz konusu gelişmelerden biri olan eklemeli imalat; üretim ihtiyaçlarına en üst düzeyde esneklik ve çok yönlülük sunmuştur. Öte yandan böylesi iyileşmeler; beraberinde, eklemeli imalat ile üretilen parçaların mekanik özelliklerinin çoğunlukla geleneksel imalat yöntemleriyle elde edilebilen mekanik iyileştirmelerden yoksun olması gibi bazı dezavantajlar da getirmektedir. Bu dezavantajların üstesinden gelmek, söz konusu çalışma alanındaki başlıca amaçlardan biri haline gelmiş olup çözüm olarak eklemeli imalat uygulamalarda kompozit malzemelere başvurulmaktadır.

Farklı bileşim ve morfolojiye sahip bazı malzemeler, istenen uygulama alanına göre potansiyel takviye malzemeleri olarak incelenmiştir. Bu malzemeler arasında titanyum dioksit nanopartikül kullanımı; beraberinde getirdiği yüksek dayanım, fotokatalitik özellik ve biyouyumluluk nedeniyle araştırmacıların ilgisini çekmiştir. Yine de; şu ana kadar gerçekleştirilmiş çalışmalar göz önüne alındığında titanium dioksit nanopartikül miktarının mekanik özelliklere etkisinde, parça kalitesine

etkiyen imalat parametreleriyle arasındaki sinerji ve ardında yatan nedenler yeteri kadar ele alınmamıştır.

Bu çalışmanın amacı, değişken takviye miktarları ile üretim parametreleri arasındaki ilişkiyi ortaya koymak ve bu özelliklere etki eden parametreleri optimize ederek yüksek sürtünme ve aşınma karşıtı özelliklere sahip titanyum dioksit takviyeli nanokompozitler elde etmektir. Parametre optimizasyonu için, faktörlerin takviye miktarı, katman kalınlığı ve UV'ye maruz kalma süresi olarak seçildiği, her parametre kombinasyonu için üç tekrarlı bir L9 Taguchi deney tasarımı hazırlandı. Buna göre, homojen olarak dağılmış çözeltiler elde etmek için değişken miktarlarda takviye malzemelerine sahip nano reçineler prob sonikasyonu ile hazırlandı. Hazırlanan nano reçineler, deney tasarımında tanımlanan üretim parametreleri ile dijital ışık işleme (DLP) tipi bir 3 boyutlu yazıcıda kullanıldı. Basılan numuneler, sürtünme özelliklerini gözlemlemek için ball-on-disk testlerine tabi tutuldu. Aşınma izleri, aşınma özelliklerini gözlemlemek için taramalı elektron mikroskobu ile görüntülendi. Her numune için sürtünme katsayısı ve özgül aşınma oranı değerleri kaydedildi ve deneysel girdiler ve çıktılar arasındaki ilişkiyi, ve optimal parameter setini elde etmek için Taguchi deney tasarımının çıktıları olarak kullanıldı. Bu parametre setini doğrulamak için bir doğrulama testi de yapıldı. Hem sürtünme hem de aşınma özellikleri teorik temellerle birlikte değerlendirildi.

Böylesi bir tez çalışmasının gerçekleştirilmesi ile eklemeli imalat ile üretilmiş kompozit parçalar optimize bir şekilde elde edilebilir ve sunulan deneysel işlemler bütünü, bundan sonraki ilgili tüm çalışmalarda uygulanabilir olacaktır. Bu çalışma aynı zamanda bu tür kompozit parçaların imalatı ve bu parçaların kayar sürtünme sistemlerinde kullanılması ile ilgili teorik temellerin sunulması açısından da bir bilgi kaynağıdır.

Anahtar Kelimeler: Titanyum dioksit nanopartiküller, nanokompozit, aşınma.

1
INTRODUCTION

1.1 Literature Review

From past to present; titanium dioxide (TiO_2), also called as titania, has been considered as an important material and mostly applied in fields of medicine, dentistry, energy harvesting, decontamination, self-cleaning products, etc. This interest comes from special properties that pertain to titania, such as photocatalysis, semiconductivity, bio-inertia against living tissue and non-toxicity [1-6].

These properties highly depend on crystallinity, crystal structure, form and size of constituents. When intended for a specific application, these material aspects can be manipulated and made desired properties come into prominence. In literature, there are applications of both crystalline and amorphous titania, according to their distinctive advantages: Although anatase has a wider band gap, which is a critical parameter in semiconductance, doped amorphous titania has been preferred, since it can be deposited easily onto surfaces and does not need high post-annealing temperatures. Nevertheless, its photocatalytic performance is still comparable to its photocatalytic polymorphs [5, 7]. On the other hand, especially for the applications that titanium dioxide is applied as a composite reinforcement agent, crystalline titanium dioxide is more desirable in terms of higher strength, since it has an ordered bond structure.

Despite most of the titanium dioxide studies are covering the fields related more with bioapplications, there is an interest in applying these materials as reinforcement material into the composite matrix, due to its high hardness properties as a metal oxide material. There are several studies that investigated their mechanical and tribological properties: Dafar et al. applied TiO_2 nanotube fillers as a reinforcement agent in a commercial dental filling material, in an amount of 3 wt % by spatulation method and obtained enhancements of 35.63% in fracture toughness and 8.39% in dynamic elasticity modulus [8]. Khaled at al.

applied same filler material into PMMA pristine resin, in an amount of 2 wt % by ultrasonication method and obtained enhancements of 18.51% in fracture toughness, 42.93% in flexural strength and 131.25% in flexural modulus. Such enhancements can be obtainable even with pure acrylic resins reinforced with TiO_2 reinforcement, by applying correct homogenization methods.

Titania has also been studied for tribological applications, since it has been applied to dental fillings, self-cleaning glasses, etc., which become worn throughout their operating time. Salim et al. used TiO_2 and $CaAl_2O_4$ nanoparticles in several volumetric ratios and obtained 71.8% decrease in coefficient of friction and 54.8% decrease in wear volume, when the nanoparticles are utilized in 5% vol. In several studies, it has been shown that addition of titania affects wear properties in a positive manner; with decrease of grain size, decrease of wear can be observed due to prevention of crack propagation through the material. However, it should also be considered that there is a risk of agglomeration with increasing surface area-to-volume ratio, which constitutes local faults in the material and promotes failure [9]. It is also worth mentioning, that there is a need of thorough investigation for the synergy of the friction and wear characteristics, in order to present how manufacturing parameters and reinforcement ratio are affecting mechanical qualities of the manufactured parts.

For aforementioned application fields, titania nanomorphologies are mostly applied onto nanocomposite materials and these materials can be fabricated by several methods such as layer-by-layer technique, electrophoretic deposition, gel-film transformation, sol-gel technique, etc. [10]. Among these methods, vat photopolymerization techniques are very promising, since they present manufacturing versatility of complex parts. Most of the studies related with the reinforcement of additively manufactured composite parts are mostly related with more popular materials such as carbon nanomaterials, but these is no such study specifically investigating the properties of TiO_2 reinforced nanocomposite parts obtained by additive manufacturing [11, 12].

1.2 Aim of the Thesis

Aim of this thesis study is to present the relation between varying amount of reinforcement and manufacturing parameters; thus, obtaining titanium dioxide reinforced nanocomposites that has high anti-friction and anti-wear properties, by optimizing the parameters that affect these properties.

By realizing such a thesis study, additively manufactured composite parts can be obtainable in an optimized way and presented set of experimental procedures will be applicable for all related future studies. This study is also a source of information in terms of presentation of theoretical bases related with manufacturing of such composite parts and utilization of these parts in sliding friction systems.

1.3 Hypothesis

- To an extent, increasing amount of reinforcement material will enhance anti-friction and anti-wear properties.
- Best results will be achieved with the suitable printing parameters, as long as the part is intact and not over-cured.

2
TITANIUM DIOXIDE: SYNTHESIS, PROPERTIES AND APPLICATIONS

2.1 Introduction

This section briefly explains various aspects of titanium dioxide, its properties, morphologies and their comparison within each other, their synthesis and applications, and its importance for this study.

2.2 Definition

Titanium dioxide (TiO_2), also called titania, is a compound of titanium and oxygen, that mostly have white/bone-colored powder appearance, according to its crystal structure and morphology. Due to its semi-conducting electronics, it exhibits photocatalytic activity by progressive electron traffic between valence and conductive electron bands, and ionization reactions due to the existence of electron-absent sites called holes, which triggers ionization of the moist in the air and makes ionized reactants such as hydrogen peroxide. This side products are harnessed for self-cleaning applications. Since the discovery of this phenomenon, it has been widely used as a self-cleaning agent for dyes, membrane filters and polymer films [13]. Since they are hard metal oxide phases, they are also used as composite reinforcement materials, mostly for dental fillings.

2.3 Allotropes of Titanium Dioxide

According to different synthesis and post-processing routes, titanium dioxide can behave in different crystal orders. The most popular and widely used allotropes of titanium dioxide are given in Figure 2.1. According to the expected properties, any allotrope can be utilized as crystalline or amorphous titanium oxide. Although anatase has a wider band gap, which is a critical parameter in semiconductance, doped amorphous titania has been preferred, since it can be deposited easily onto surfaces and does not need high post-annealing temperatures. Where high strength is expected from the allotrope, amorphous phase obtained right after the

synthesis should be annealed, or “calcinated”, at a specific temperature, mostly between 300-600 °C [14].

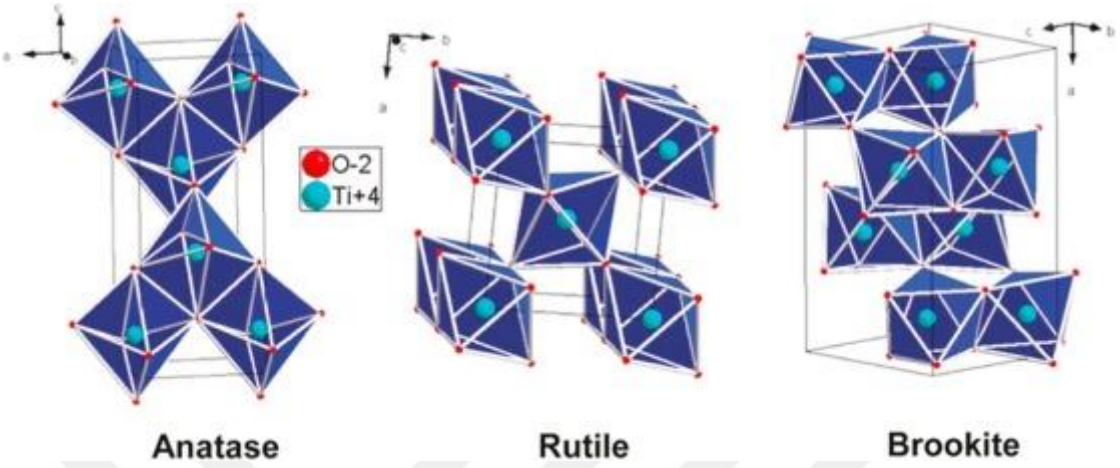

Figure 2.1 Different allotropes of titanium dioxide [13].

2.4 Synthesis Methods and Obtainable Morphologies

In addition to the crystallinity of the titanium dioxide, morphology of the material is also crucial for its respective application field. How it is synthesized and post-processed highly affects its crystal and morphological qualities. Most of the titanium dioxide allotrope can be synthesized with generally used methods, such as sol-gel method, hydrothermal method, etc., if required chemical and thermodynamical conditions has been provided. An extensive schematic about obtainable morphologies is given on Figure 2.2. According to applicational considerations, one must choose all this factors, to utilize most suitable reinforcement material for the respective application field. For composite materials application, crystallinity and aspect ratio of the constituent is important; utilizing low-aspect ratio morphologies can increase hardness and wear resistance of the composite, whereas high-aspect ratio morphologies can increase tensile and flexural properties. If reinforcement phase is homogeneously distributed throughout the matrix, it can span through the matrix in wide regions, resulting in better interfacial properties.

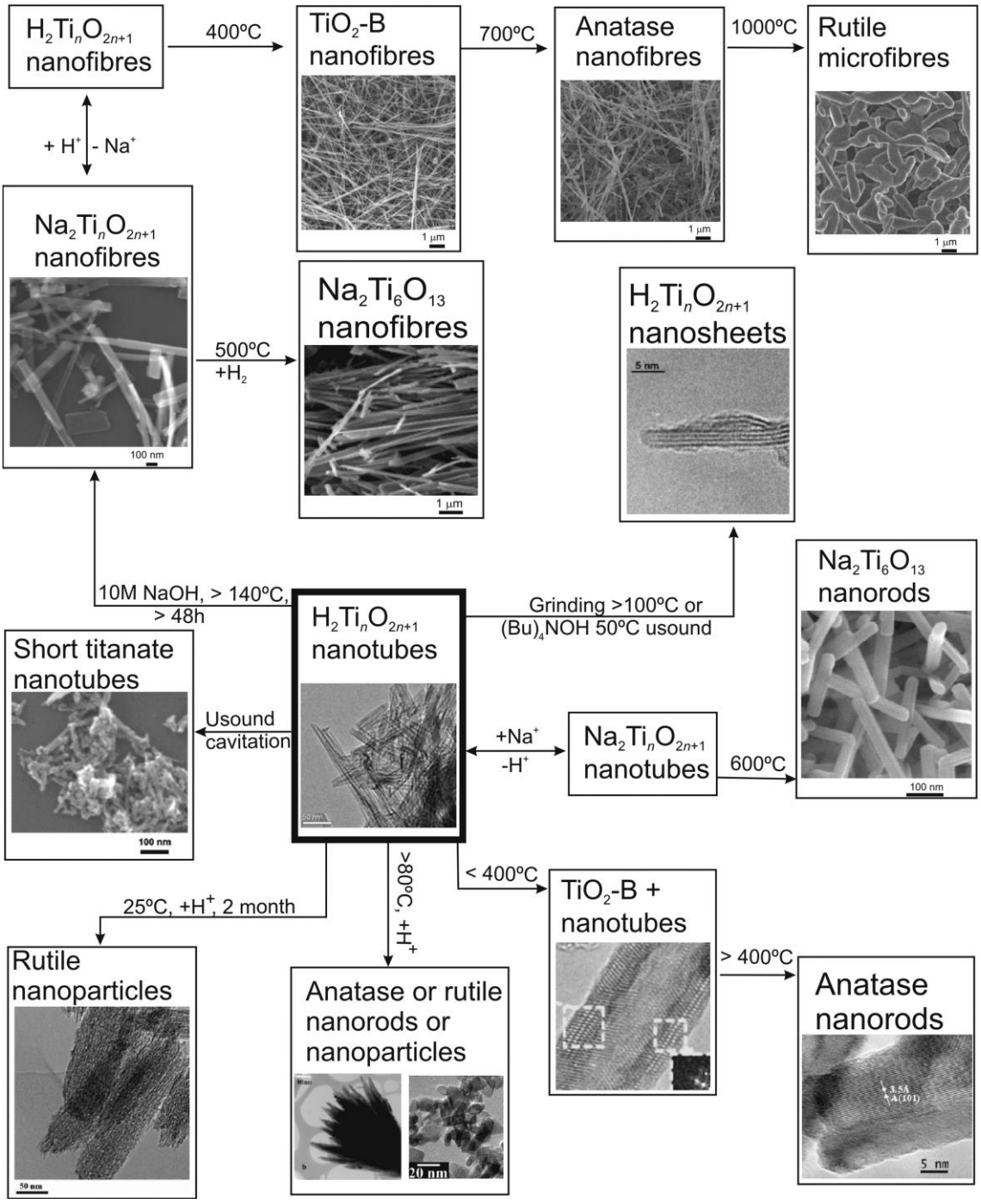

Figure 2.2 Different synthesis and post-processing routes of titanium dioxide and resulting allotropes and morphologies [15].

3
COMPOSITE MATERIALS

3.1 Definition

A composite is a combination of two or more materials, to obtain an utterly different material that consists of properties of each constituent. Mostly, each constituent of a composite material is chosen according to their best properties that can be combined, which makes composite materials widely applied in most of the industrial fields. Each composite material consists of a main phase called matrix that holds all together, and reinforcement phases that transfers their property throughout the matrix, by the interface between the reinforcement and the matrix. According to the reinforcement and matrix material separately, composite materials can be classified as shown in Figure 3.1.

3.2 Classification of Composite Materials

According to the reinforcement and matrix material separately, composite materials can be classified as shown in Figure 3.1.

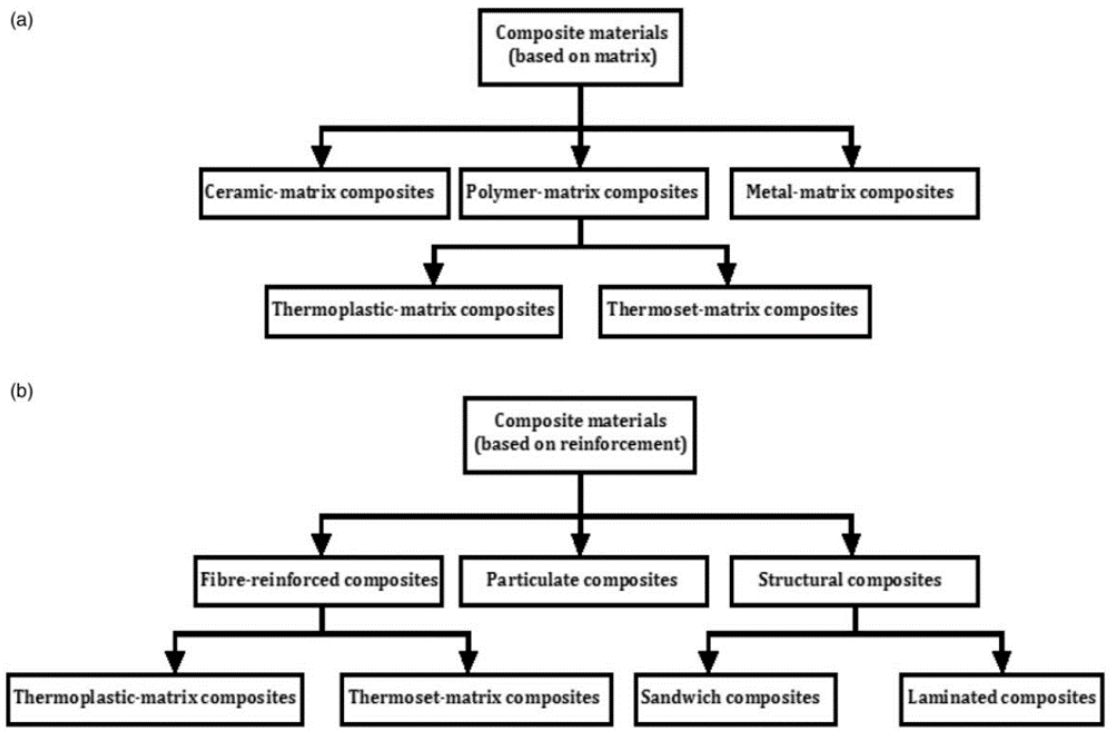

Figure 3.1 Classification of composite materials: a) based on matrix, b)based on reinforcement.

3.2.1 Composite Materials Based on Their Matrix

3.2.1.1 Ceramic Matrix Composites (CMCs)

CMCs are types of composite materials that their matrix materials are ceramics such as oxides, carbides, etc. They are mostly preferred due to their high tensile strength, high hardness, high wear resistance, high thermal resistance, and low density, which makes them very useful for high temperature and high friction applications. As a downside, CMCs are very brittle materials, and very vulnerable against impact. To overcome these downsides, suitable reinforcement materials can be added into their structure: To increase their fracture toughness, an even harder phase can be used inside these ceramic matrices, which behaves as obstacles against any crack proceeding through the matrix. To increase their toughness and impact strength, they can be combined either with metals or polymers, according to the service temperature that CMC will be operating.

3.2.1.2 Metal Matrix Composites (MMCs)

MMCs are types of composite materials that their matrix materials are metals that are either ferrous or non-ferrous. When high strength steels are considered, their superior mechanical properties come with high density, which makes most of these materials inapplicable for the applications such as aviation. To overcome this weight problem, MMCs are utilized, where there is a need of high strength, high fracture toughness and relatively low density, which is only obtainable by applying high hardness dispersions as reinforcement material, into low density non-ferrous matrices such as aluminum and magnesium.

3.2.1.3 Polymer Matrix Composites (PMCs)

PMCs are types of composite materials that their matrix materials are polymers. According to the expected field of application, fabrication-related or economical constraints, there are vast alternative of polymer matrices. When compared to ceramics and metals, polymers have the lowest density and the most flexibility in terms of manufacturing. Yet, they are very susceptible to environmental conditions such as heat and moist and have lower strength and hardness attributes. To overcome these downsides, they are reinforced either by the polymers that have higher performance, in the form of fibers such as carbon fiber, or by the ceramics of several morphologies such as particulates or short fibers, etc. Such reinforcement solutions can increase strength and fracture toughness of the polymers significantly.

3.2.2 Nanocomposites

As a very special subclass of composite materials, nanocomposites consist of a reinforcement material, that any of its dimensions is lower than approximately 100 nm. Such a decrease in dimensions comes with special properties that arise from the alteration of the mechanics that applies in nanoscales. One of these special phenomena is called quantum confinement, that is related with altering any aspect of a material, namely one of its physical properties, by decreasing the physical dimensions that the aspect is taking place, making it “squeezed” into that diminished dimension and either making it cease to exist, or behave dramatically

different compared to its macro- or micro-scale alternative case. Most popular reinforcement materials currently, such as graphene, carbon nanotubes, MXenes, etc. gain their superior properties such as high electrical and thermal conductivity, peculiar electrical and optical properties and high strength and elasticity, due to this phenomenon.

To transfer these superior properties, interface between the matrix and the reinforcement has to be increased. As the second phenomenon, and the most important one in composite materials practices, increase in surface area-to-volume ratio is crucial for obtaining higher enhancements that are normally obtainable by conventional means. For same mass fractions, if any material is split into smaller parts, total surface area increases according to geometrical features of the split parts. Increase of the surface area also means more atomic interactions between in-contact elements in same medium, since there will be more atoms per total surface area, which results in increase in chemical reaction rate, van der Waals forces between same or alike constituents, etc. An example to exhibit the significance of this can be given in Table 3.1.

Table 3.1 Surface-atomic features for n-layer-atomic FCC nanoparticle [16].

n	Surface Atoms	Bulk Atoms	Surface/Bulk Ratio	Surface Atoms (%)
1	14	0	-	100
2	50	13	3.85	79.3
3	110	62	1.78	63.9
4	194	171	1.13	53.1
5	302	364	0.83	45.3
6	434	665	0.655	39.4
7	590	1098	0.535	34.9
8	770	1687	0.455	31.3
9	974	2456	0.395	28.3
10	1202	3429	0.350	25.9
11	1454	4630	0.314	23.8
12	1730	6083	0.284	22.1
100	120,002	3,940,299	0.0304	2.9

3.2.3 Composite Materials Based on Their Reinforcement

Based on their reinforcement material, composites can be subclassed according to either their material, or their morphology. In terms of material choice, especially for brittle materials such as ceramics, more ductile phases such as polymers or metals can be utilized as reinforcement materials, to increase toughness of the composite. To increase strength of the material, deploying reinforcements that have even higher strength or hardness compared to their matrix can be used.

Beyond the right choice of the reinforcement material, the geometrical features of the reinforcement have to be taken into the account, to optimize the isotrophy of the composite material. For most of the cases, high aspect ratio reinforcement materials such as fibers can be utilized to enhance tensile or flexural properties, whereas low aspect ratio reinforcements such as particles can be utilized to enhance compressive properties, hardness and wear resistance.

Particle reinforced composites can also be subdivided into “large-particle” and “dispersion-strengthened” composites, which differs essentially in particle size; in large-particle composites, particle size is relatively large, atomic-level interactions are weak and properties for these composites can be calculated by simple rule of mixture. However, in dispersion-strengthened composites, particle size is at about 10-100 nm. Since particles are nanosized, surface area-to-volume ratio is increased compared to large-particle composites, atomic-level interactions like van der Waals appears to affect properties of the composite. Assuming that nanoparticles are high-quality, it is also possible to obtain materials that has high compressive strength, as long as breakdown limit of Hall-Petch relation is not reached [16, 17]. Such a condition for titanium dioxide particles has been shown in Figure 3.2.

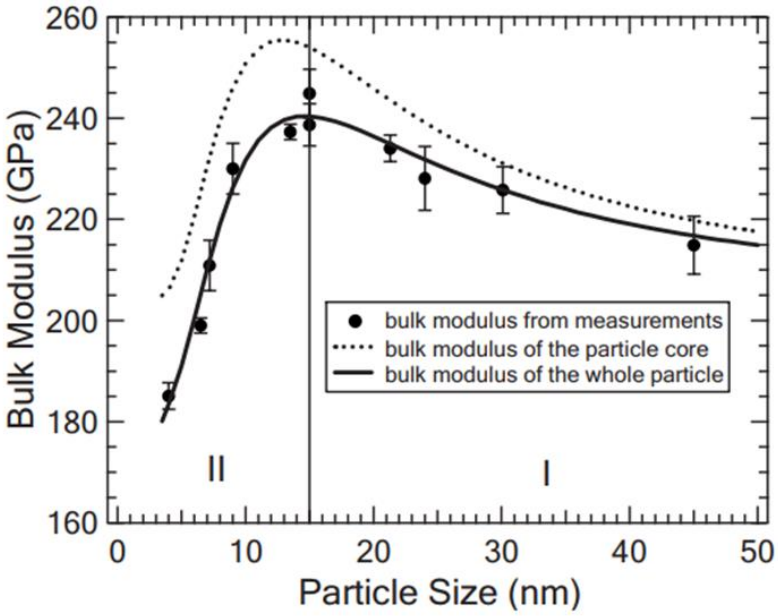

Figure 3.2 Dependence of bulk modulus on particle size and Hall-Petch breakdown limit at around 15 nm of particle size **[18]**.

4
ADDITIVE MANUFACTURING

4.1 Definition and Main Principles

Additive Manufacturing (AM) involves all manufacturing techniques that consist of constructing a part layer by layer and has been attracting attention among many bottom-up manufacturing techniques. AM techniques present their practitioners high versatility at fabricating complex-shaped parts and highly applicable in industrial scale nowadays. By applying correct route of techniques, one can obtain parts with high quality. By AM, any type of material can be used for fabrication of a part, with correct type of AM technique, according to the specifications of to-be-used material.

Main steps of a typical AM route can be named as follows: Digitalization of a part by CAD; extracting digital data of the part as STL; digitalization of the AM process by transferring STL to a slicing software, defining process parameters, printing orientation and support structures, if necessary; introducing the digitalized process data to a printer user interface; realization of the AM and obtaining the part; post-processes such as cleaning, getting rid of the excessive structures, extra processes for further solidification of the part, etc.

According to the type of material and how each layer is constructed during AM, the techniques are classified.

4.2 Classification of AM Techniques

AM techniques can be simply classified according to the form of the material, as solid, powder and liquid.

Solid-based AM techniques mainly consist of an initial material in solid phase and constructing the part layer by layer, by different means. As long as the initial material phase is solid, it can be in the form of laminates. filaments, etc.

Accordingly, these materials can be utilized in extrusion-based methods such as fused deposition modeling (FDM), contour cutting-based methods such as laminated object manufacturing (LOM), and ultrasonic consolidation-based methods such as ultrasonic metal welding (UMW) [19].

Powder-based AM techniques use initial material in the form of solid powder, and the powder can be any type of material, if the powder material can be consolidated layer by layer, by the means of either melting-solidifying, or sintering. Such processes need high-density heat application in the form of focused high-energy radiation such as laser beam, electron beam, etc. If optimized, AM techniques belonging to this subclass can present good quality results [20].

Liquid-based AM techniques use initial material in liquid phase and solidify the material layer by layer, by different means of curing. As curing technique, most techniques utilize high-energy light sources, preferably ultraviolet (UV), in forms of focused light or pixels. Applying UV in different means has separate advantages, according to the applicational constraints. In either way, liquid-based AM techniques presents results with very good surface features [20]. As the most popular types of liquid-based AM techniques, vat photopolymerization techniques such as Stereolithographic Apparatus (SLA) and Digital Light Processing (DLP) can be presented, which are also schematized in Figure 4.1.

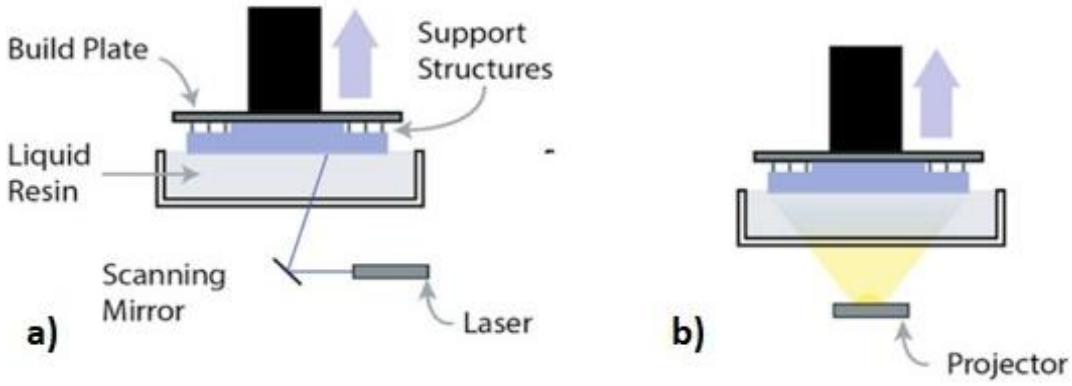

Figure 4.1 Working principles of a) SLA and b) DLP printers [21].

Due to how UV light is applied, there are some differences between SLA and DLP printing methods. Mainly, surface quality of the printed part depends on the size

of the UV beam that is applied onto the resin. For SLA, this corresponds to the spot size of the laser, whereas for DLP, to the pixel size of the projector. Due to the small size of the laser spot, SLA may yield better surface quality results, but with improvements in LCD technologies, DLP methods that adapt LCD light source that has higher resolution, instead of a projector, will be equally good in time. In terms of infill quality and the requirements for achieving a total infilling of the printed part, DLP is more practical, since to-be-cured layer can be projected instantly, whereas for SLA, the layer must be hatched.

As it will be discussed further in the experimental section, if it is intended to develop composite resins, their behavior under UV light will be easier to investigate, since diffusion of UV through a layer of the resin is mostly in a linear absorbance gradient, whereas for SLA, it becomes more Gaussian, which is achievable with more effort. Choosing a DLP printer for this study makes the investigation more related with the further studies that will be investigating UV absorbance of the nanoresins by UV-vis spectrophotometry, since both DLP and UV-vis spectrophotometry methods, UV behavior will be depending on Beer-Lambert's Law.

4.3 Downsides of AM Techniques

Despite its flexibility on part geometry, each of AM techniques have their downsides, due to the materials that are used, and the principles behind the construction of each layer. For powder-based techniques, powder size highly affects potential porosity density that the part has. To prevent such void defects, higher amount of energy must be given to the system, to liquify the powder until the porosity decreases to an acceptable level, then solidify the part, or sinter the powder until a consolidation with an acceptable level of porosity is obtained. As a post-process, pressurized heating processes such as hot isostatic pressing (HIP) can also be applied, but it results in extra time and energy expense.

According to the application field of the part, surface quality can be also a constraint. Almost all AM technique need a surface treatment as a post-process. This can be additional polishing or sandblasting for a powder-bed fusion part, or

simply washing away all excessive resin that is left on the printed part obtained from a vat photopolymerization-based printer.

Due to the layer-by-layer-constructed nature of the parts obtained by AM techniques, interfacial differences between each layer may result in different physical/mechanical property gradients throughout the part. As an example, for a DLP-printed part, interfaces between each layer will have different mechanical properties, even each layer is cured properly, since overcuring for the regions between each layer is likely to occur. When compared to its equivalent that is fabricated by conventional means, namely plastic injection molding, the mechanical properties of the part will become less. Similar property-diminishing factors due to the interfacial differences are very common for most of the AM techniques.

To overcome such problems, aside from optimizing the fabrication parameters, utilizing composite materials as additively-manufacturable materials can be significantly effective. Among the other AM techniques, vat photopolymerization techniques are very suitable for this task, since preparation of homogeneously-dispersed reinforcement-resin mixture is relatively easy and can yield better results when compared with the other composite AM studies [22-24].

4.4 Fabrication of Titanium Dioxide Reinforced Polymer Composites by AM

As both interfacial and mechanical improvement agent, titanium dioxide nanoparticles can be used as the reinforcement material into the acrylic resin specialized for vat photopolymerization. Due to the photocatalytic properties of titanium dioxide, the parts fabricated by the prepared nanoresin will have self-cleaning and antimicrobial properties, which is also shown in the previous studies [25]. In the literature, despite the current studies on the usage of popular carbon nanomaterials as reinforcement, there is no titanium dioxide reinforced polymer composite AM study conducted, in a way that fabrication parameters are optimized and consequences are evaluated by theoretical bases [11, 12]. This thesis study will encompass development of nanoresins reinforced by titanium dioxide nanoparticles, usage of prepared nanoresins with optimized fabrication

parameters and investigation of the influence of the quality parameters on the behavior of the material under sliding friction.

5
EXPERIMENTAL STUDIES

5.1 Preliminary Studies

Most of the methodology related with the preparation of nanoresins and materials testing were practiced beforehand. Before applying titanium dioxide reinforced nanoresins to a DLP, first it was tested, that the prepared resin is either curable or not. Nanocomposite specimens with reinforcement ratios of 0, 0.05 and 0.1 wt % respectively, were tried to fabricated in simple molds, using a hand-held UV light source. For the simplicity of the prestudy, UV was applied in a manner that the specimens were completely cured, and the only parameter that would affect the mechanical quality of the parts would be reinforcement ratio and homogeneity of the nanoparticles throughout the matrix. For each reinforcement ratio, the specimens were obtained successfully and subjected to microvickers hardness measurements and ball-on-disk tests. It has been shown, that anti-friction, anti-wear and hardness properties were obtained best for 0.05 wt % of titanium dioxide nanoparticle reinforcement. Beyond that ratio, utilizing more nanoparticles into the matrix was resulted in diminishing all the properties. Obtained results are given in Figure 5.1, and supported with Figure 5.2 and Figure 5.3, by presenting friction and wear mechanisms occured onto the test specimens [26].

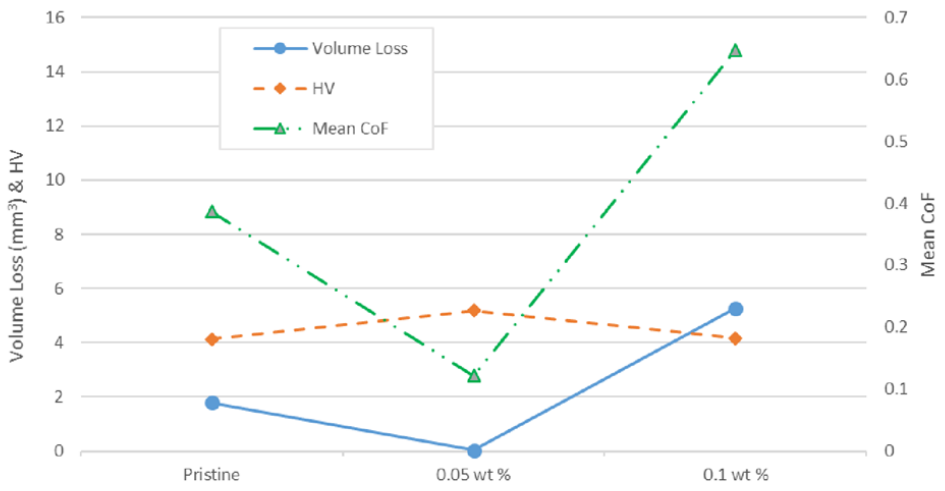

	Pristine	0.05 wt %	0.1 wt %
Volume Loss	1.789 ± 0.811	0.033 ± 0.006	5.273 ± 1.357
HV	4.130 ± 1.450	5.187 ± 3.180	4.159 ± 0.995
Mean CoF	0.387	0.122	0.648

Figure 5.1 Classification Change in volume loss, hardness and mean coefficient of friction (CoF) with varying nanoparticle amount.

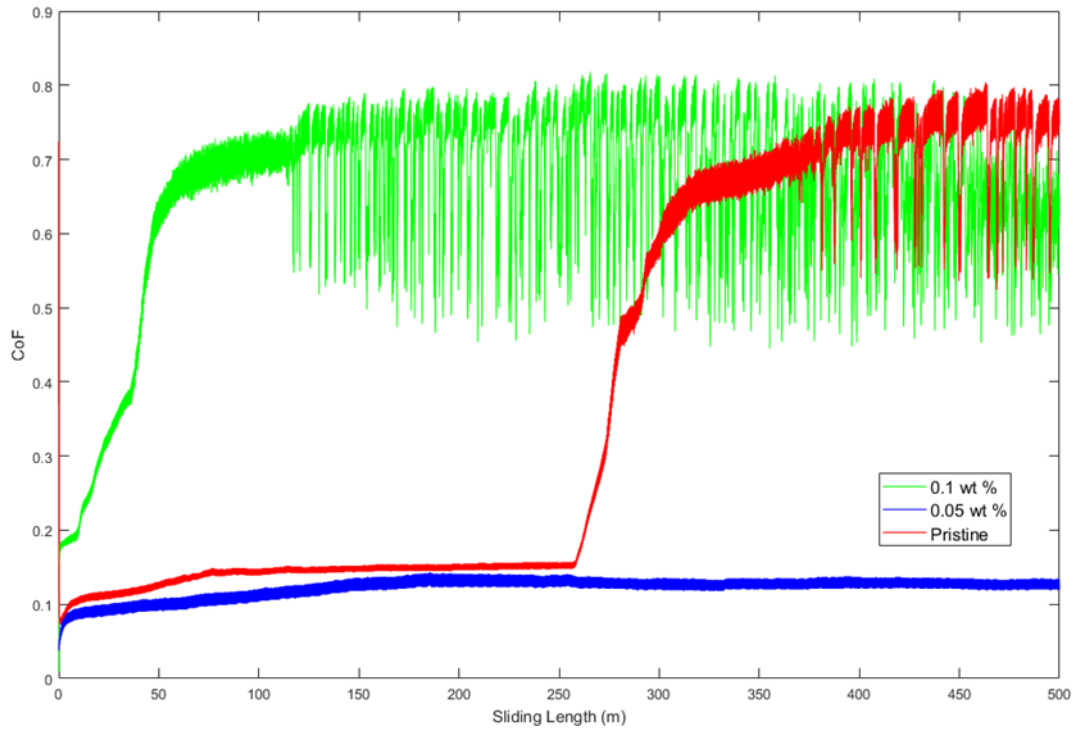

Figure 5.2 Ball-on-disk test results: Change in coefficient of friction throughout the test.

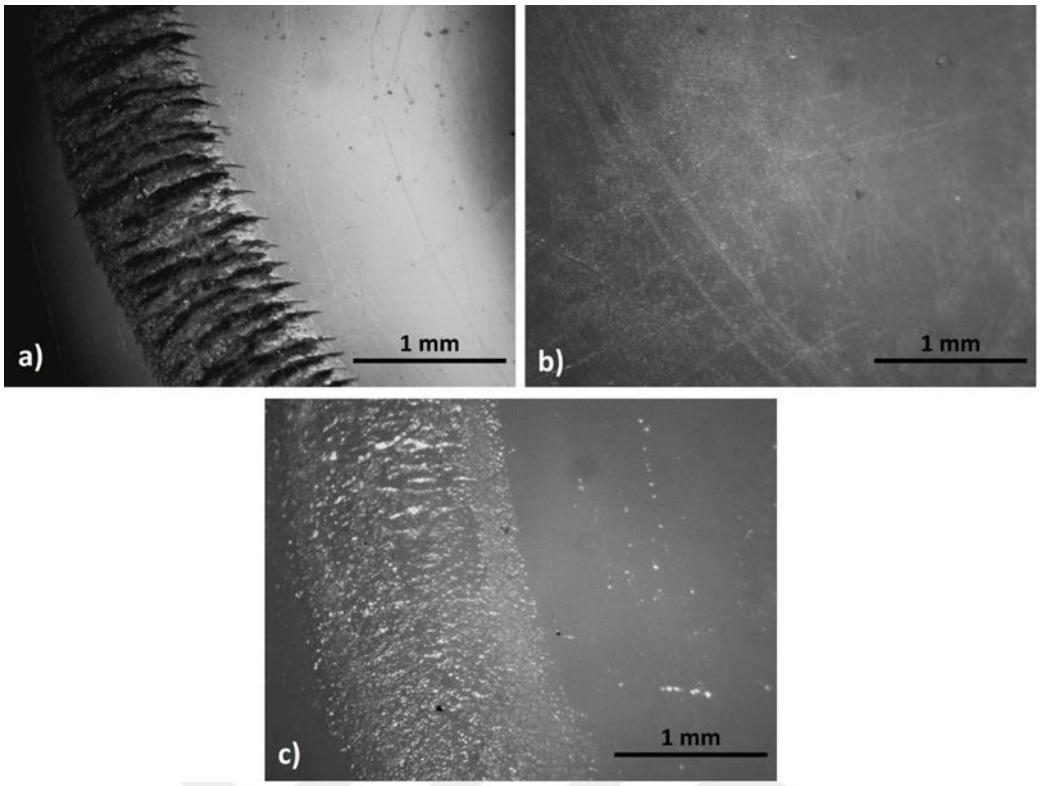

Figure 5.3 Wear track images: (a) Pristine PMMA, (b) 0.05 wt % TiO2/PMMA, (c) 0.1 wt % TiO2/PMMA.

5.2 Materials and Methods

This section explains the materials and the methodology that was applied throughout the thesis study extensively.

As the reinforcement material, titanium dioxide nanoparticles were obtained from Aldrich. Material specifications for the specific lot was provided from Aldrich and given in Table 5.1 [26].

Table 5.1 Material specifications for titanium dioxide nanoparticles [26].

Property	Result
Appearance (Color)	White
Appearance (Form)	Powder
XRD	Conforms to structure (anatase)
Particle Size	20 nm
Surface Area	52 m^2/g (between the specified range of 45-55 m^2/g)
Trace Metal Analysis	125.9 ppm (meets the requirement of ≤ 4000 ppm)

As the matrix material, polyurethane acrylate (PUA) resin was obtained from Anycubic. Material specifications for the resin is given in Table 5.2 [27]. In terms of physical and mechanical properties, PUA behaves very likely to polymethyl methacrylate (PMMA), so it can be chosen as a more affordable counterpart.

Table 5.2 Material specifications for acrylic resin [27].

Parameter	Value	Parameter	Value
Viscosity (mPa; 25 °C)	150-200	Density (g/cm^3)	1.05-1.25
Wavelength (nm)	405	Hardness (Shore D)	82D
Tensile Strength (MPa)	36-45	Elongation (%)	8-12
Flexural Strength (MPa)	50-65	Impact Toughness (J/m)	25

Table 5.2 Material specifications for acrylic resin (continued) [27].

Volumetric Shrinkage (%)	4.5-5.5	Shell Life (year)	1
Heat deflection temperature (°C, at 0.45 MPa)	65-70	Flexural Modulus (MPa)	1200-1600

5.2.1 Design of Experiments

Properties of the obtained part are affected by several factors such as parameters related with the AM technique and the material properties. For this study, quality of the part was affected by reinforcement ratio, exposure time and layer thickness of the part, which also affect how the resin was cured throughout the process. Minimizing the layer thickness and maximizing the exposure ratio yield the best results in terms of mechanical strength, yet it is not time efficient. On the other hand, aiming the fastest printing process may result in inefficiently cured parts that lack of sufficient mechanical strength. Optimizing all these parameters is crucial for obtaining enhanced mechanical properties and maintaining time efficiency for the printing, at the same time. Accordingly, an L9 Taguchi Design of Experiments (DoE) with three repetitions for each test parameter set was prepared as shown in Table 5.3. For defining suitable test parameters, several screening tests were conducted, to determine the most extreme printing parameters that hard to print a part, yet has integrity within itself. Parameter levels of 7 s of minimum exposure time and 0.075 mm of maximum layer thickness were chosen accordingly. 0.025 mm minimum layer thickness was chosen, as the minimum layer thickness that the printer can operate is this specific value. Maximum exposure time of 13 s was chosen by trial experiments. Accordingly, median values for the factor levels were defined as the average values of the extrema. p-values for each factor were also found to present the significance of the factors. While conducting the design, both wear rate and CoF were taken as quality characteristics and evaluated together, since both characteristics affect each other.

Table 5.3 Design of Experiments.

Specimen No.	Reinforcement Ratio (% wt)	Exposure Time (s)	Layer Thickness (mm)
S1	0	7	0.025
S2	0	10	0.050
S3	0	13	0.075
S4	0.05	7	0.050
S5	0.05	10	0.075
S6	0.05	13	0.025
S7	0.10	7	0.075
S8	0.10	10	0.025
S9	0.10	13	0.050

Since it was expected to obtain coefficient of friction and wear rate in minimum, “smaller is better” approach was chosen. The set of parameters which gives the smallest value for both wear rate and CoF at the same time was subjected to a verification test.

5.2.2 Preparation of Nanoresins

Before weighing titanium dioxide nanoparticles and adding them into the resins, to get rid of any agglomeration that possibly occurred during its unused shell life,

the nanoparticles are mixed with isopropyl alcohol and subjected to ultrasonication for 2 hours. The nanoparticles for respective weight ratios were separately weighed with a precision scale and added into the resins of respective amounts, in a way that desired reinforcement ratios were obtained. Prepared nanoresins were also homogenized by probe sonication for 1 hour. The duration of the sonication was defined in this way, to prevent any unintended curing during the homogenization, due to the excessive temperature increase. Sonication processes are shown in Figure 5.4.

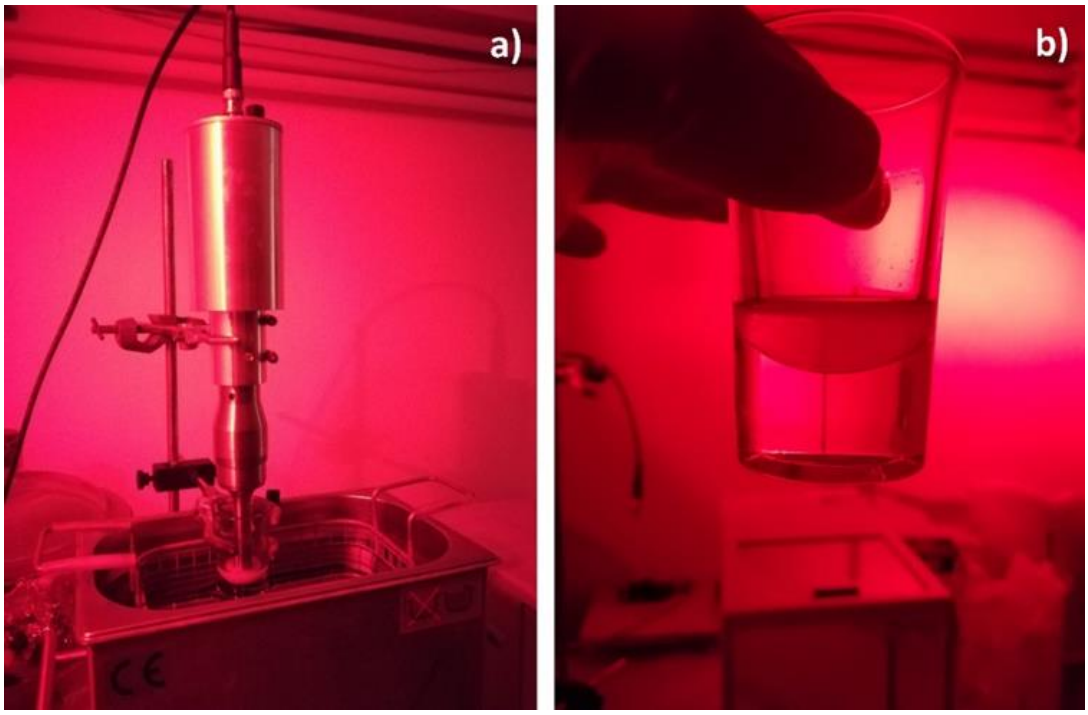

Figure 5.4 a) Homogenization process, b) obtained nanoresin.

5.2.3 Printing of Nanocomposite Parts

According to the prepared DoE, each set of specimens were printed with their respective printing parameter. Slicing software of Anycubic Photon was used for slicing and printing parameter definition, since the capabilities of the software was enough for our experimental expectations and relatively easy to use. According to each set of printing parameters, printing duration takes between approximately 30 minutes to 90 minutes. Printing setup has been shown in Figure 5.5.

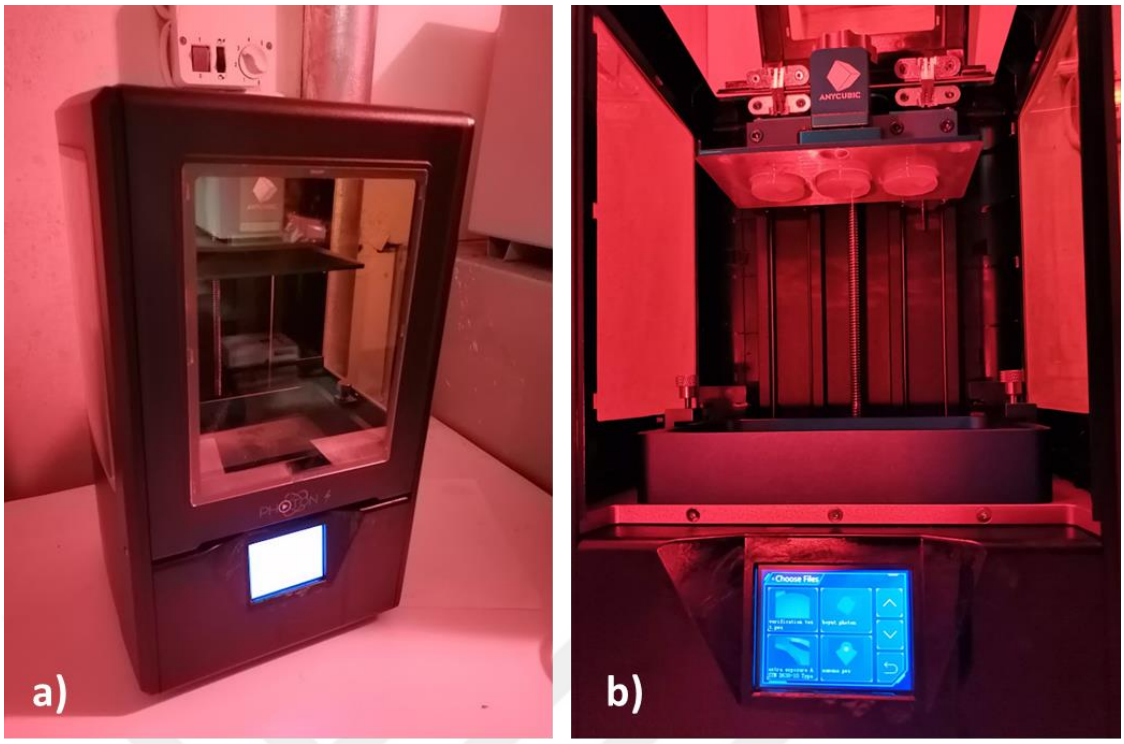

Figure 5.5 Printing setup: a) The printer, b) specimens after the printing.

After the specimens were printed, they were taken from the plate by a spatula and washed in isopropyl alcohol, to get rid of the excessive resin. To observe the influence of the printing parameters better, no post-curing in a UV bath was applied. After the alcohol wash, to completely clean the specimen surface and make it ready for further ball-on-disk tests, the specimens were grinded with a paper with 2000 grit size.

5.2.4 Ball-on-Disk Tests

To observe friction and wear behavior of the specimens, they were subjected to ball-on-disk tests, which is a versatile type of sliding tests that can simulate different sliding friction pair materials with high contact pressures. In principle, the test setup consists of a stationary ball that is applying constant load onto a rotating disk specimen. During the test, all vertical and horizontal loads are recorded by strain gages located onto the test apparatus, which is used for calculation of time-dependent CoF. This way, friction behavior of a specimen can

be observed during the test period, and can be related with wear characteristics that will be observed by visual inspection of worn specimens after the test. All ball-on-disk tests were conducted according to the ASTM G99-95a [28]. The test setup is shown in Figure 5.6.

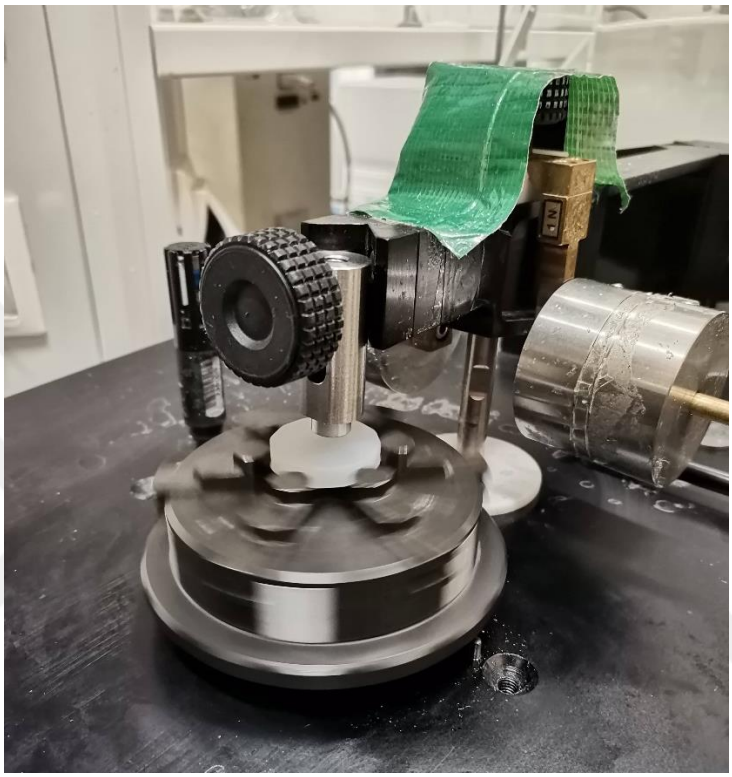

Figure 5.6 Ball-on-disk testing setup.

For the study, test parameters were chosen as 10 N of applied normal load, 30 mm/s of sliding speed, sliding length of 214 m, ball specimen radius of 3 mm and wear track radius of 3 mm. This test parameters were defined, in a way that the same specific conditions with the pre-study tests were provided with a shorter test duration.

5.2.5 Imaging and Evaluation of Worn Specimens

Macroscopic images are taken from each wear track to observe how surfaces are worn and how varying amount of reinforcement affected wear behavior. Volume loss can also be calculated by measuring wear track widths and applying these values to volume loss formula obtained from ASTM G99-95a [28]:

$$Volume\ Loss\ (mm^3): V = 2\pi R\left[r^2 \arcsin\left(\frac{d}{2r}\right) - \left(\frac{d}{4}\right)\sqrt{4r^2 - d^2}\right] \quad (5.1)$$

As it is also shown both in light macrographs and scanning electron micrographs, wear tracks were developed properly, without significant smearing of the material to the sides of the wear tracks, which makes the Eq. 5.1 applicable for the wear tracks. Also, there did not developed any wear track onto the ball specimens.

For an in-depth analysis of wear characteristics, scanning electron microscopy (SEM) images of the wear tracks were also taken with 1000x magnification, at secondary electron mode for a better observation of surface features. Both macroscope and SEM as imaging instruments are shown in Figure 5.7.

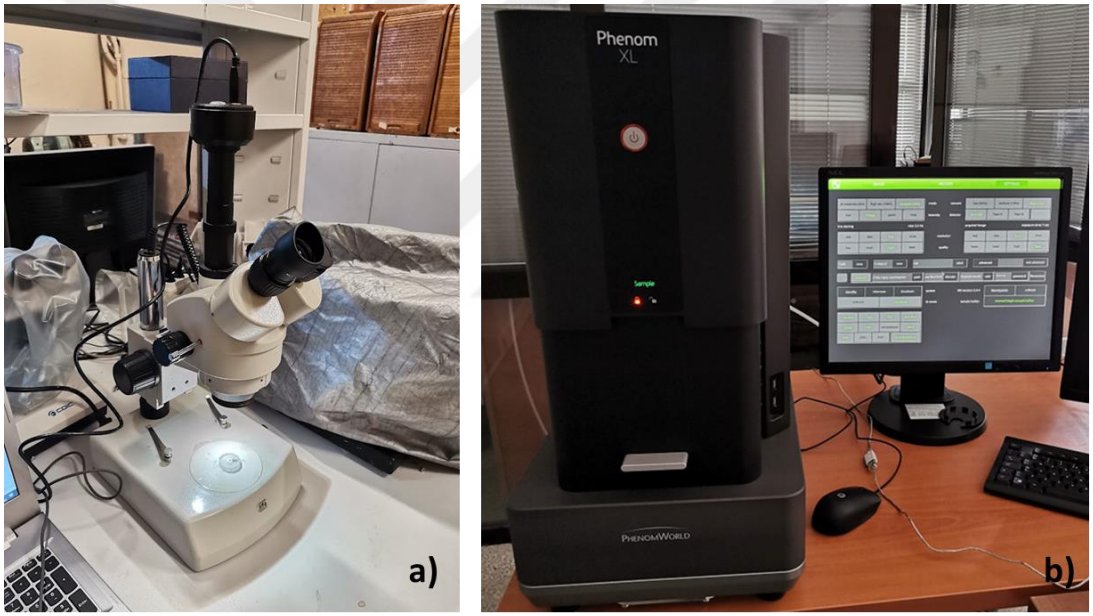

Figure 5.7 Imaging instruments: a) light macroscope, b) SEM.

6
RESULTS AND DISCUSSION

The specimens were fabricated according to the printing parameters specified in DoE, and subjected to ball-on-disk tests. Worn specimens were inspected under light macroscope for wear volume loss calculation and SEM for wear characterization. Taguchi optimization has been done according to the CoF and wear volume loss, ass quality characteristics. Accordingly, an optimum set of printing parameters has been obtained, that the best quality characteristics would be achieved. In order to validate this, validation tests were conducted according to the previous methodology. Main effect plots for SN ratios and means are given in Figure 6.1 and Figure 6.2, respectively. CoF and wear volume loss values corresponding to the printing parameters are also given in Table 6.1. More data on wear tracks and friction coefficients can be found in Appendices A and B.

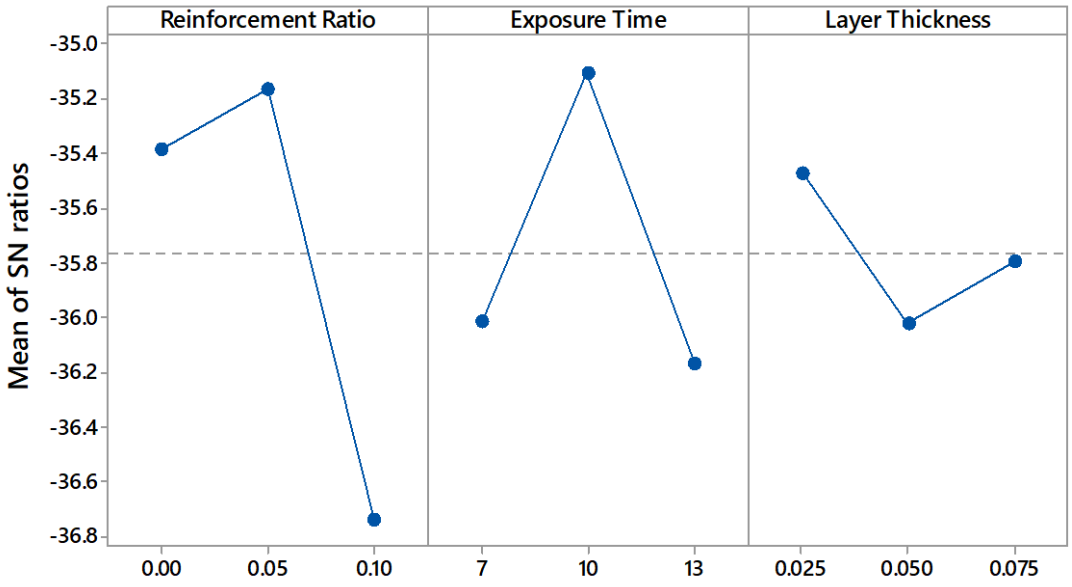

Figure 6.1 Main effects plot for SN ratios.

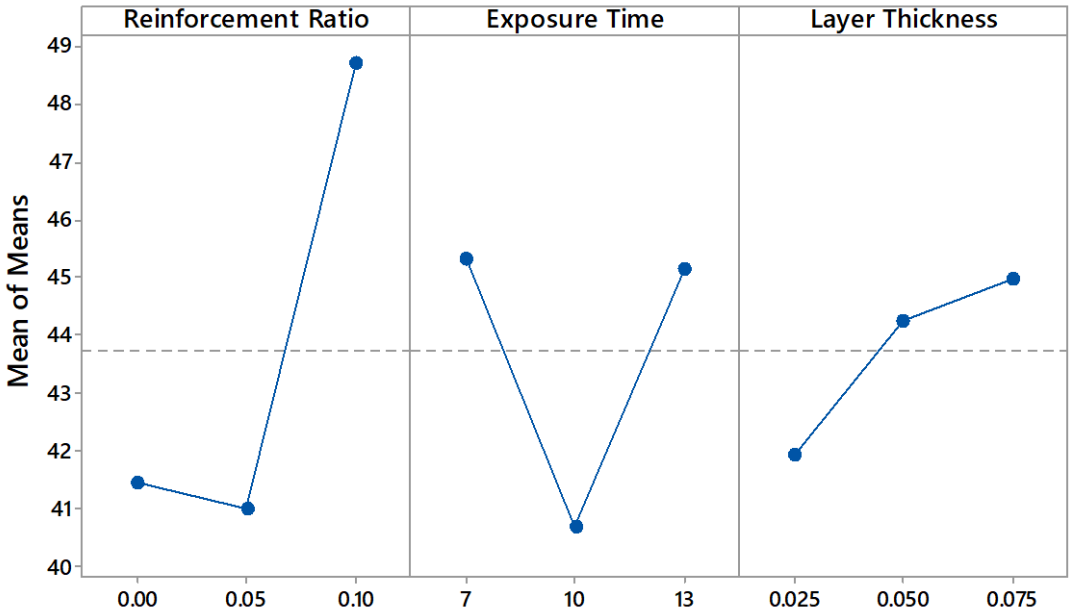

Figure 6.2 Main effects plot for means.

Table 6.1 CoF and wear volume loss values of each specimen set.

Specimen No.	Reinforcement Ratio (% wt)	Exposure Time (s)	Layer Thickness (mm)	CoF	Wear Volume Loss (mm^3)
S1	0	7	0.025	0.262	51.224
S2	0	10	0.05	0.697	96.038
S3	0	13	0.075	0.715	99.950
S4	0.05	7	0.05	0.605	98.065
S5	0.05	10	0.075	0.264	47.039
S6	0.05	13	0.025	0.744	99.290
S7	0.1	7	0.075	0.726	121.156
S8	0.1	10	0.025	0.729	99.479
S9	0.1	13	0.05	0.438	69.805
Verification	0.05	10	0.025	0.176	45.404

In Figure 6.1, the factor levels that affect SN ratio most can be stated as optimum levels that yield best results for printing. Accordingly, 0.05 wt % reinforcement ratio, 10 s of exposure time and 0.025 mm of layer thickness are the optimal printing parameters. Also in Figure 6.1, the difference between maximum and minimum values of SN ratios for each factor shows how much influence have these factors on the quality characteristics. Accordingly; reinforcement ratio has the most influence on the quality of the printed parts, then exposure time and layer thickness, respectively.

p-values for each factor were calculated as 0.9, which is higher than 0.05 that indicates the rejection of the null hypothesis. Such high p-values indicate that factors have no significant effect over quality characteristics. On the other hand, high p-values can be frequently encountered for small sample sizes or unpredictability of any factor that makes the system behave non-linearly, which may be the case for the resin solutions with nano-sized additives. To overcome the inadequateness of the statistical outputs, experimental observations were used to corroborate the evaluation.

When CoF and wear volume loss values were taken into consideration, best results were obtained for verification tests, whereas worst results were obtained for the 0.1 wt % reinforcement ratio, 7 s exposure time and 0.075 mm layer thickness. This specific set of printing parameters was intentionally defined for better constitution of a DoE that could properly cover the thesis problem (see also 5.2.1 Design of Experiments), therefore such results are very reasonable. On the contrary, better results were obtained, where the printing parameters are more suitable for higher part quality. Both applying UV light longer and taking the layer thickness less can provide better layer curing, thus better friction and wear properties. Obtaining better quality with 0.025 mm layer thickness when compared to 0.075 mm verifies this argument. Increasing reinforcement ratio to 0.1 wt % significantly decreases lubricity and wear resistance of the part, which was also shown in the prestudy section of the thesis.

Obtained results can be related with the friction and wear characteristics throughout the ball-on-disk tests. Friction coefficient curves and wear track

micrographs of the best specimens are given in Figure 6.3, 6.4 and 6.5, respectively.

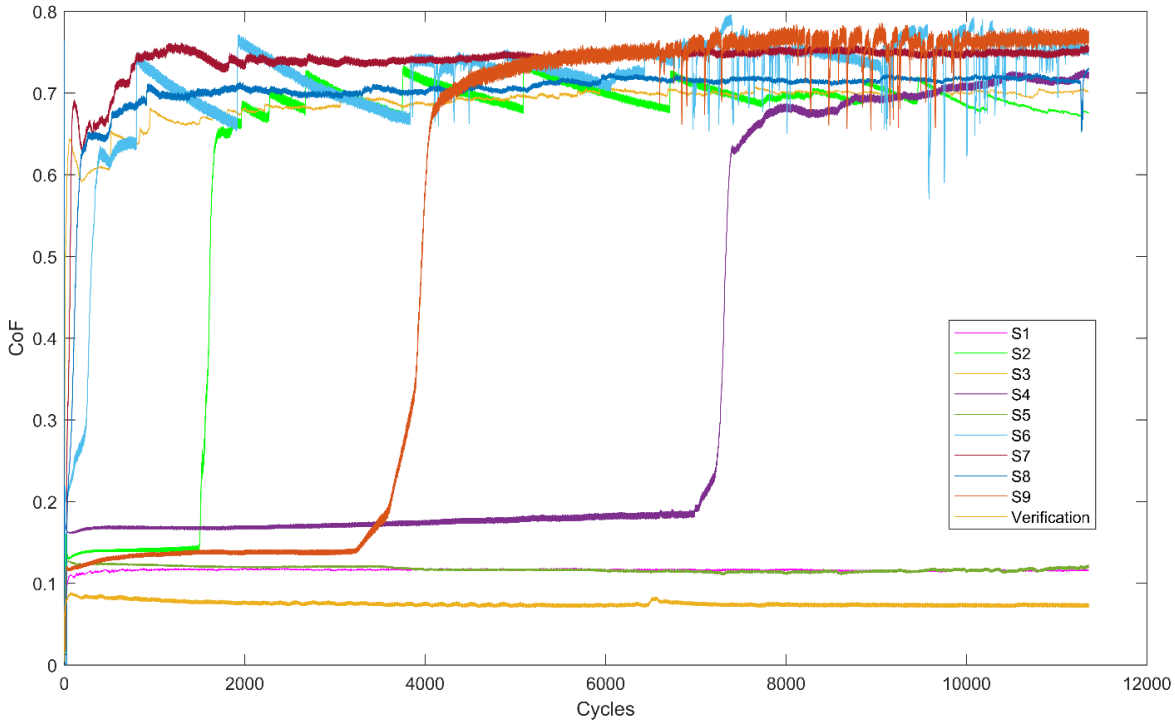

Figure 6.3 Change in CoF with cycles during the ball-on-disk tests.

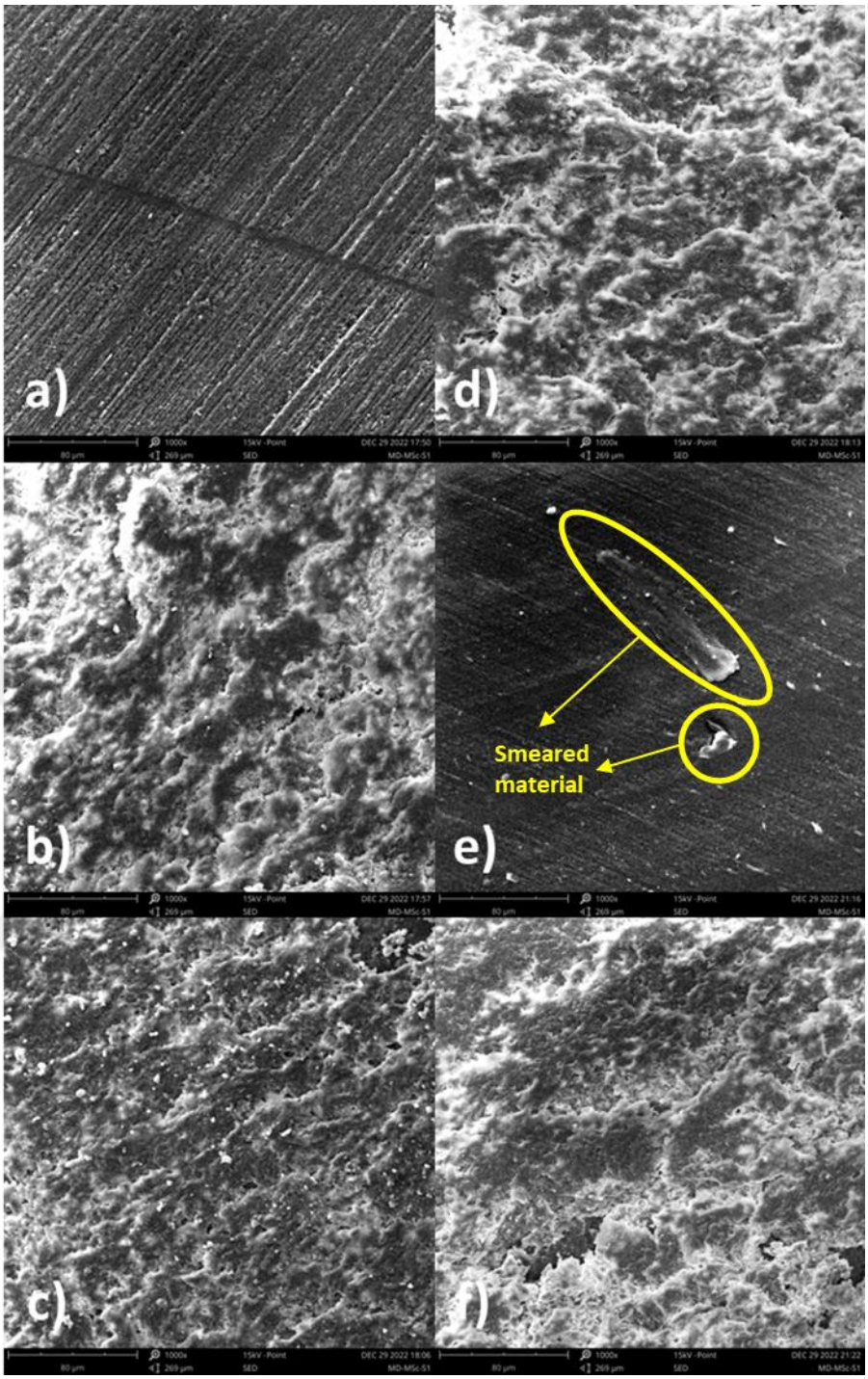

Figure 6.4 Scanning electron micrographs of the specimens: a) S1, b) S2, c) S3, d) S4, e) S5, f) S6.

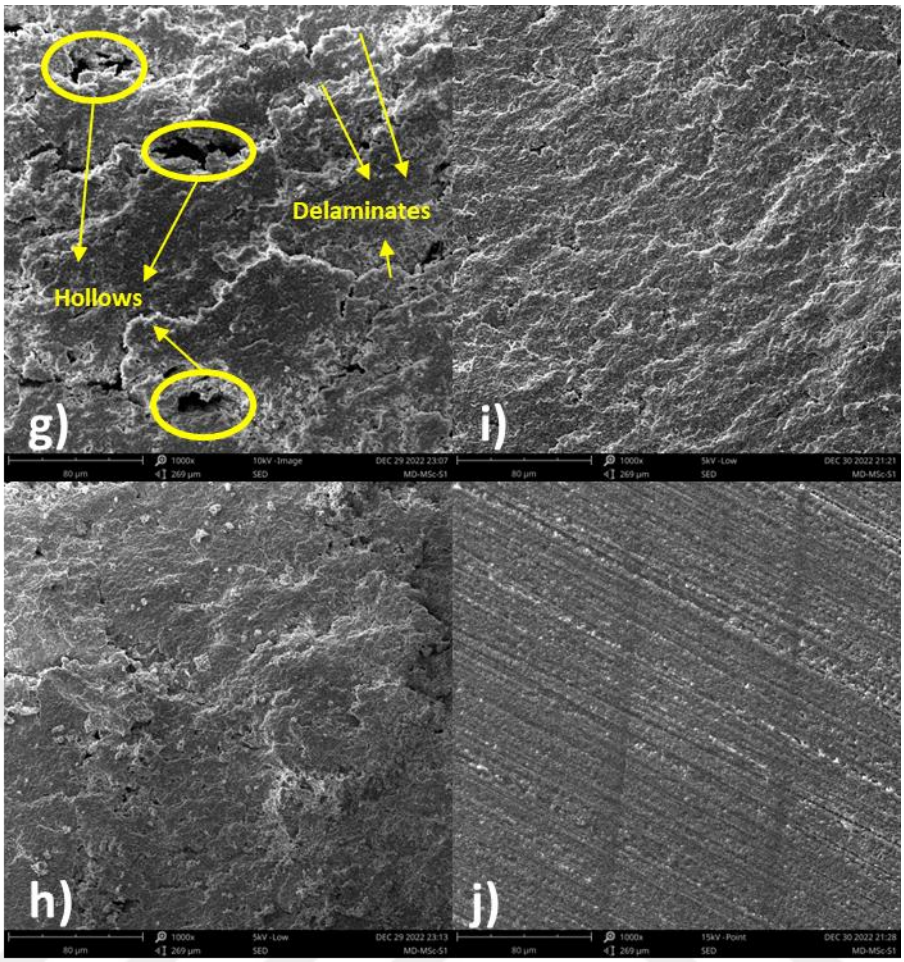

Figure 6.5 Scanning electron micrographs of the specimens: g) S7, h) S8, i) S9, j) verification.

When change in friction coefficient and wear characteristics are evaluated together, it can be stated, that in every case, there occurs adhesive wear mechanism, that consists of sticking of friction pairs, or wear side products smeared onto the friction pairs. Throughout the tests, this mechanism mostly occurs in different forms, but there are obvious indicators of stick-slip mechanism, especially for the specimens S2 and S6, as larger-stepped waves. When both friction and wear mechanisms are considered, both S6 and S7 exhibits severe conditions, since friction coefficient of these tests start to behave more sharply fluctuating and wear track of these specimens consist of more distinct masses of materials that smeared onto the surface during the tests, which can also be seen as delaminated layers. As the wear mechanisms become

more severe, hollow structures between delaminates can also be observed. Evaluating the specimens S6 and S7 is important, since S6 has the printing parameters that allows the printed layers be cured most, whereas S7 offers the exact opposite printing conditions. Determining such results reveals the possibility, that there may be over-curing of layers that makes the surface properties worse, in a comparable degree with the parameters that offers less curing of the layers during printing.

In terms of property enhancement, regardless of its degree, decreasing the layer thickness increased the enhancements. Despite the fact that verification tests yield slightly better results than S5, they are very comparable in terms of surface lubricity and anti-wear properties, that both of the surfaces did not exhibit any severe wear regime. Additionally, layer thickness of 0.075 may be a better choice in terms of printing speed, if there is no significant difference between choosing the layer thickness 0.025 or 0.075, in terms of anti-friction and anti-wear properties. In this regard, usage of titanium dioxide nanoparticle reinforcement can achieve better results, even if the layer thickness is increased, as long as there is no over-curing due to excessive UV exposure.

CONCLUSION

1. Titanium dioxide nanoparticle reinforced nanocomposite parts are successfully obtained by DLP printing. The parts maintain their structural integrity and exhibits their mechanical properties.
2. Nanocomposite part fabrication is successfully optimized by Taguchi method, where the printing parameters are the reinforcement ratio of the nanocomposite, UV exposure time and layer thickness. Influence of these parameters onto the quality characteristics of the parts also varies as follows: Reinforcement ratio affects the properties most, then exposure time and layer thickness, respectively.
3. Best properties are obtained, where reinforcement ratio is 0.05 wt %, exposure time 10 s, and layer thickness 0.025 mm. Further addition of nanoparticles results in worsening of properties, possibly due to ineffective curing or agglomerates, whereas excessing UV exposure of the layers results in possible over-curing of the part, which either way increases friction and wear, and severity of the wear regime.
4. Optimal enhancements obtained by 0.05 wt % / 10 s / 0.025 mm printing parameters are very comparable of the case that the layer thickness is chosen as 0.075 mm and the other parameters are held same. Usage of 0.05 wt % of nanoparticles inside the composite parts still maintains optimal properties, even if the layer thickness is increased, which allows 33.3% faster printing of the parts.
5. The findings that this thesis study present allows enhanced anti-friction and anti-wear properties comparable to the other printing cases with different printing parameter combinations, and yet the printing can be faster, in a very optimal way.

REFERENCES

[1] X. Guan, J. Du, X. Meng, Y. Sun, B. Sun, and Q. Hu, "Application of titanium dioxide in arsenic removal from water: A review," *Journal of Hazardous Materials,* vol. 215-216, pp. 1-16, 2012/05/15/ 2012.

[2] A. J. Haider, R. H. Al– Anbari, G. R. Kadhim, and C. T. Salame, "Exploring potential Environmental applications of TiO2 Nanoparticles," *Energy Procedia,* vol. 119, pp. 332-345, 2017/07/01/ 2017.

[3] A. J. Haider, Z. N. Jameel, and I. H. M. Al-Hussaini, "Review on: Titanium Dioxide Applications," *Energy Procedia,* vol. 157, pp. 17-29, 2019/01/01/ 2019.

[4] F. Han, V. S. R. Kambala, M. Srinivasan, D. Rajarathnam, and R. Naidu, "Tailored titanium dioxide photocatalysts for the degradation of organic dyes in wastewater treatment: A review," *Applied Catalysis A: General,* vol. 359, pp. 25-40, 2009/05/15/ 2009.

[5] Y. Lan, Y. Lu, and Z. Ren, "Mini review on photocatalysis of titanium dioxide nanoparticles and their solar applications," *Nano Energy,* vol. 2, pp. 1031-1045, 2013/09/01/ 2013.

[6] F. M. Salim, "Tribological and Mechanical Characteristics of Dental Fillings Nanocomposites," *Energy Procedia,* vol. 157, pp. 512-521, 2019/01/01/ 2019.

[7] P.-Y. Li, H.-W. Liu, T.-H. Chen, C.-H. Chang, Y.-S. Lu, and D.-S. Liu, "Characterization of an Amorphous Titanium Oxide Film Deposited onto a Nano-Textured Fluorination Surface," *Materials,* vol. 9, p. 429, 2016.

[8] M. O. Dafar, M. W. Grol, P. B. Canham, S. J. Dixon, and A. S. Rizkalla, "Reinforcement of flowable dental composites with titanium dioxide nanotubes," *Dental Materials,* vol. 32, pp. 817-826, 2016.

[9] W. Żórawski, A. Góral, O. Bokuvka, L. Lityńska-Dobrzyńska, and K. Berent, "Microstructure and tribological properties of nanostructured and conventional plasma sprayed alumina–titania coatings," *Surface and Coatings Technology,* vol. 268, pp. 190-197, 2015/04/25/ 2015.

[10] J. George and H. Ishida, "A review on the very high nanofiller-content nanocomposites: Their preparation methods and properties with high aspect ratio fillers," *Progress in Polymer Science,* vol. 86, pp. 1-39, 2018.

[11] M. Hassan, K. Dave, R. Chandrawati, F. Dehghani, and V. G. Gomes, "3D printing of biopolymer nanocomposites for tissue engineering: Nanomaterials, processing and structure-function relation," *European Polymer Journal,* p. 109340, 2019.

[12] H. Wu, W. Fahy, S. Kim, H. Kim, N. Zhao, L. Pilato*, et al.*, "Recent Developments in Polymers/Polymer Nanocomposites for Additive Manufacturing," *Progress in Materials Science,* p. 100638, 2020.

[13] S. Shen, J. Chen, M. Wang, X. Sheng, X. Chen, X. Feng*, et al.*, "Titanium dioxide nanostructures for photoelectrochemical applications," *Progress in Materials Science,* vol. 98, pp. 299-385, 2018/10/01/ 2018.

[14] M. Á. López Zavala, S. A. Lozano Morales, and M. Ávila-Santos, "Synthesis of stable TiO2 nanotubes: effect of hydrothermal treatment, acid washing and annealing temperature," *Heliyon,* vol. 3, p. e00456, 2017/11/01/ 2017.

[15] D. V. Bavykin and F. C. Walsh, *Titanate and titania nanotubes: synthesis*: Royal Society of Chemistry, 2009.

[16] D. L. Schodek, P. Ferreira, and M. F. Ashby, *Nanomaterials, nanotechnologies and design: an introduction for engineers and architects*: Butterworth-Heinemann, 2009.

[17] W. D. Callister and D. G. Rethwisch, *Materials science and engineering: an introduction* vol. 7: John Wiley & Sons New York, 2007.

[18] B. Chen, H. Zhang, K. Dunphy-Guzman, D. Spagnoli, M. Kruger, D. Muthu*, et al.*, "Size-dependent elasticity of nanocrystalline titania," *Physical Review B,* vol. 79, p. 125406, 2009.

[19] F. W. Liou, *Rapid prototyping and engineering applications: a toolbox for prototype development*: Crc Press, 2007.

[20] I. Gibson, D. W. Rosen, B. Stucker, M. Khorasani, D. Rosen, B. Stucker*, et al.*, *Additive manufacturing technologies* vol. 17: Springer, 2021.

[21] B. Yilmaz, A. Al Rashid, Y. A. Mou, Z. Evis, and M. Koç, "Bioprinting: A review of processes, materials and applications," *Bioprinting,* vol. 23, p. e00148, 2021/08/01/ 2021.

[22] E. Kuram, B. Ozcelik, F. Yilmaz, G. Timur, and Z. M. Sahin, "The effect of recycling number on the mechanical, chemical, thermal, and rheological properties of PBT/PC/ABS ternary blends: With and without glass-fiber," *Polymer Composites,* vol. 35, pp. 2074-2084, 2014.

[23] S. Mallakpour and V. Behranvand, "Using recycled polymers for the preparation of polymer nanocomposites: properties and applications," in *Hybrid Polymer Composite Materials*, ed: Elsevier, 2017, pp. 197-226.

[24] R. H. Sanatgar, A. Cayla, C. Campagne, and V. Nierstrasz, "Morphological and electrical characterization of conductive polylactic acid based nanocomposite before and after FDM 3D printing," *Journal of Applied Polymer Science,* vol. 136, p. 47040, 2019.

[25] R. H. Enginler Özlen, N. Topcuoğlu, E. Dalkılıç, B. O. Küçükyıldırım, A. Akdoğan Eker, and H. G. Külekçi, "Effect of TiO2-n on the Antibacterial Properties of Low–Viscosity Bulk-Fill Composite," 2021.

[26] Sigma-Aldrich, "Certificate of Analysis for Titanium(IV) oxide, anatase - nanopowder, <25 nm particle size, 99.7% trace metal basis; Production number: 637254, Batch number: MKCD5233," 2017.

[27] Anycubic, "Standard Resin User Manual."

[28] ASTM, "G99–95a Standard Test Method for Wear Testing with a Pin-on-Disk Apparatus," in *ASTM International*, ed, 2000.

A
BALL-ON-DISK TEST RESULTS

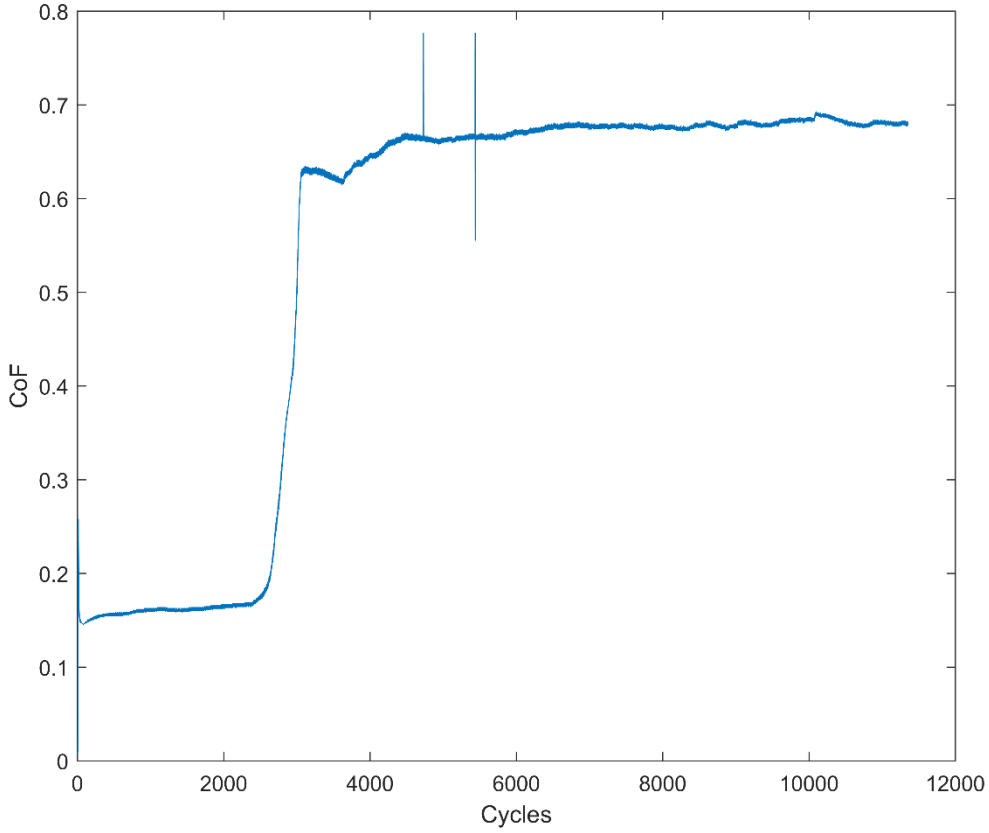

Figure A.1 Change in friction coefficient with cycle: S1-1.

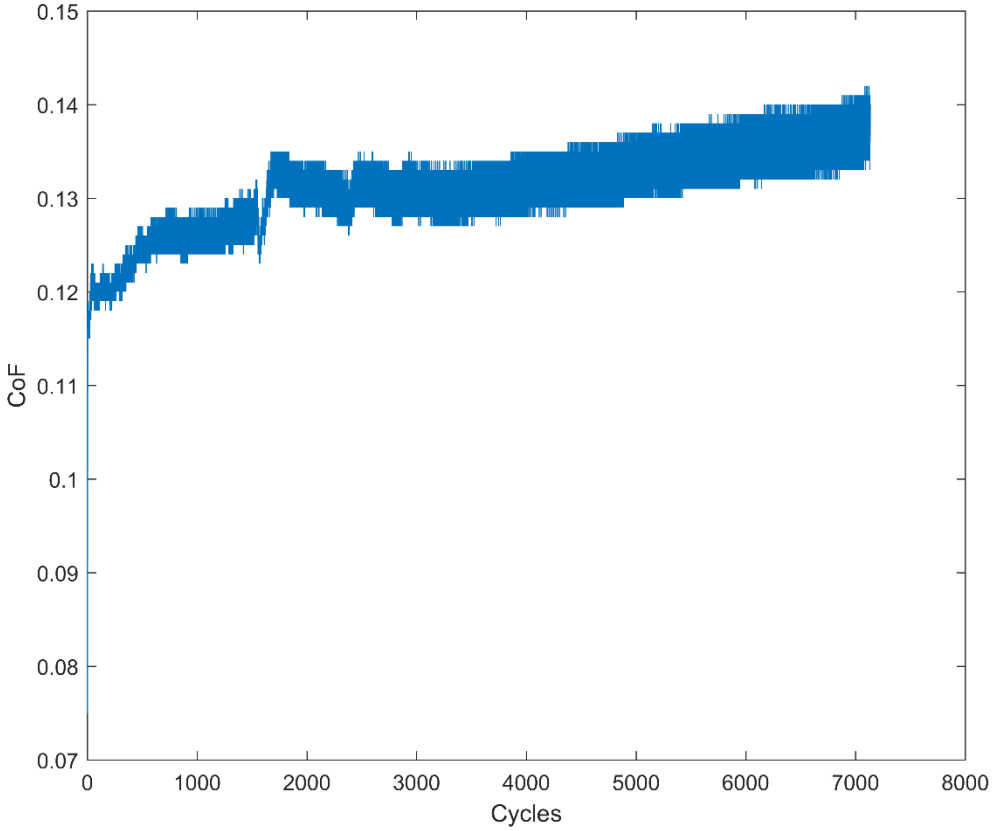

Figure A.2 Change in friction coefficient with cycle: S1-2.

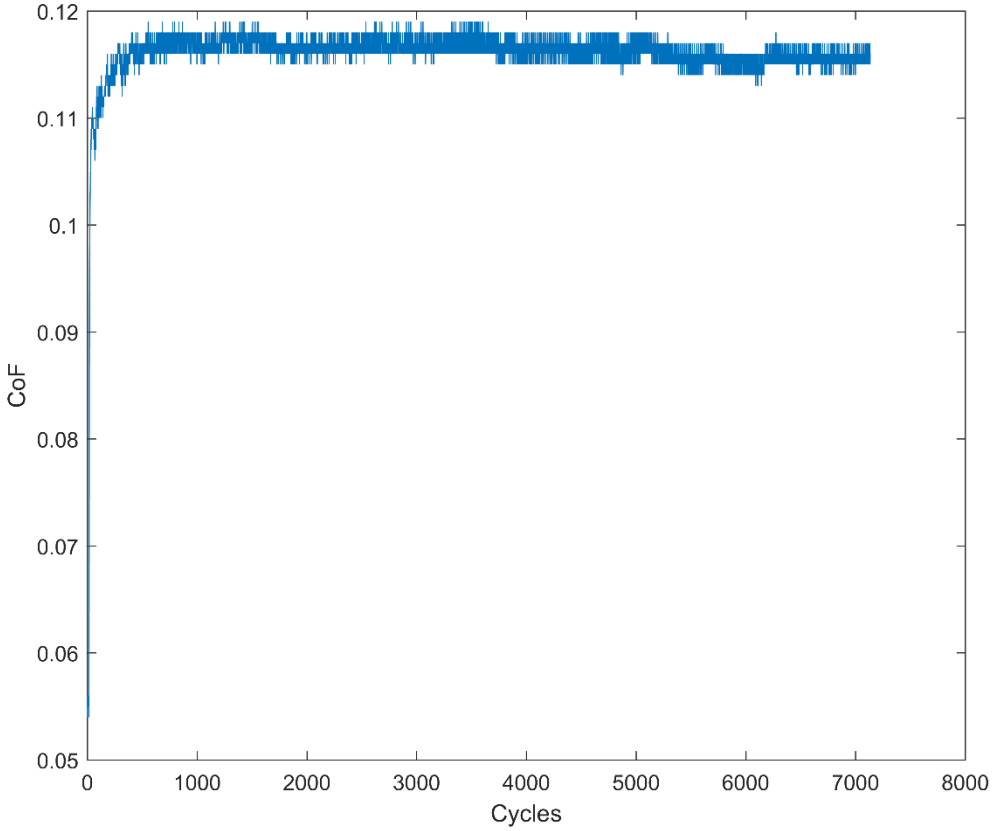

Figure A.3 Change in friction coefficient with cycle: S1-3.

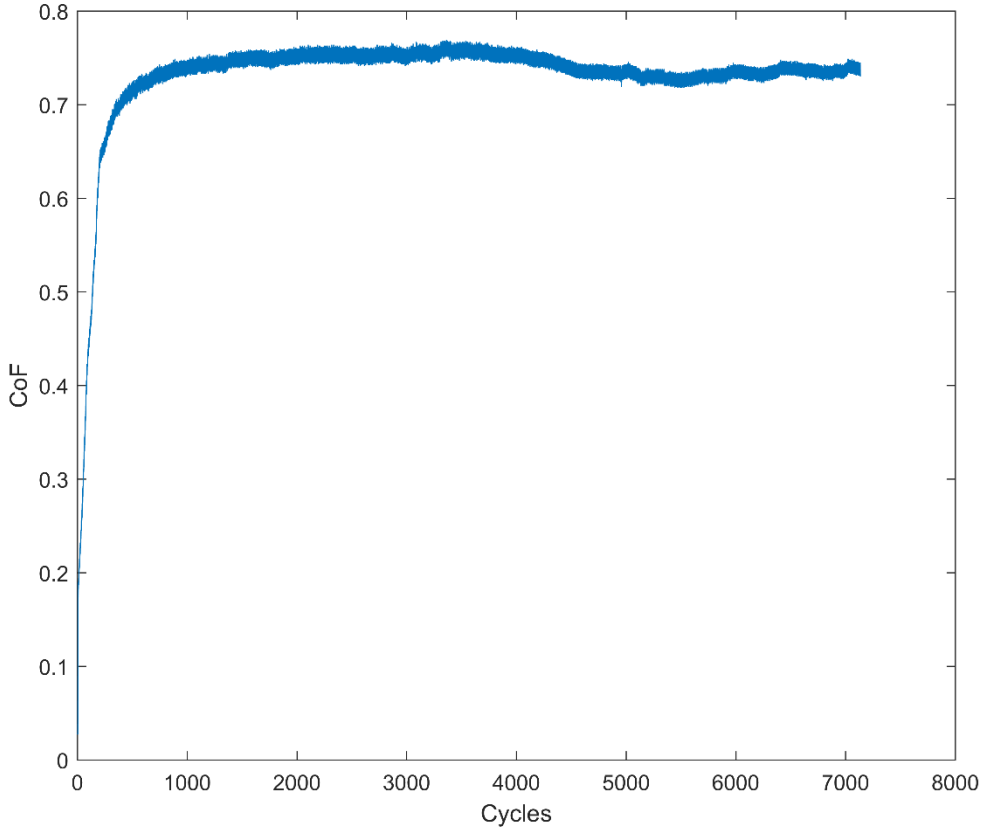

Figure A.4 Change in friction coefficient with cycle: S2-1.

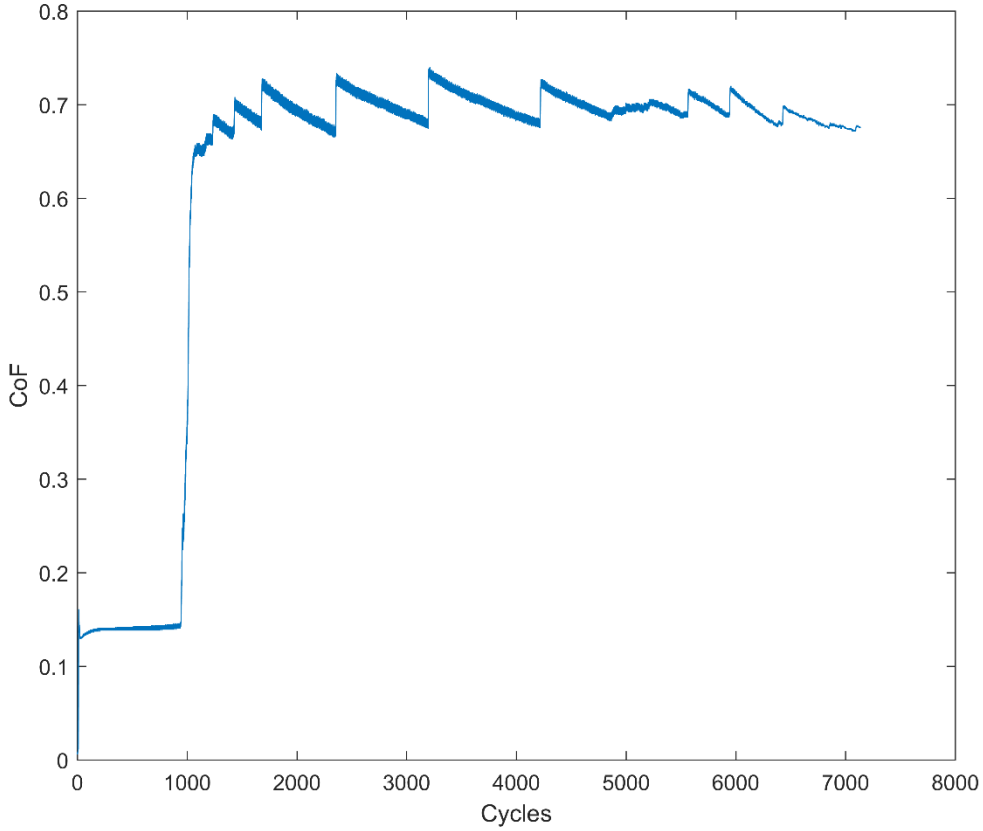

Figure A.5 Change in friction coefficient with cycle: S2-2.

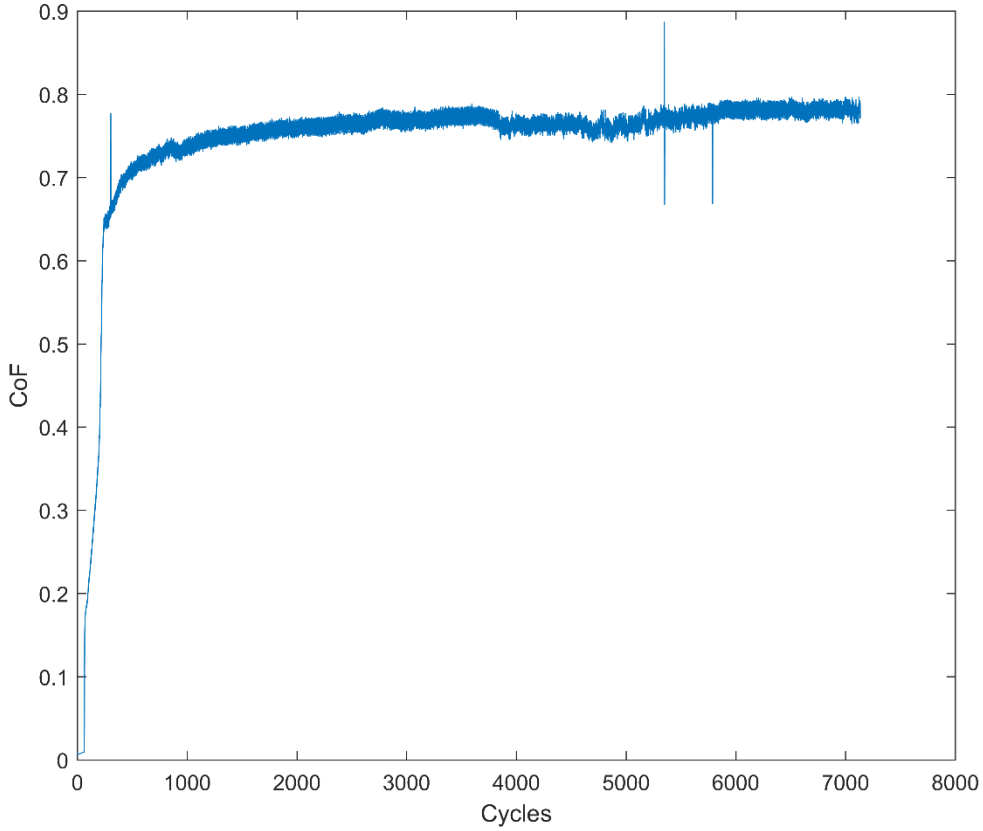

Figure A.6 Change in friction coefficient with cycle: S2-3.

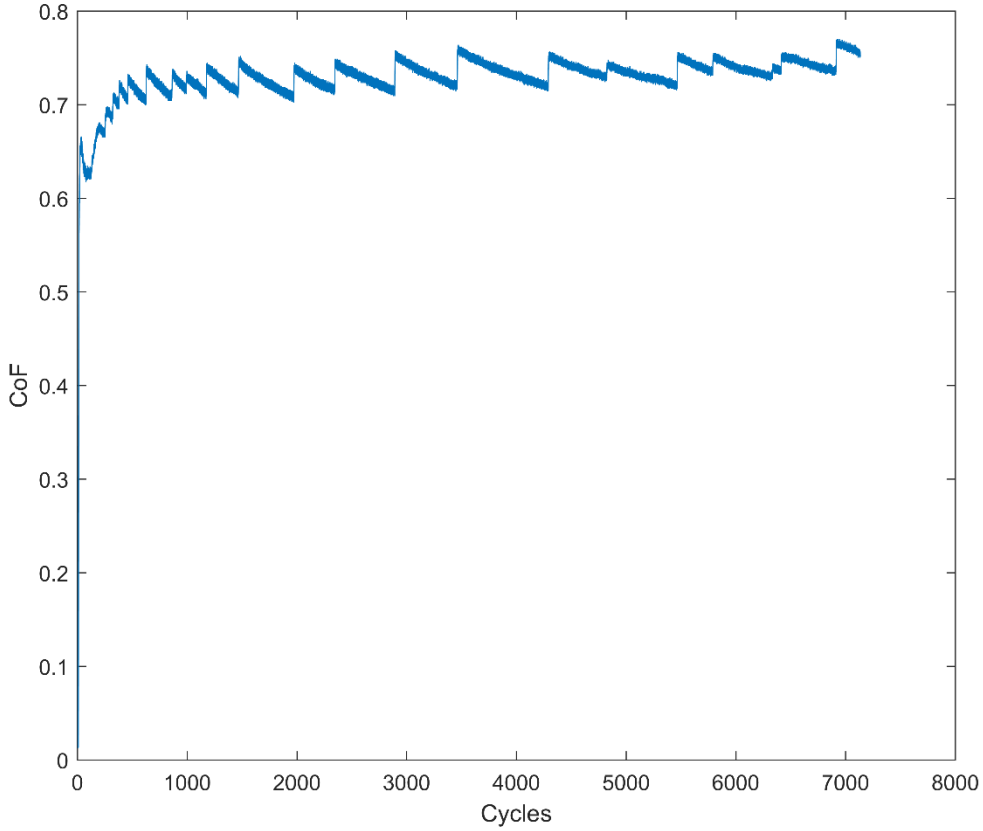

Figure A.7 Change in friction coefficient with cycle: S3-1.

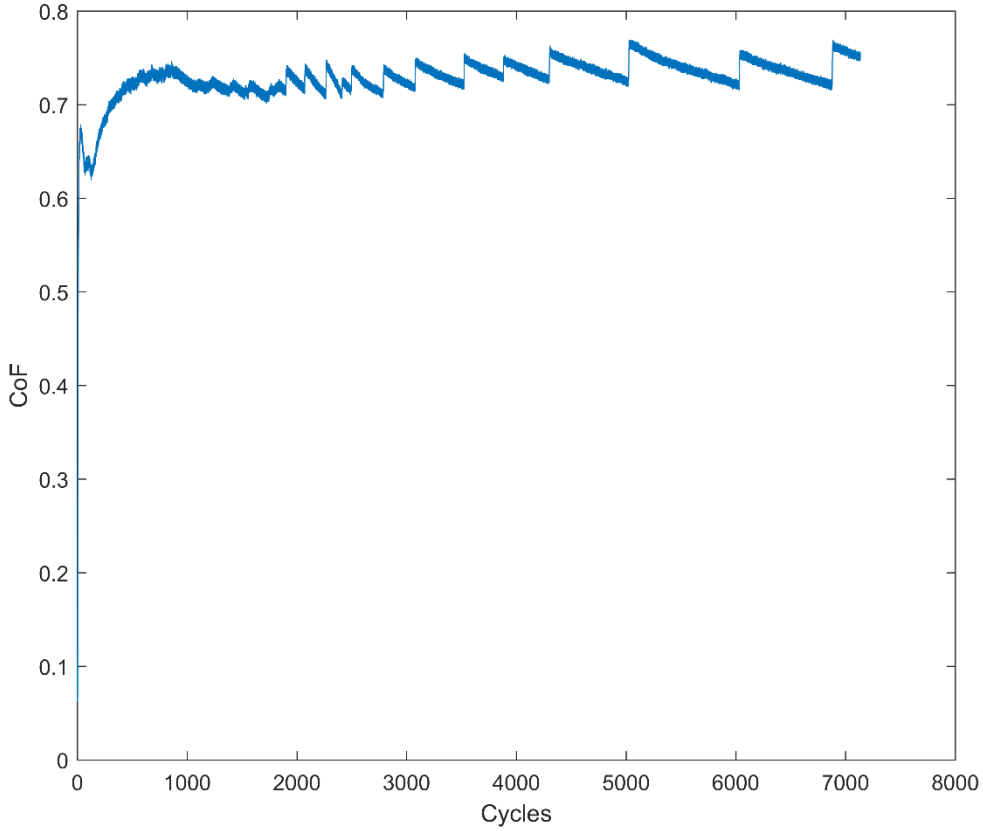

Figure A.8 Change in friction coefficient with cycle: S3-2.

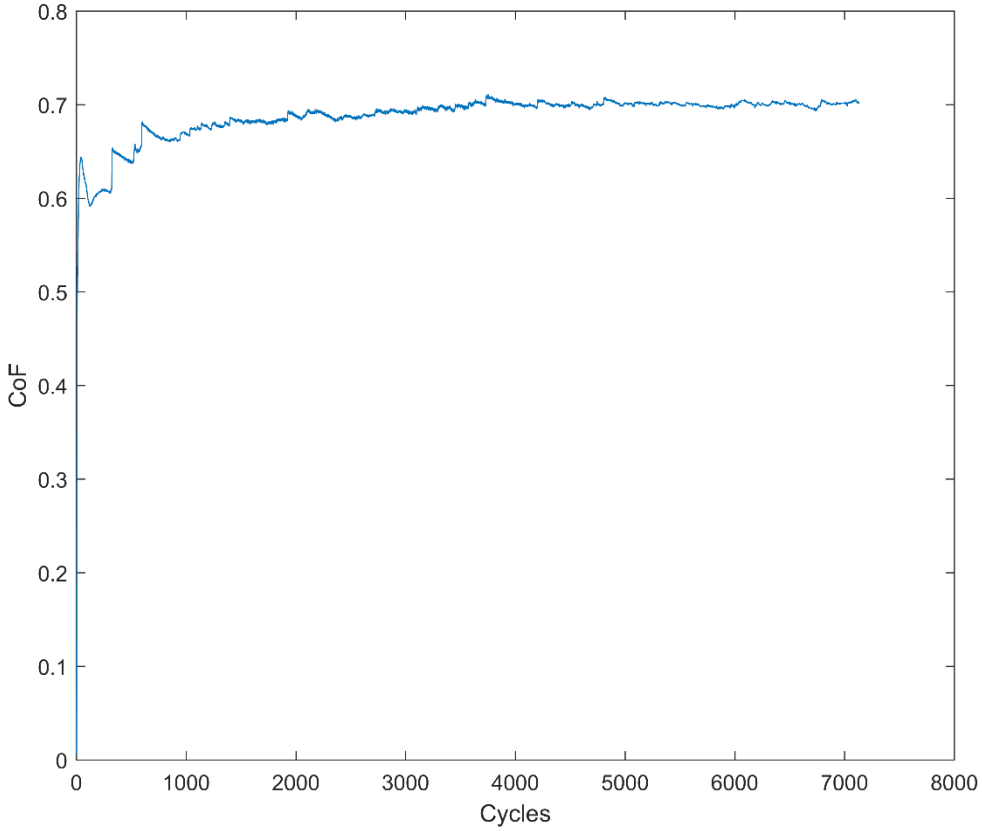

Figure A.9 Change in friction coefficient with cycle: S3-3.

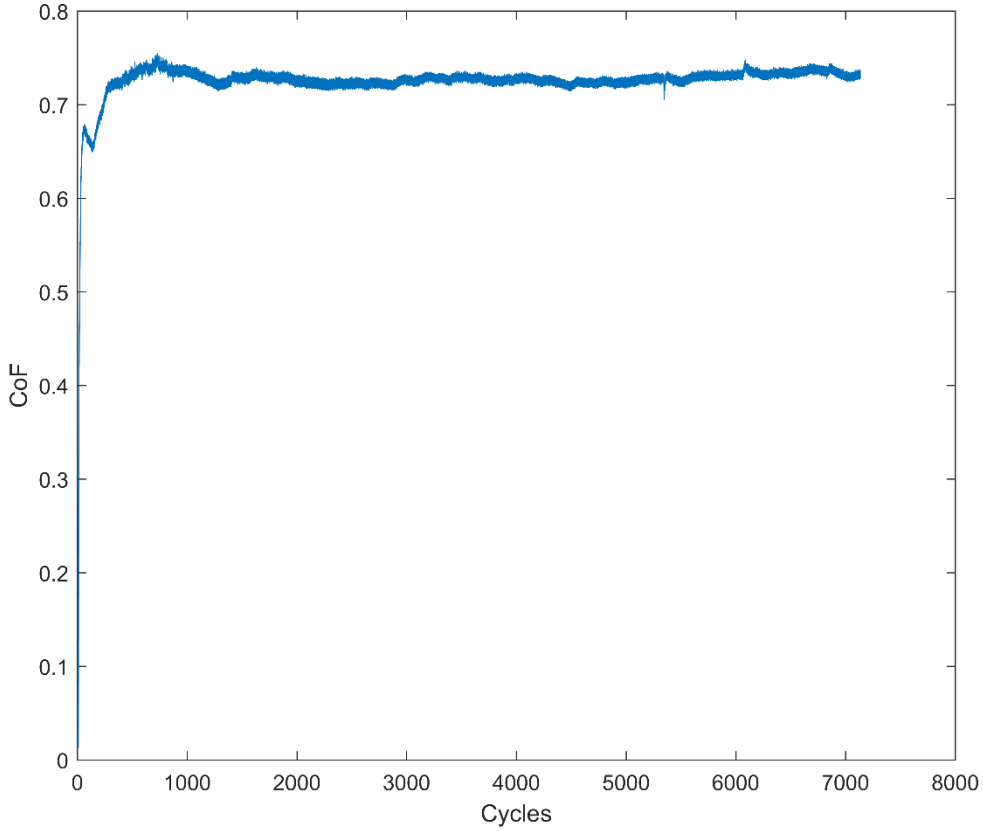

Figure A.10 Change in friction coefficient with cycle: S4-1.

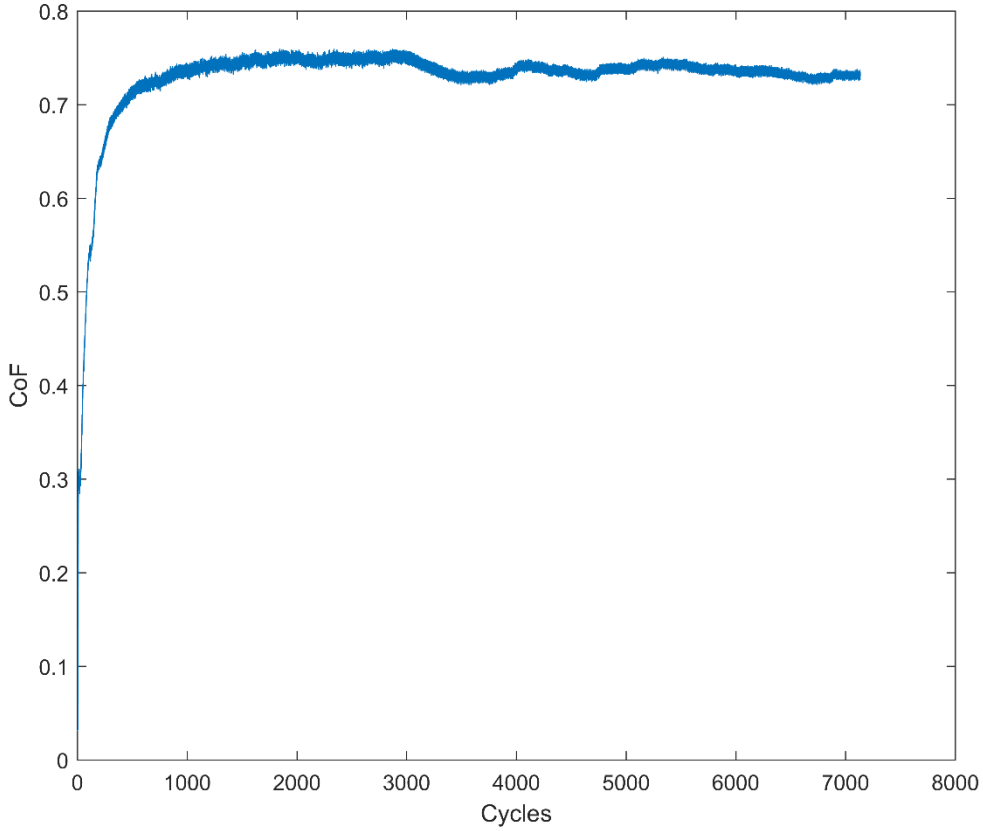

Figure A.11 Change in friction coefficient with cycle: S4-2.

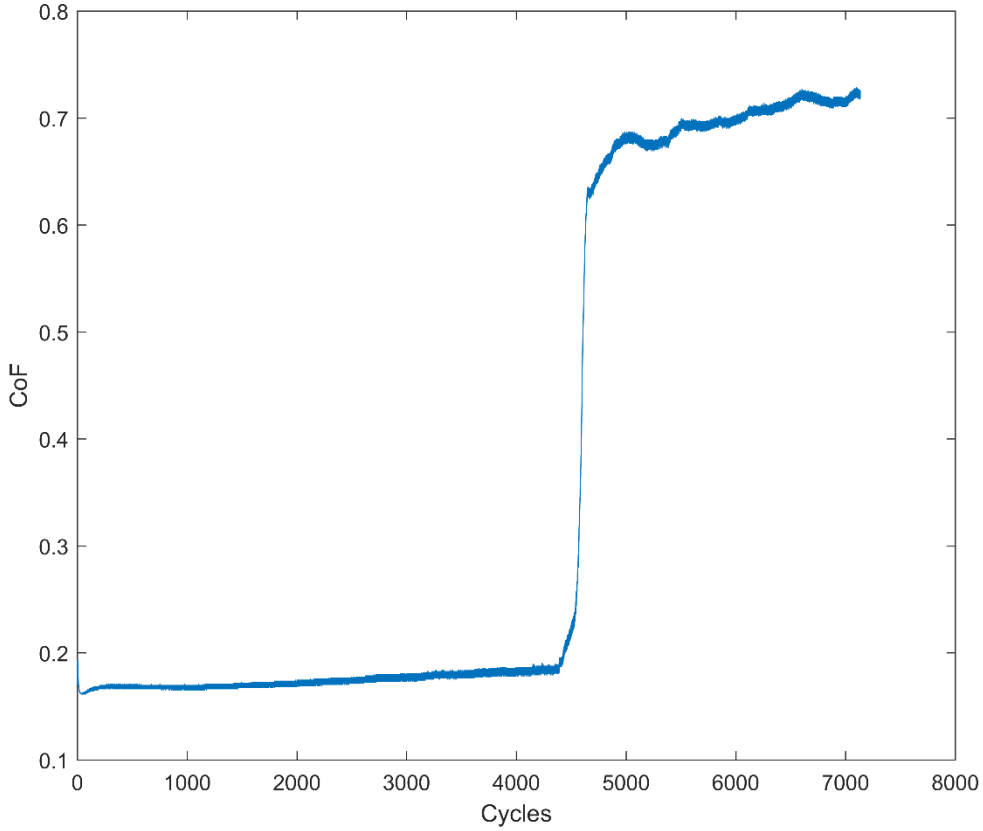

Figure A.12 Change in friction coefficient with cycle: S4-3.

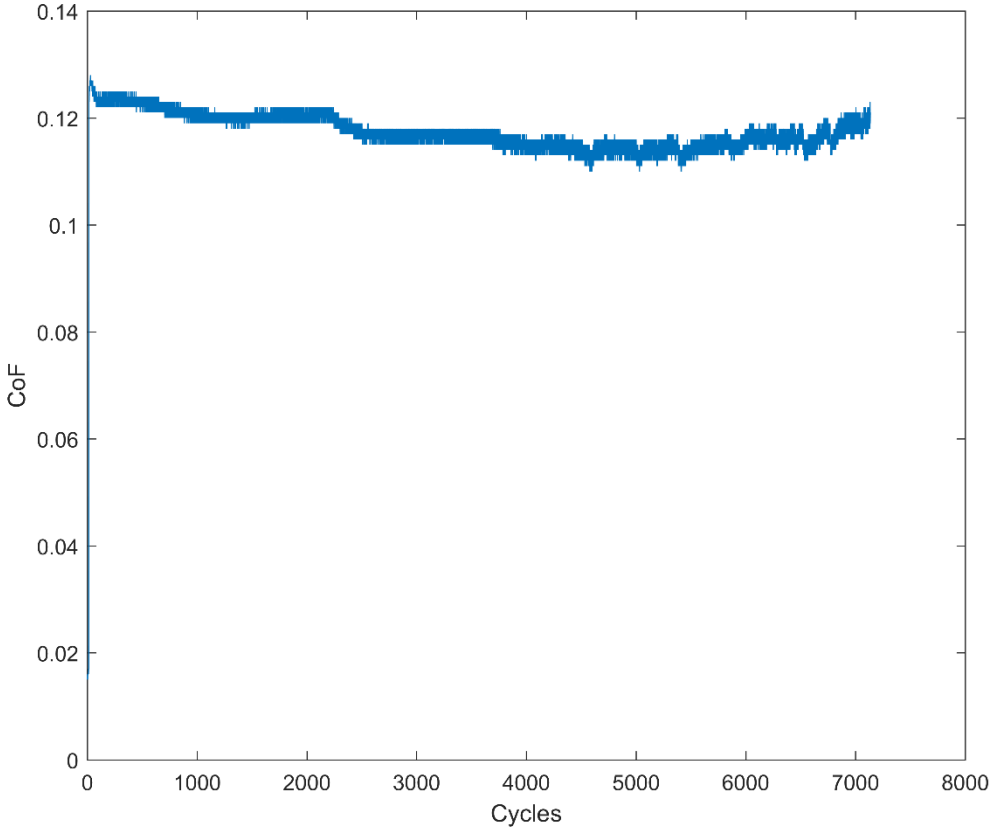

Figure A.13 Change in friction coefficient with cycle: S5-1.

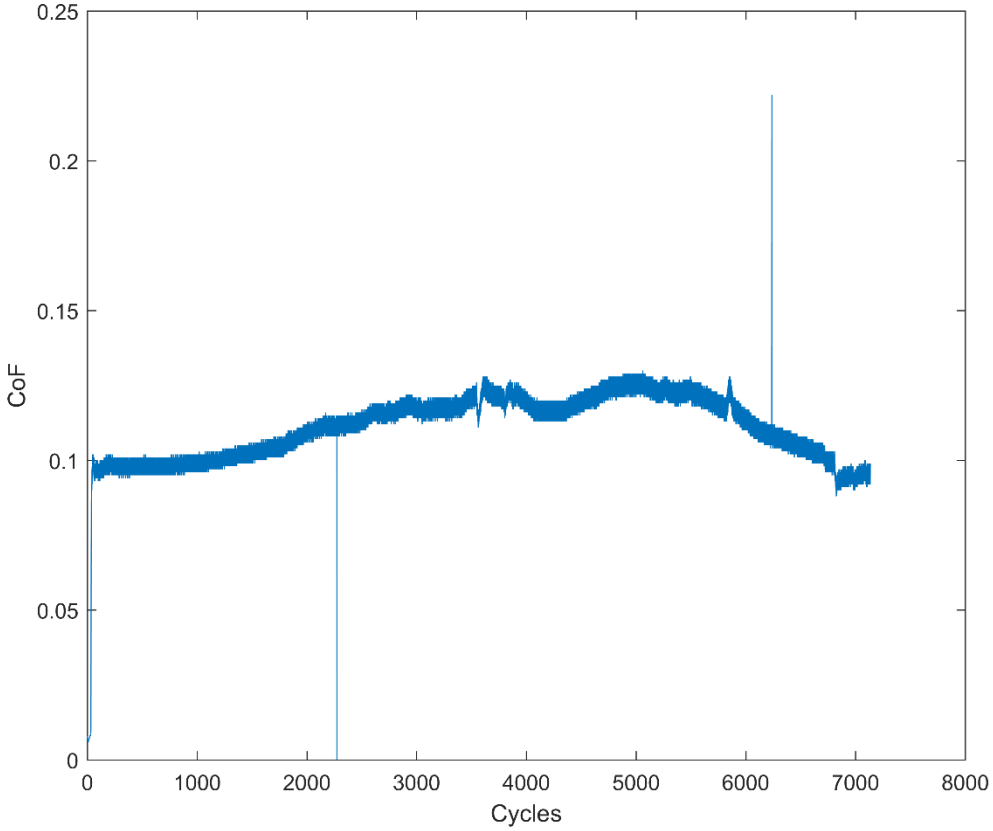

Figure A.14 Change in friction coefficient with cycle: S5-2.

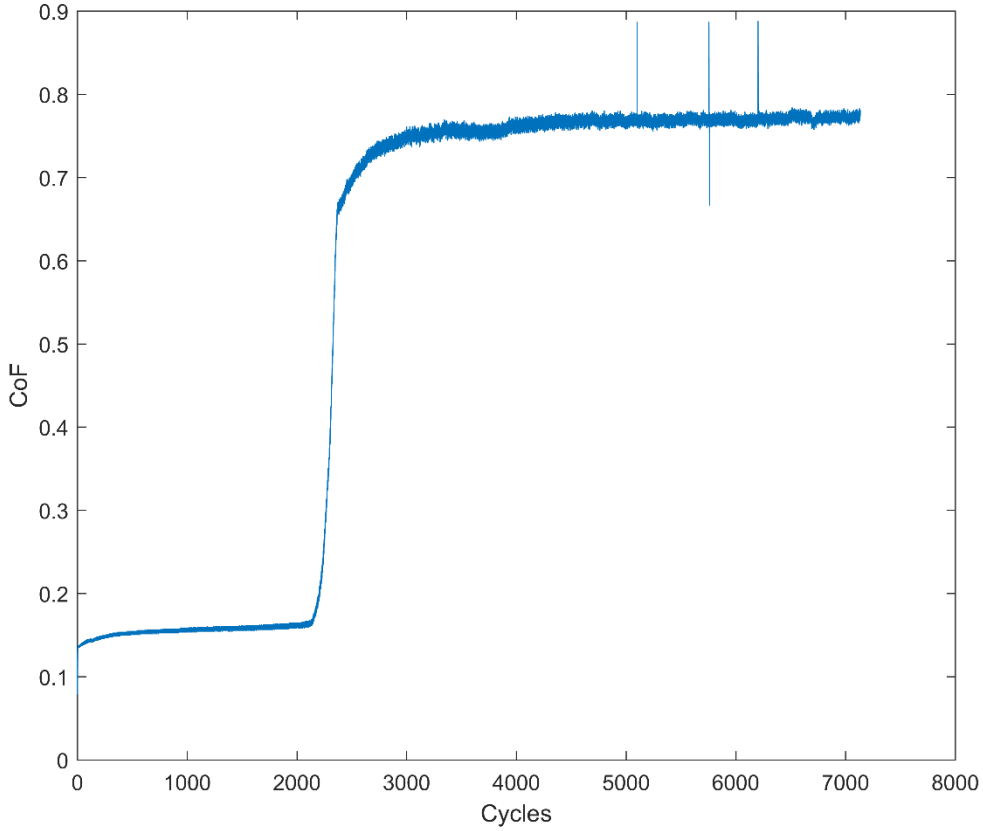

Figure A.15 Change in friction coefficient with cycle: S5-3.

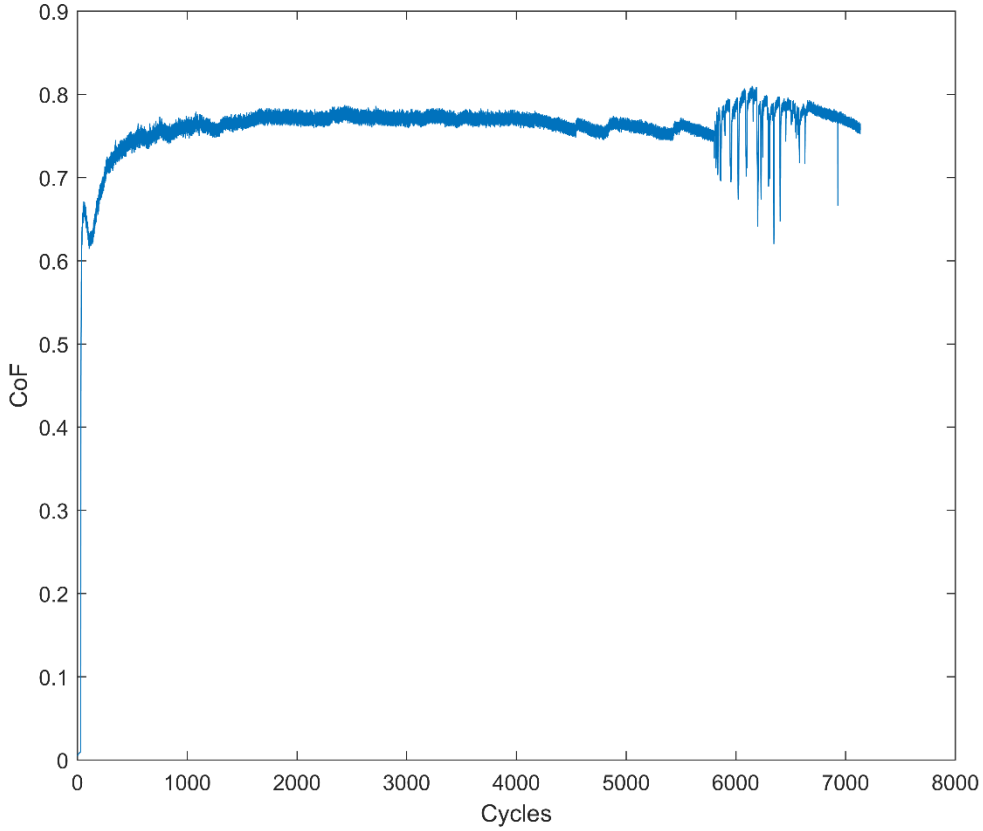

Figure A.16 Change in friction coefficient with cycle: S6-1.

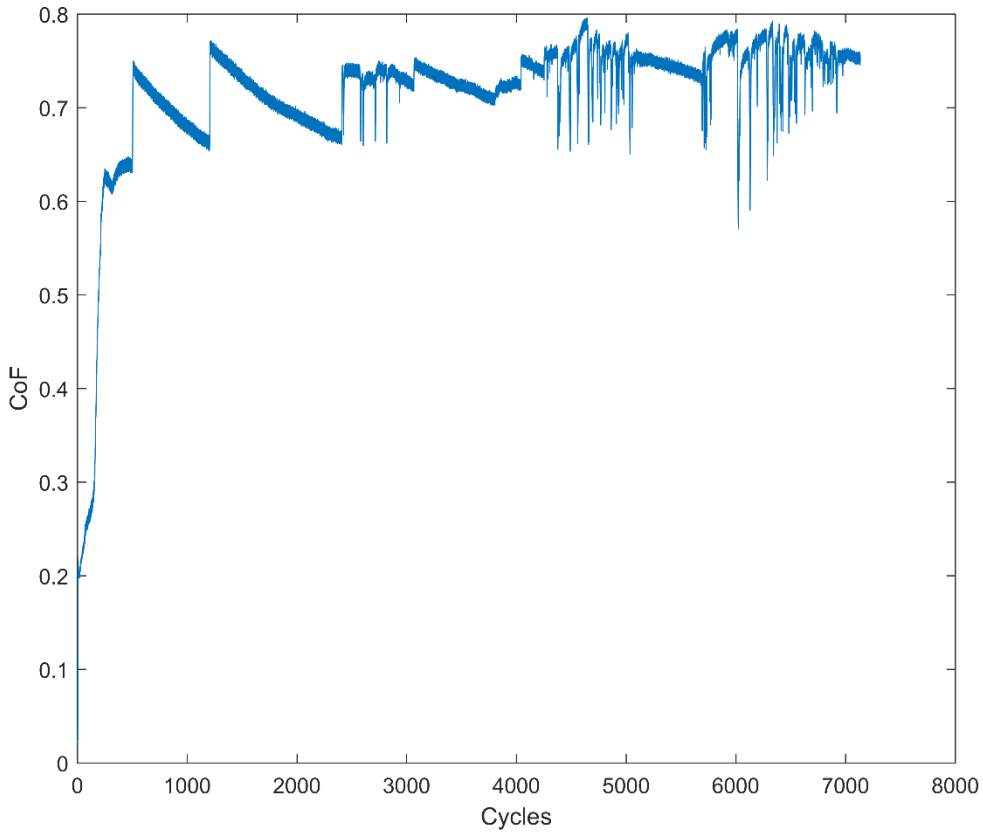

Figure A.17 Change in friction coefficient with cycle: S6-2.

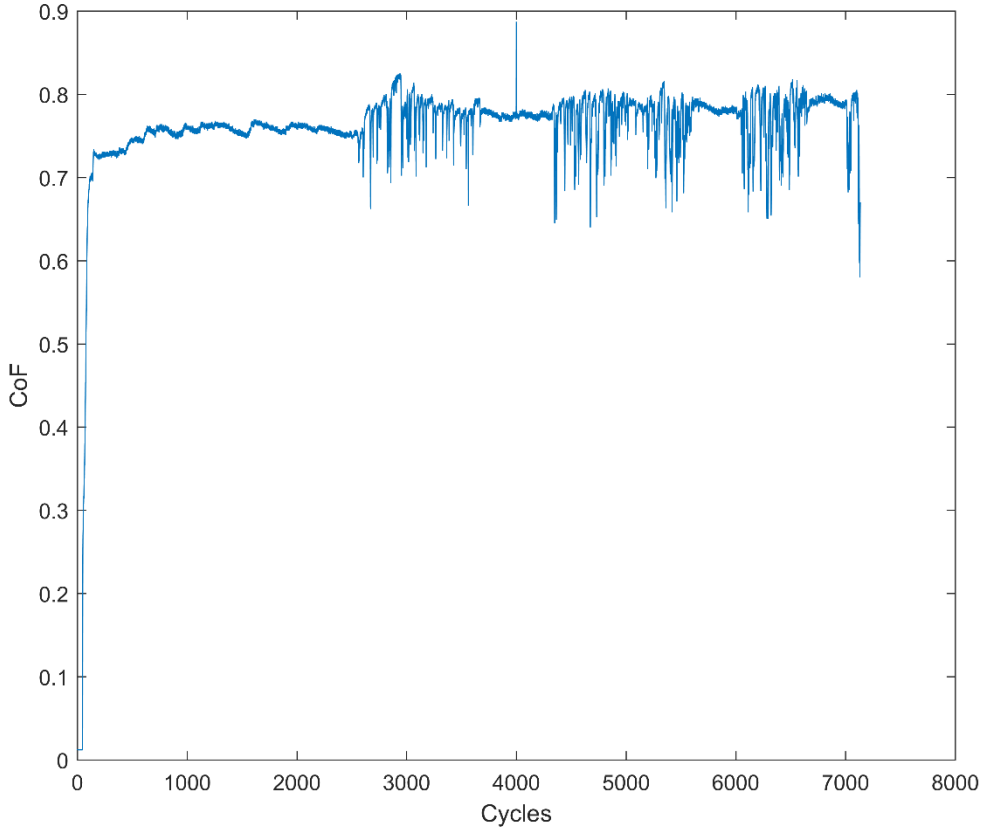

Figure A.18 Change in friction coefficient with cycle: S6-3.

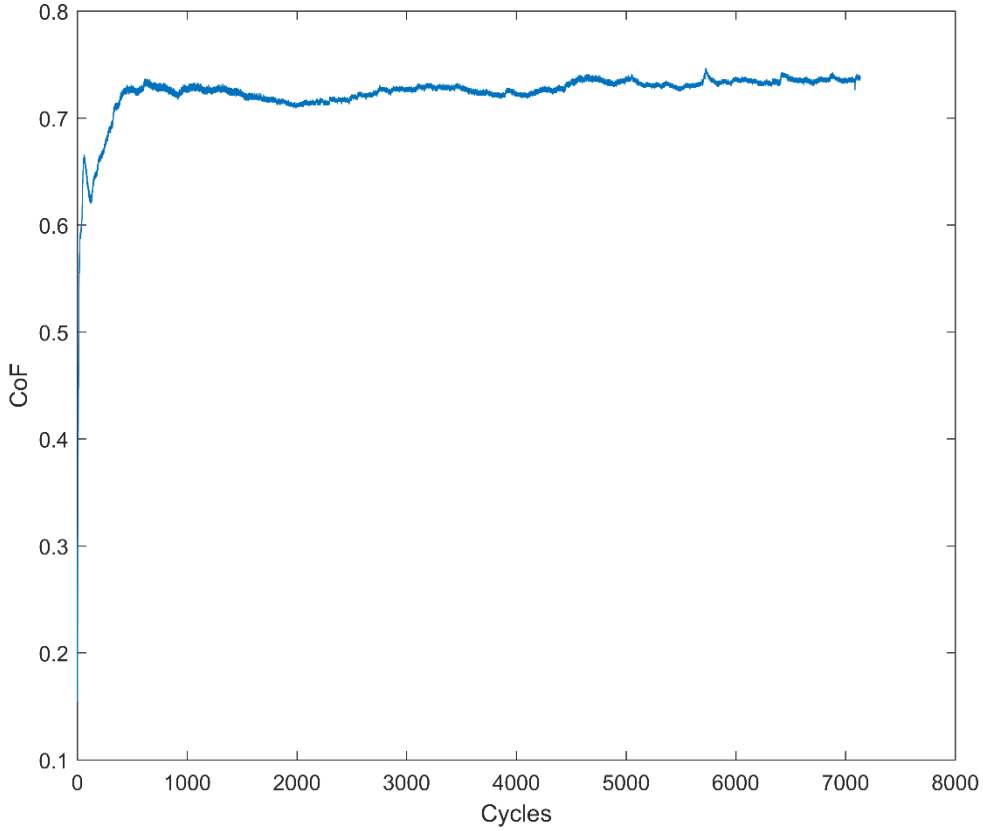

Figure A.19 Change in friction coefficient with cycle: S7-1.

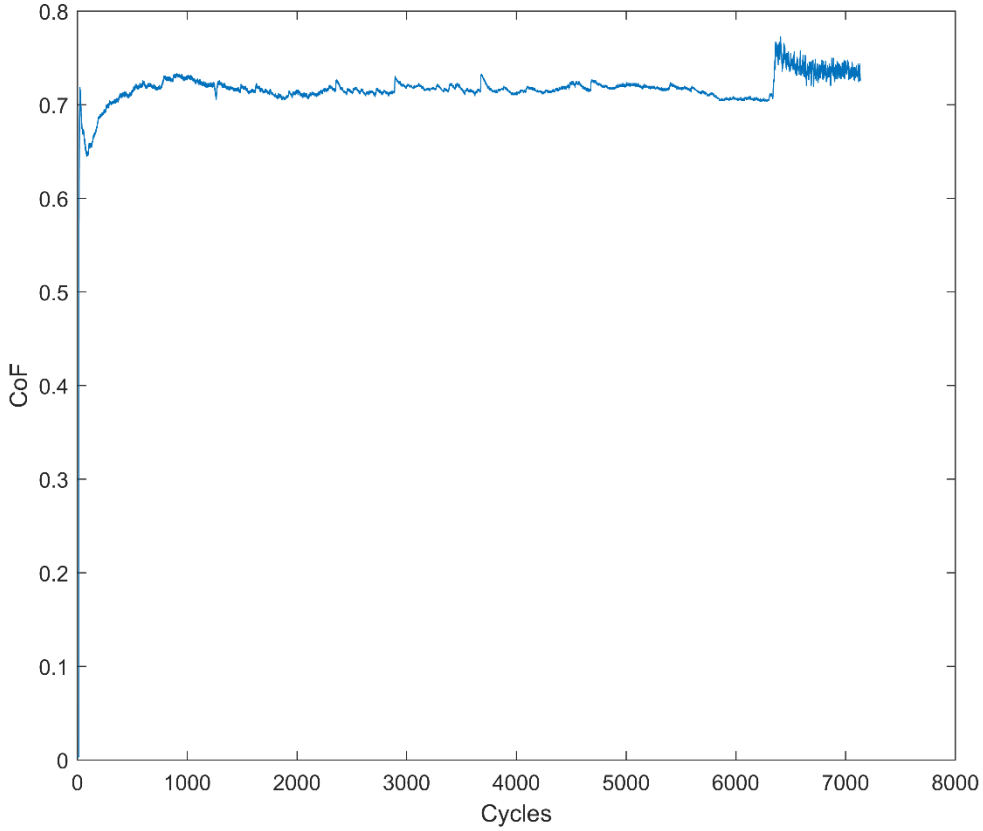

Figure A.20 Change in friction coefficient with cycle: S7-2.

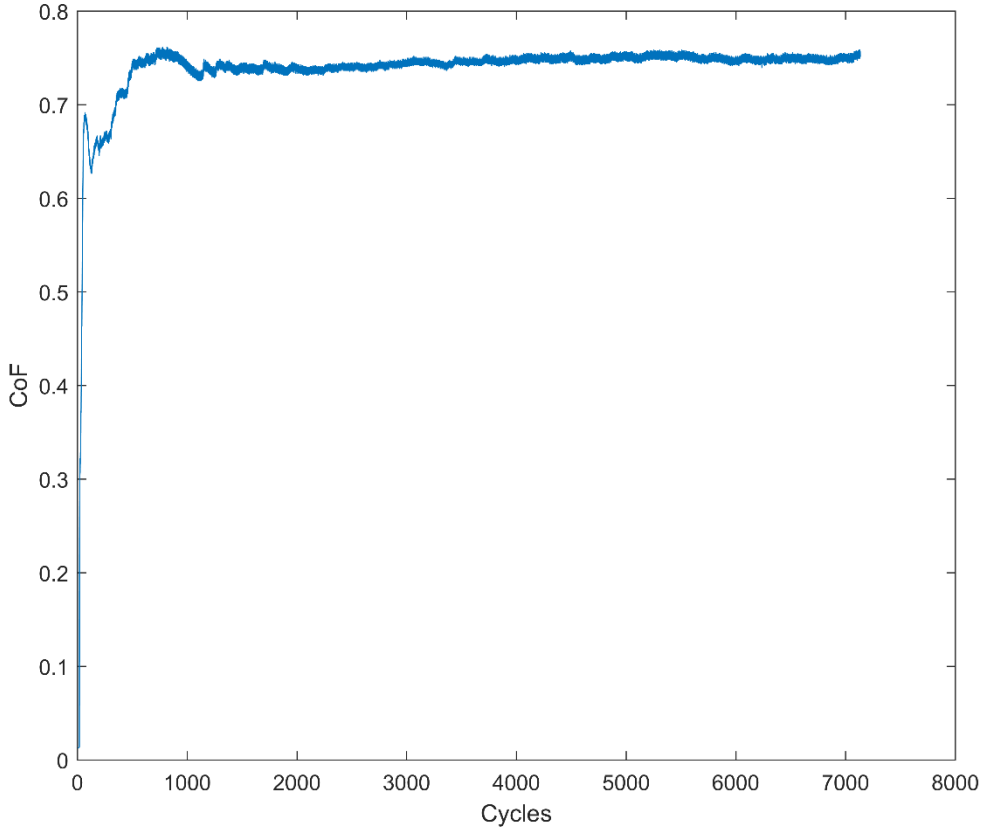

Figure A.21 Change in friction coefficient with cycle: S7-3.

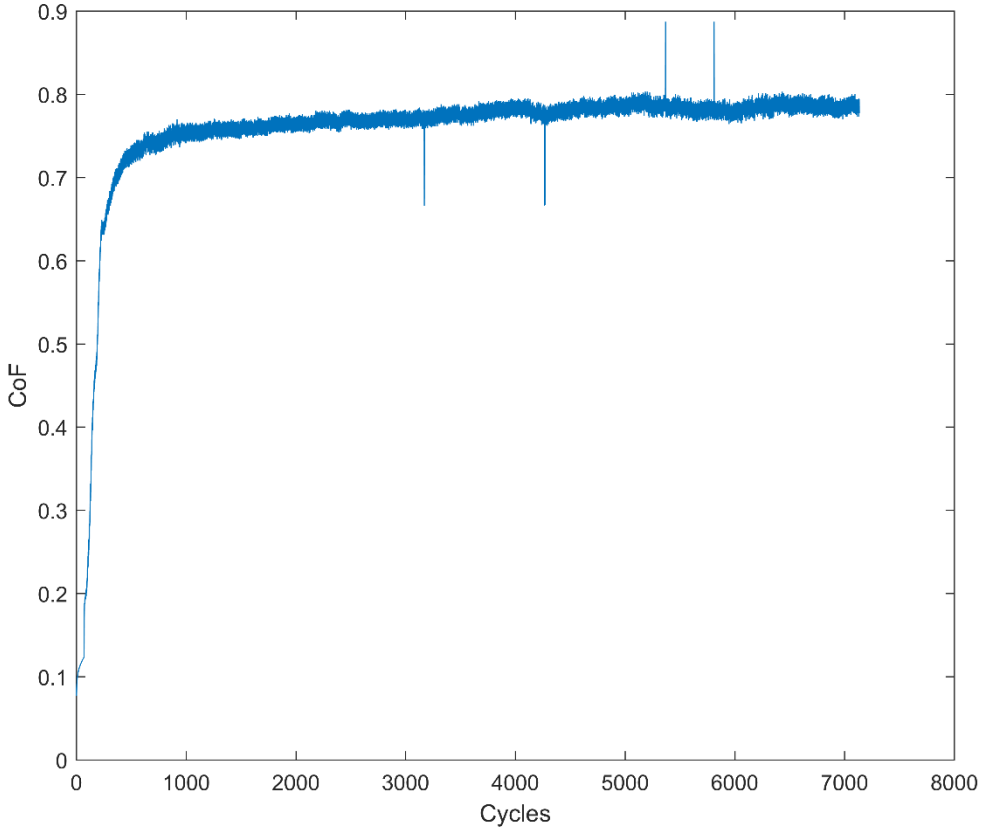

Figure A.22 Change in friction coefficient with cycle: S8-1.

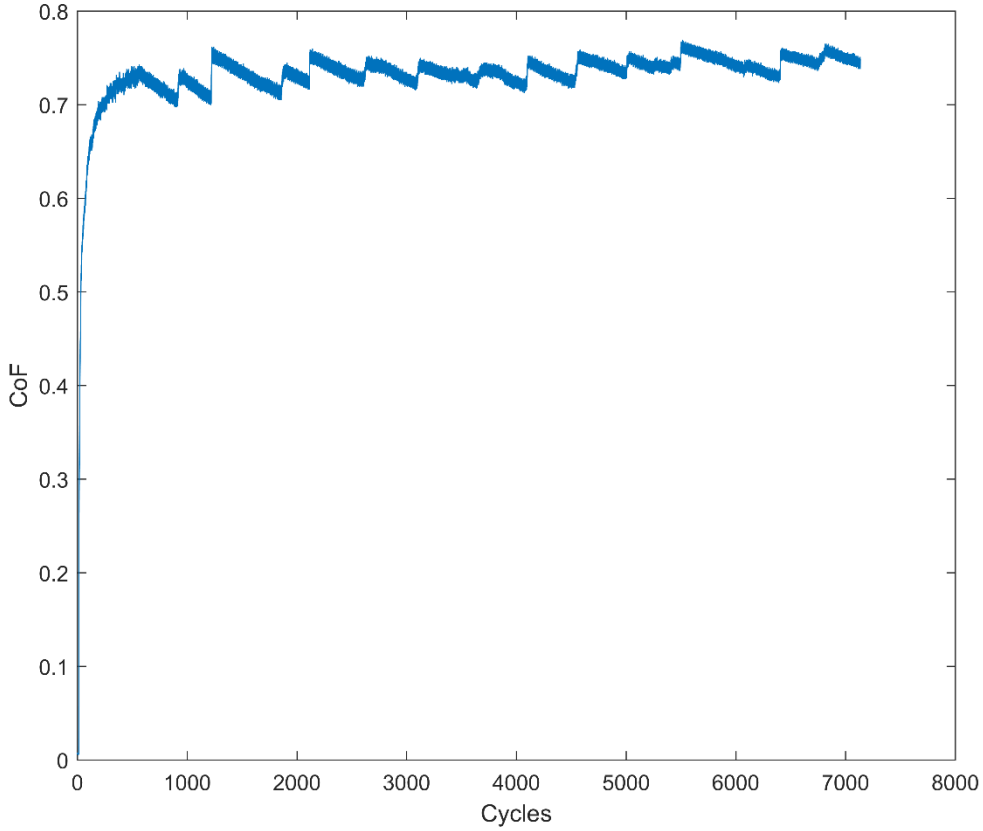

Figure A.23 Change in friction coefficient with cycle: S8-2.

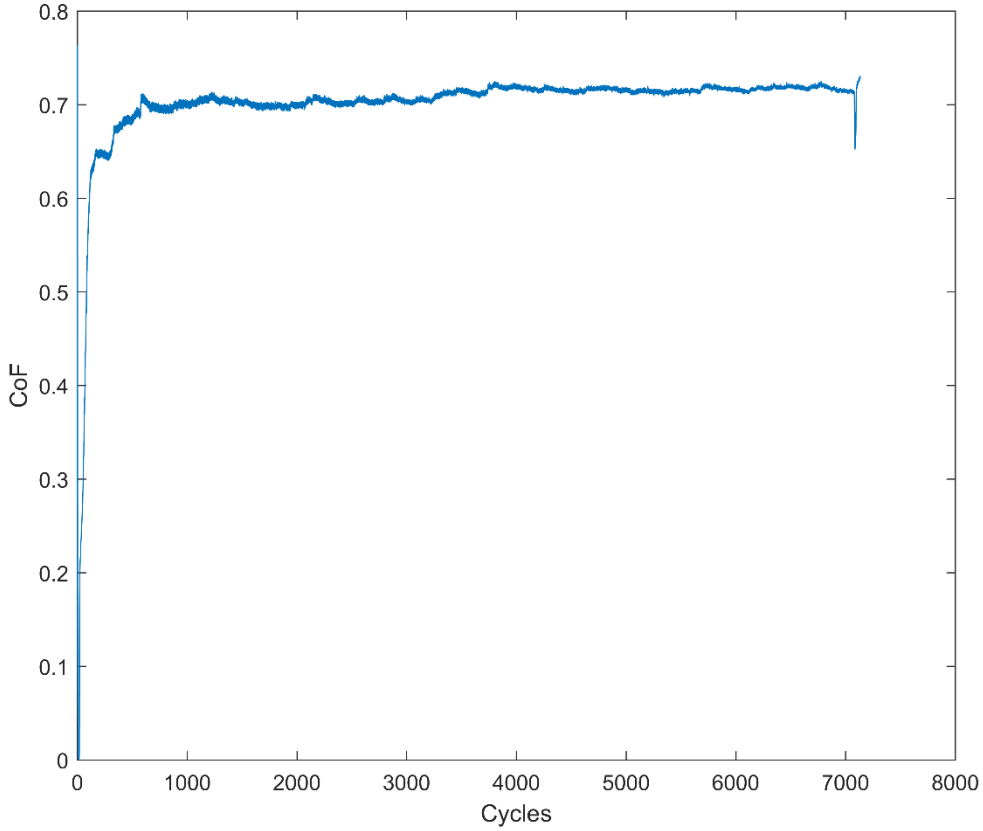

Figure A.24 Change in friction coefficient with cycle: S8-3.

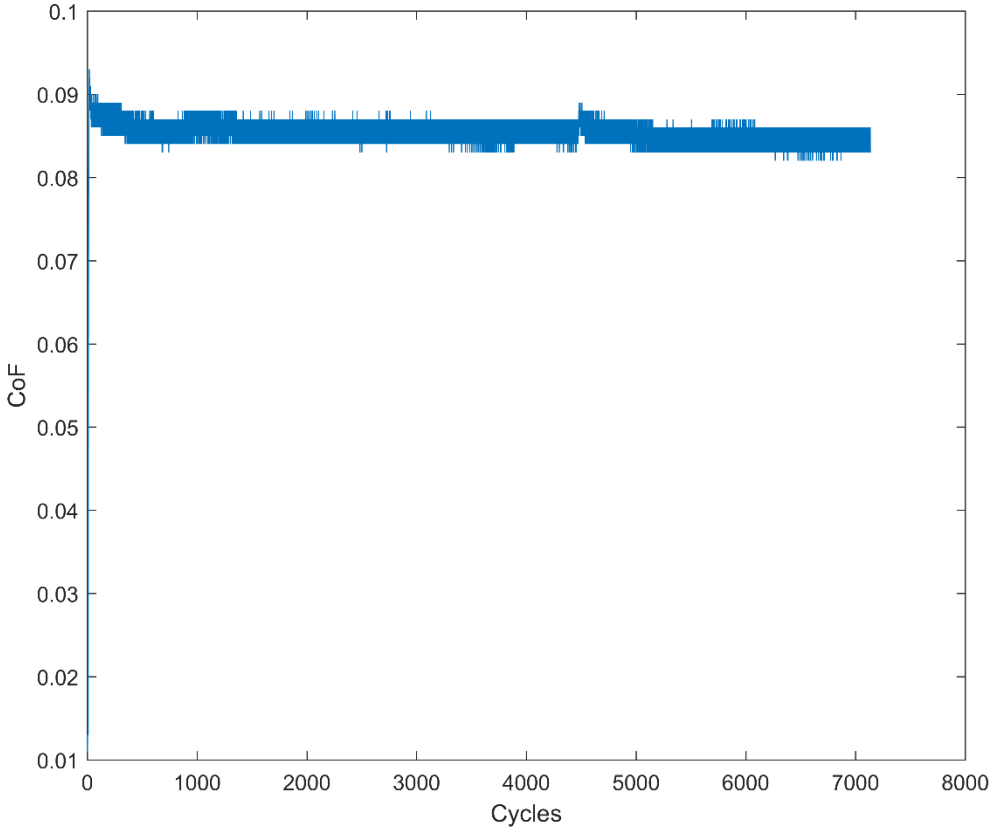

Figure A.25 Change in friction coefficient with cycle: S9-1.

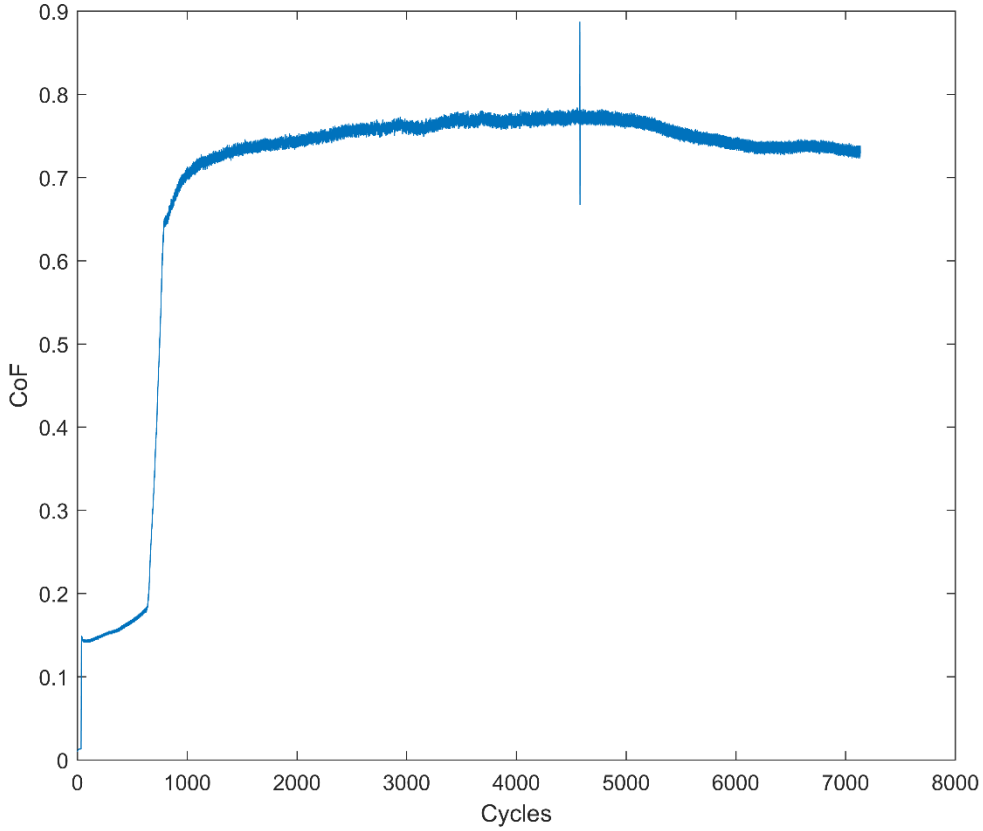

Figure A.26 Change in friction coefficient with cycle: S9-2.

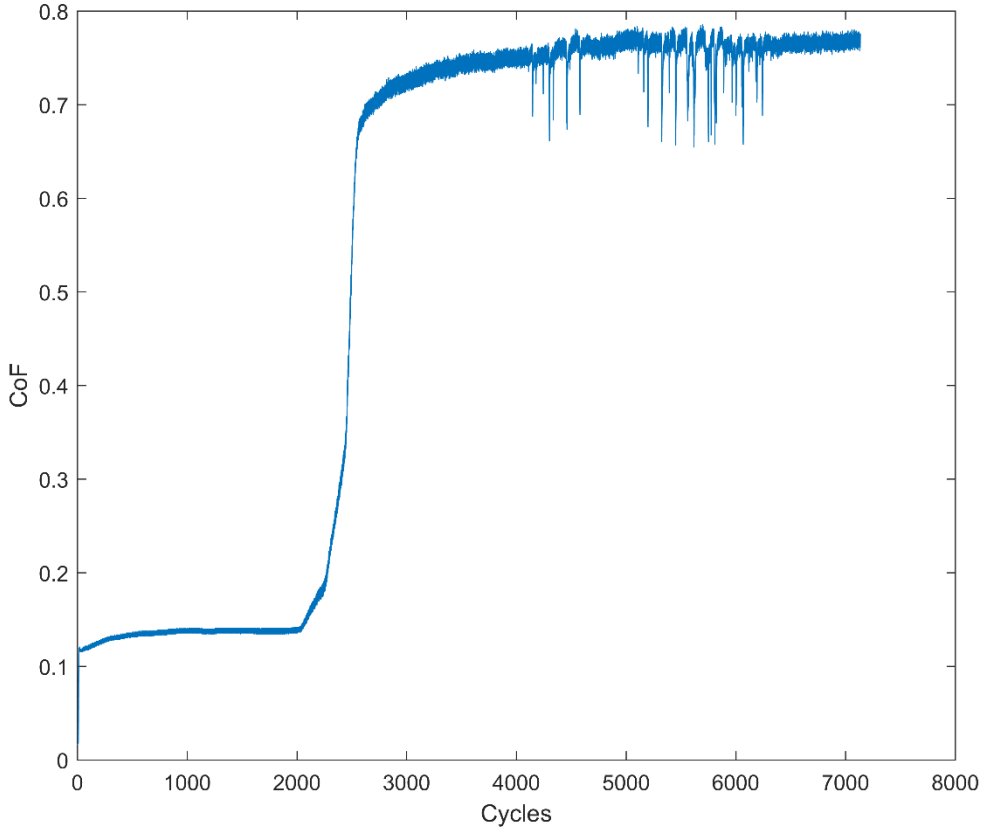

Figure A.27 Change in friction coefficient with cycle: S9-3.

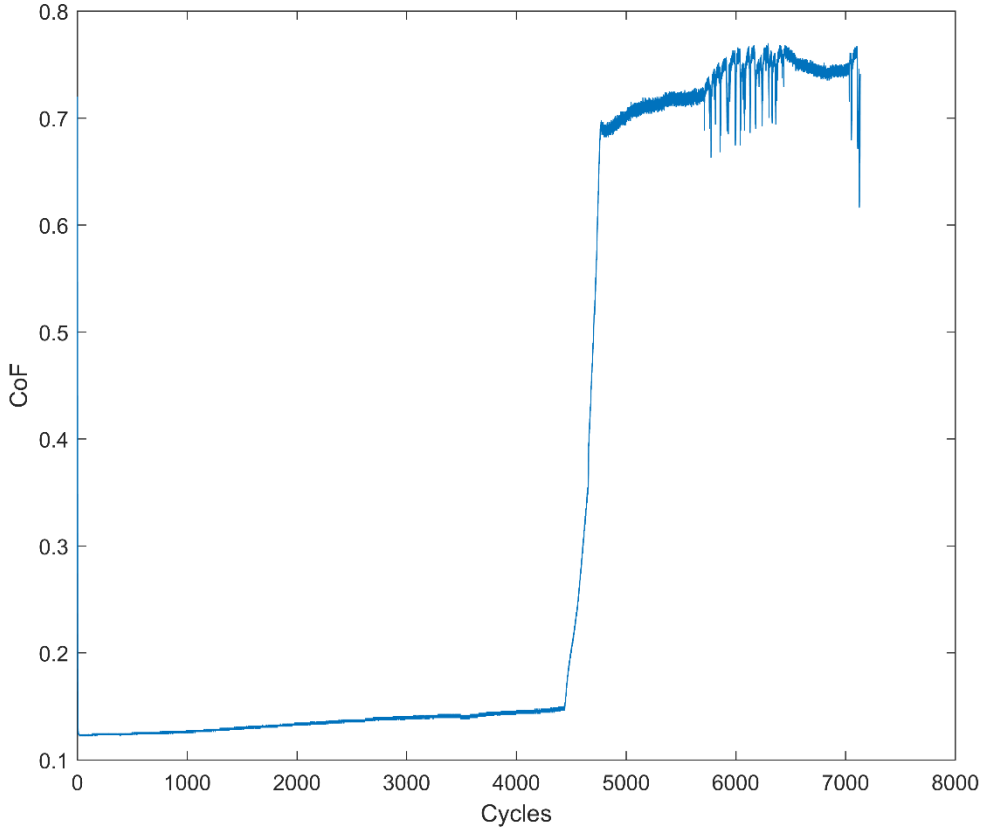

Figure A.28 Change in friction coefficient with cycle: Verification-1.

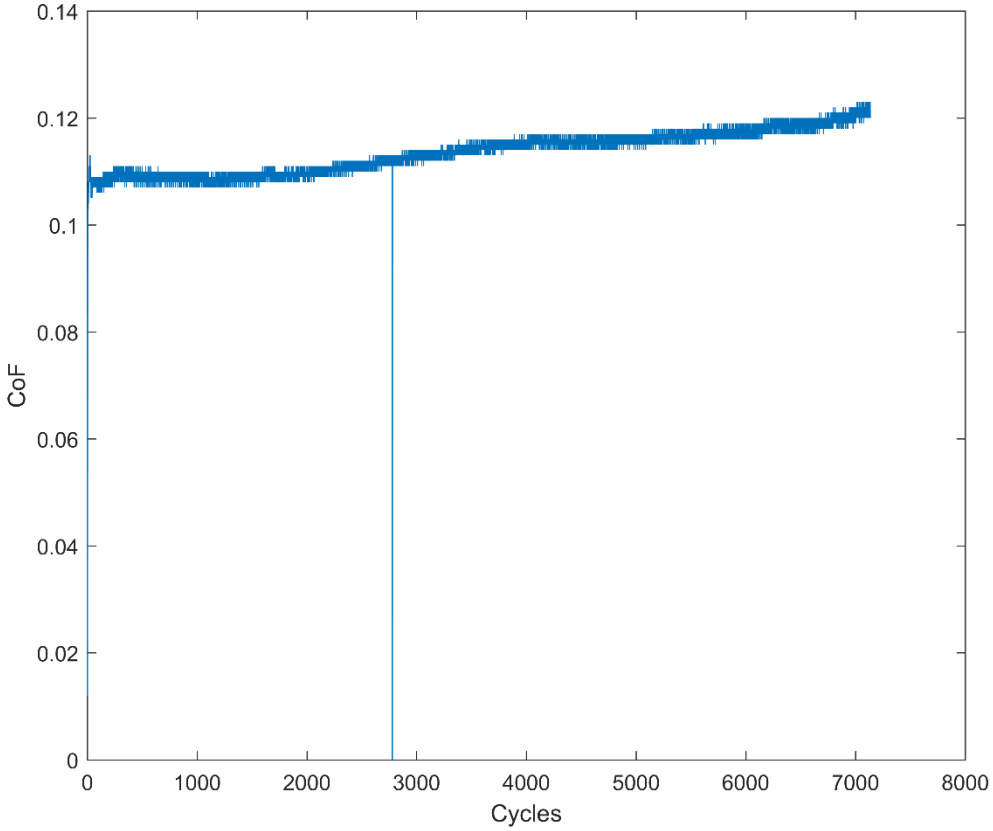

Figure A.29 Change in friction coefficient with cycle: Verification-2.

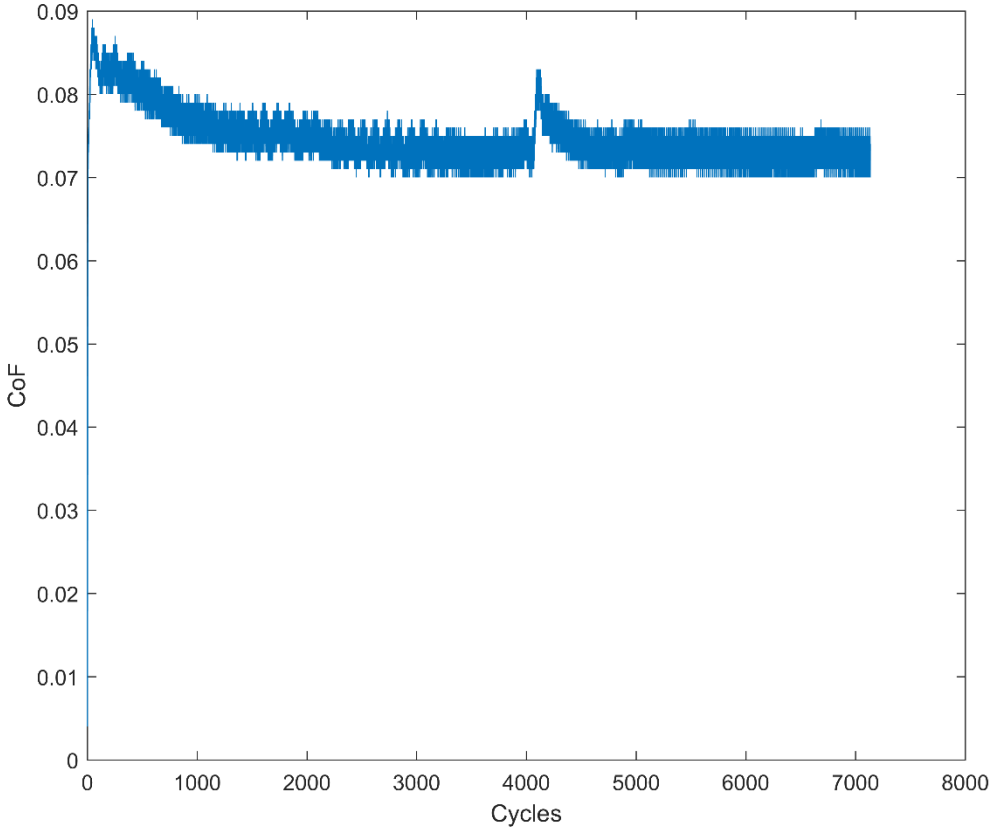

Figure A.30 Change in friction coefficient with cycle: Verification-3.

B
MACROSCOPY IMAGES

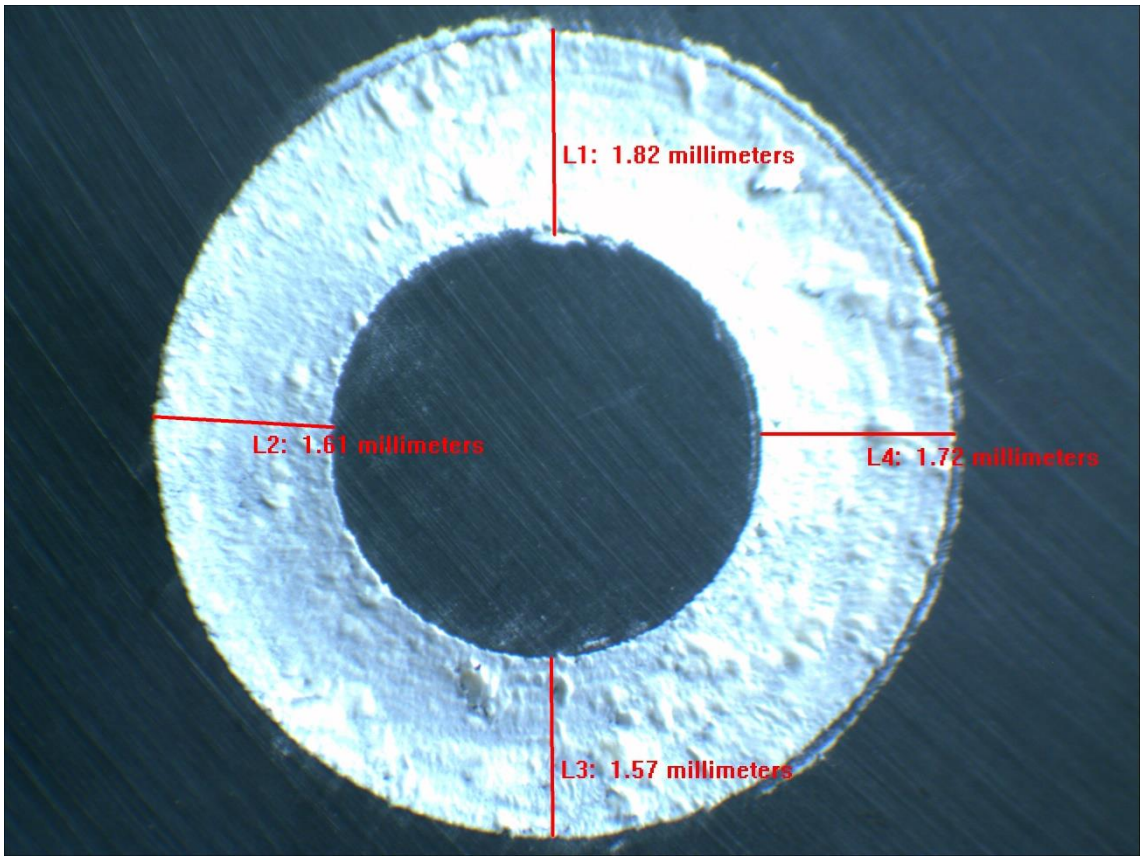

Figure B.1 Macroscopy image and wear track measurement of S1-1.

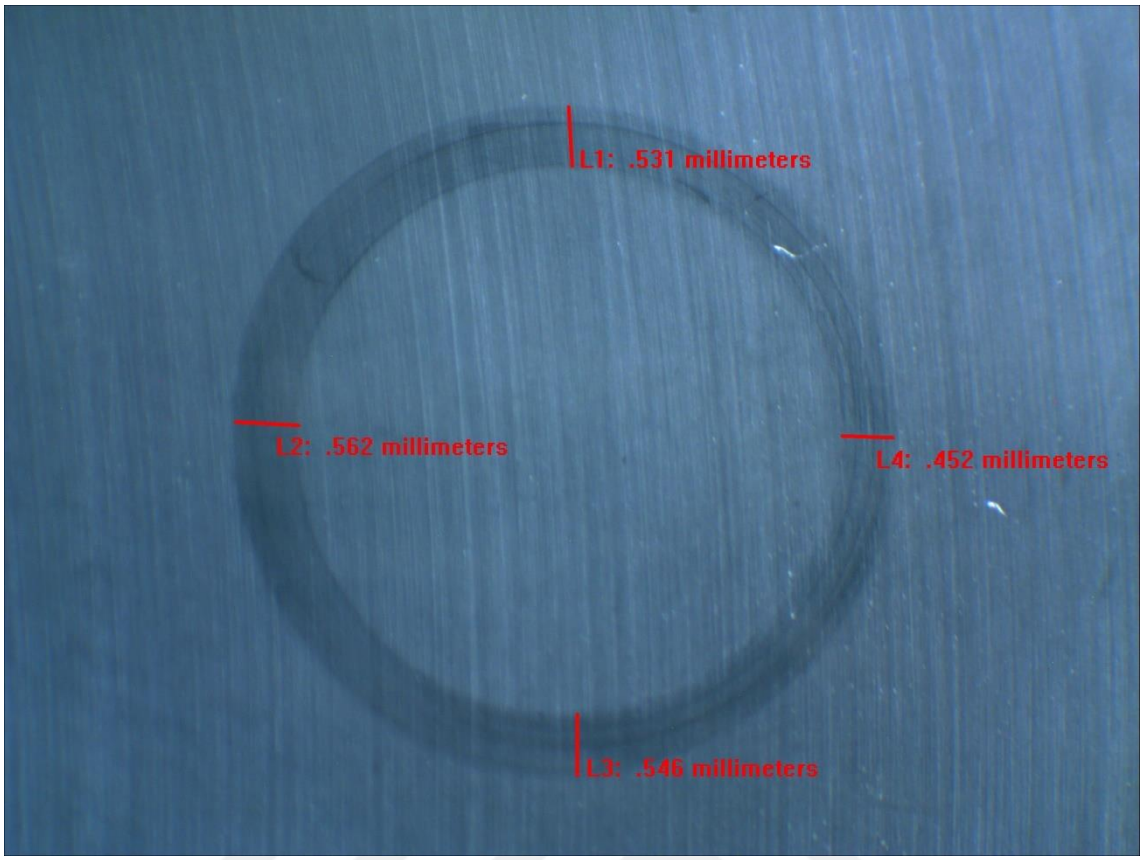

Figure B.2 Macroscopy image and wear track measurement of S1-2.

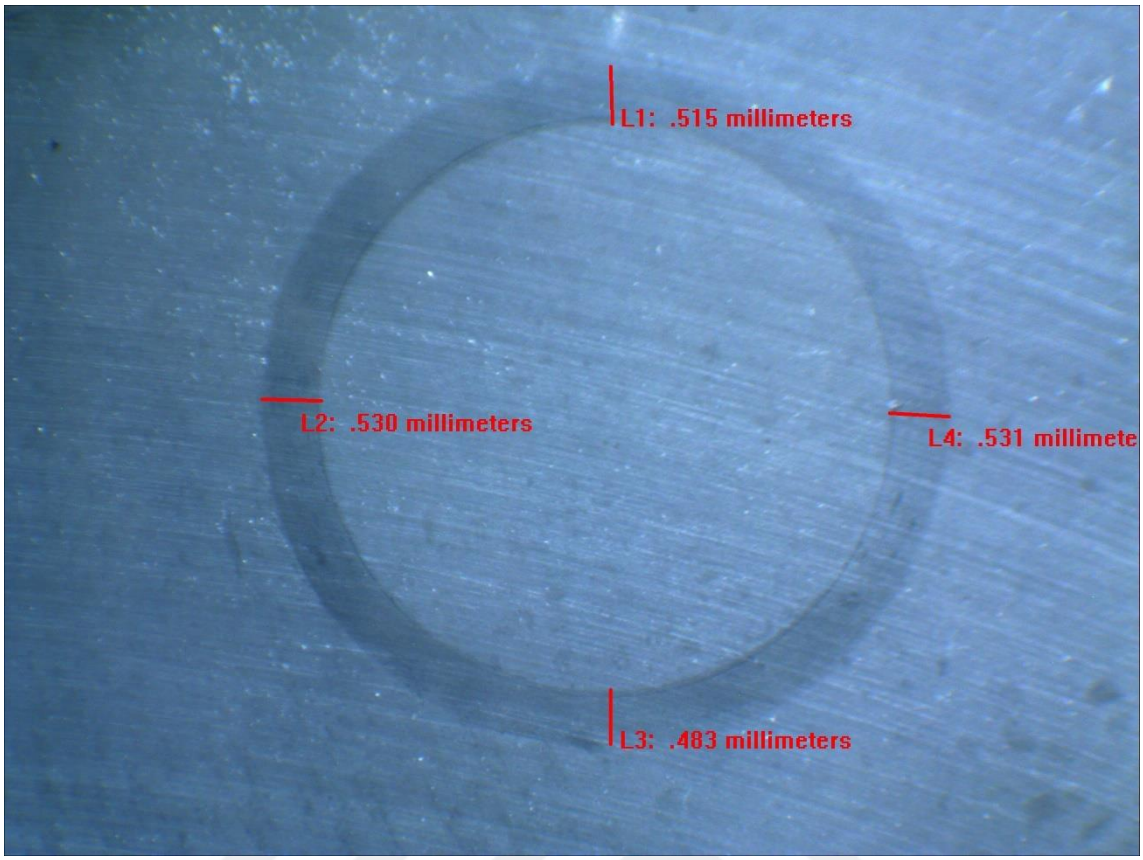

Figure B.3 Macroscopy image and wear track measurement of S1-3.

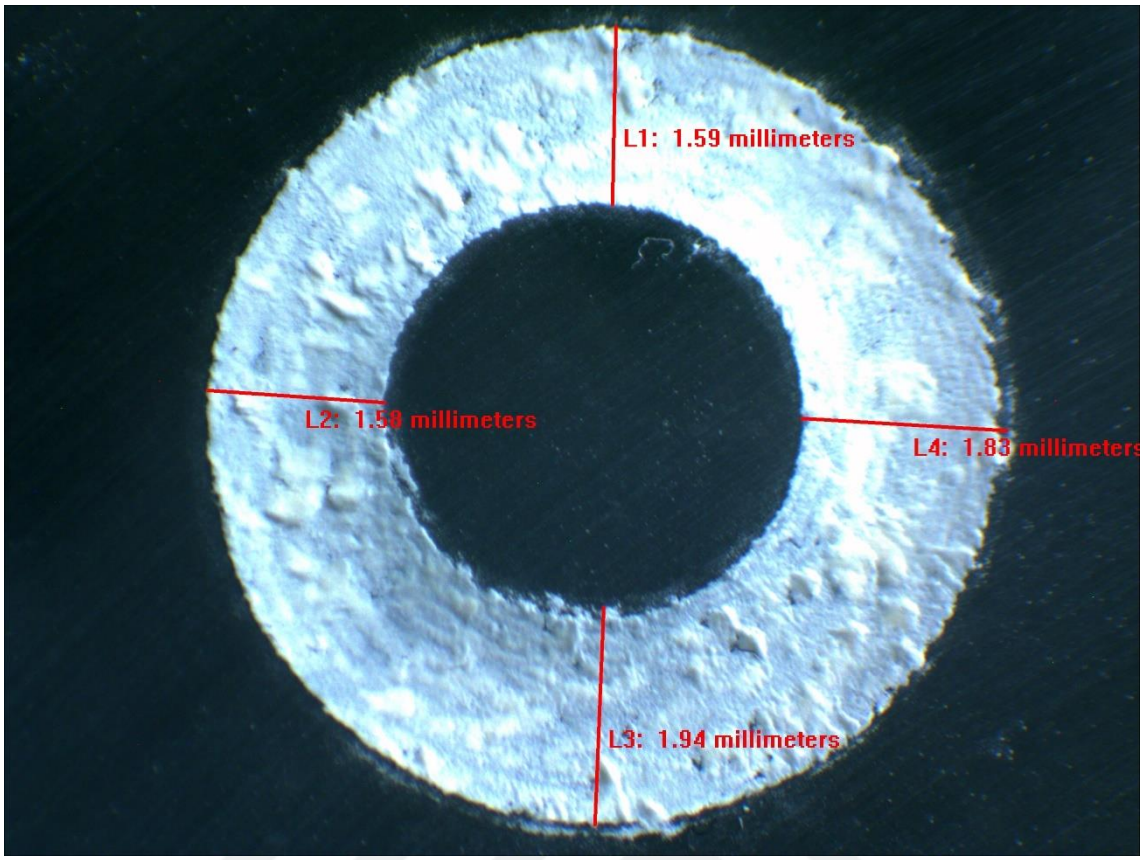

Figure B.4 Macroscopy image and wear track measurement of S2-1.

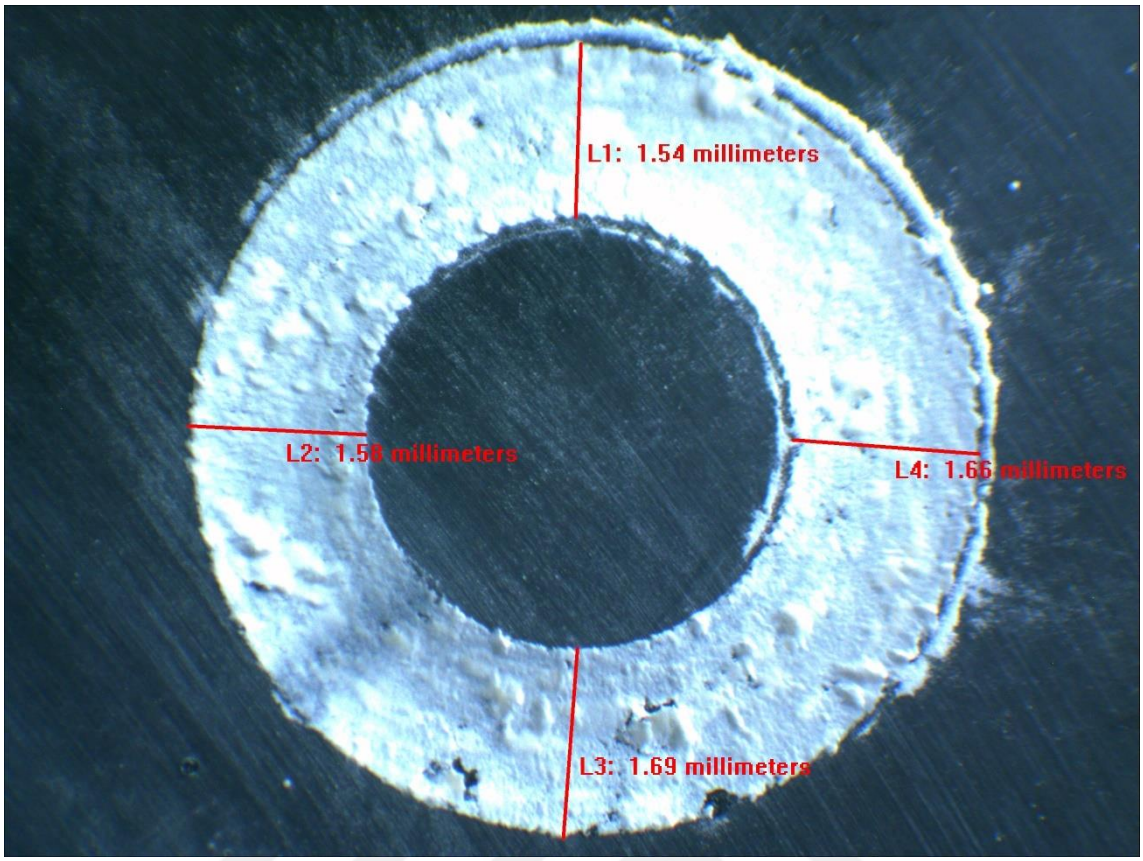

Figure B.5 Macroscopy image and wear track measurement of S2-2.

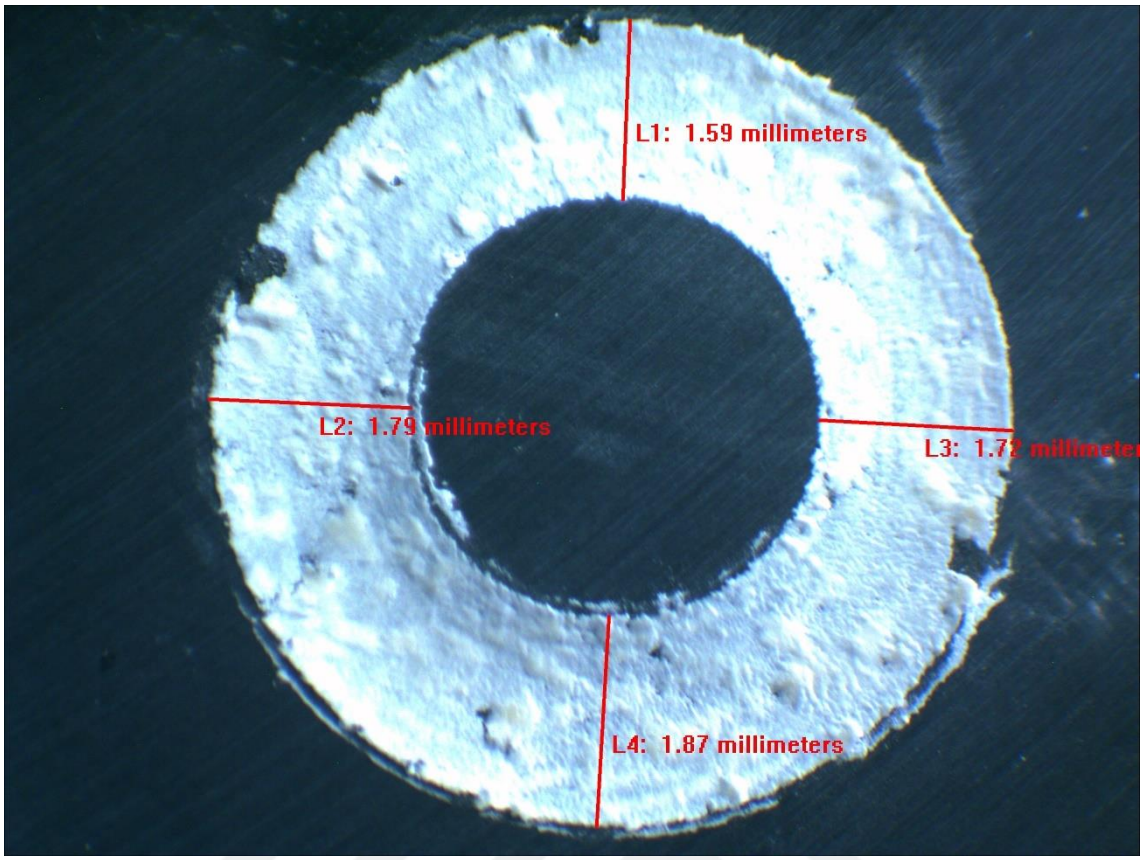

Figure B.6 Macroscopy image and wear track measurement of S2-3.

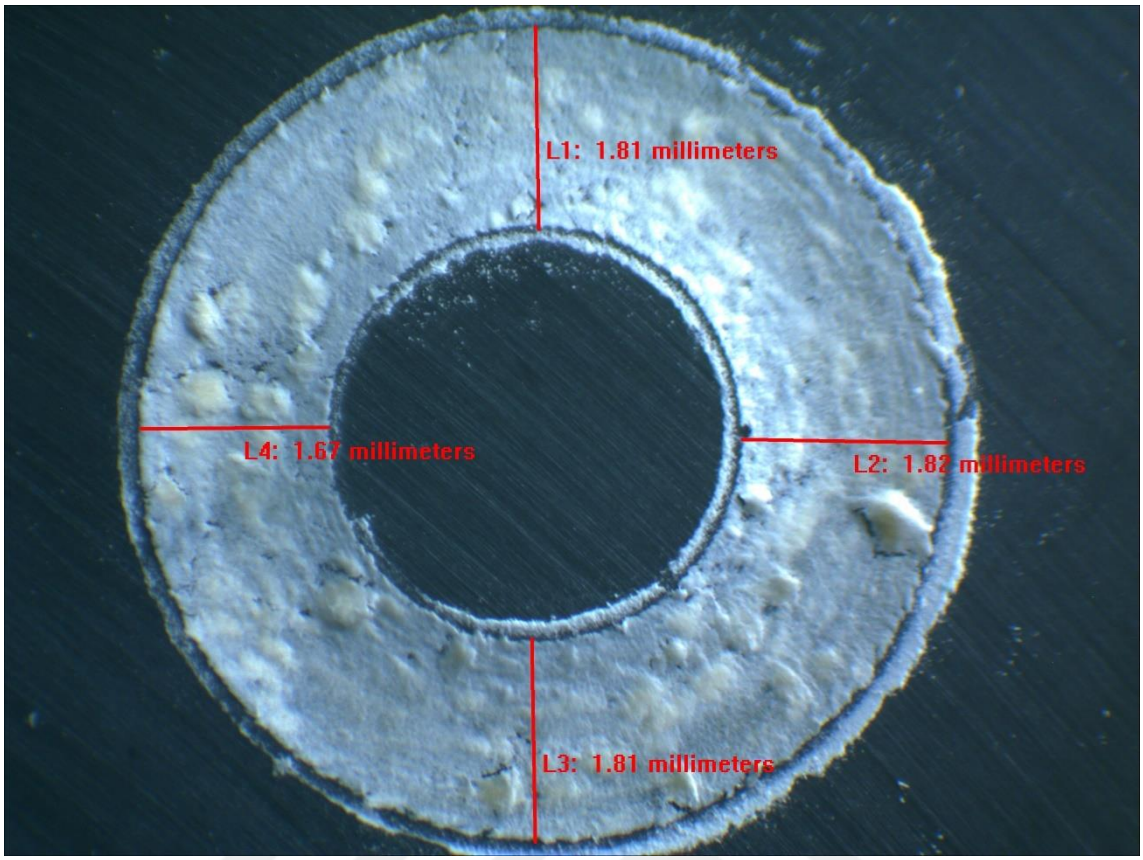

Figure B.7 Macroscopy image and wear track measurement of S3-1.

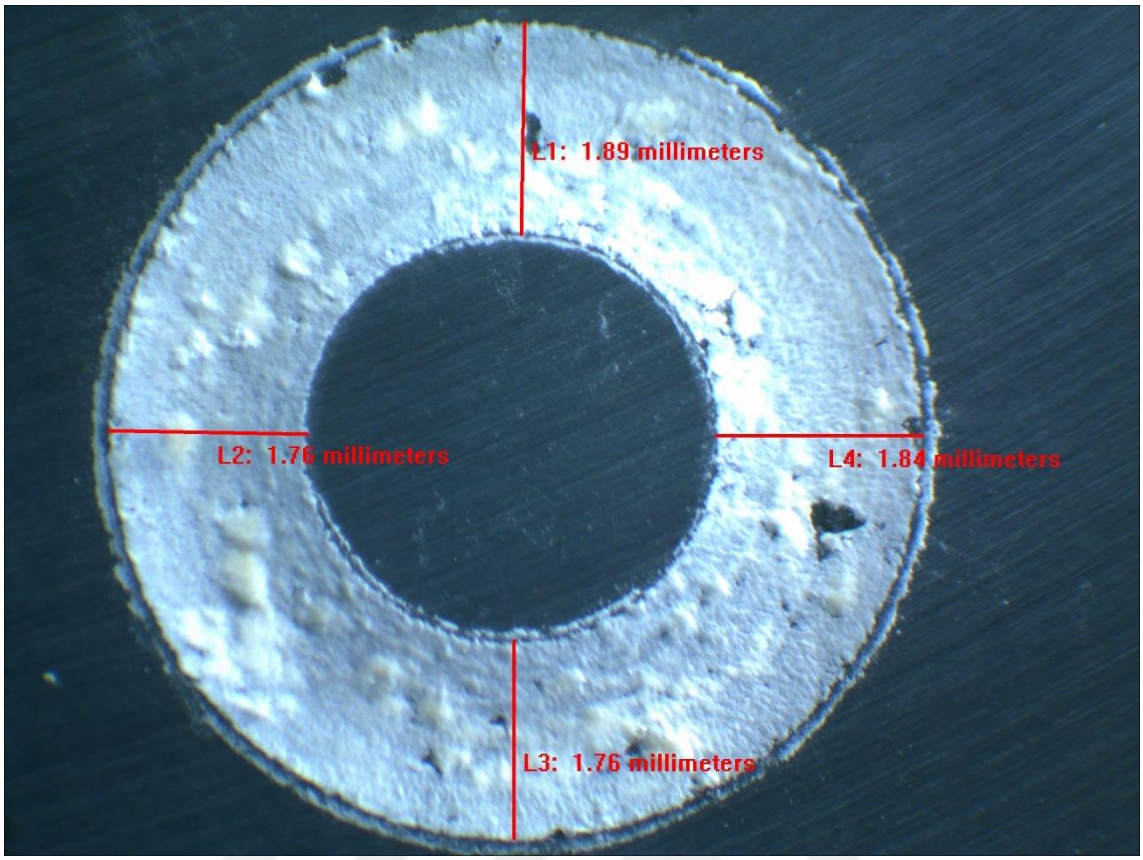

Figure B.8 Macroscopy image and wear track measurement of S3-2.

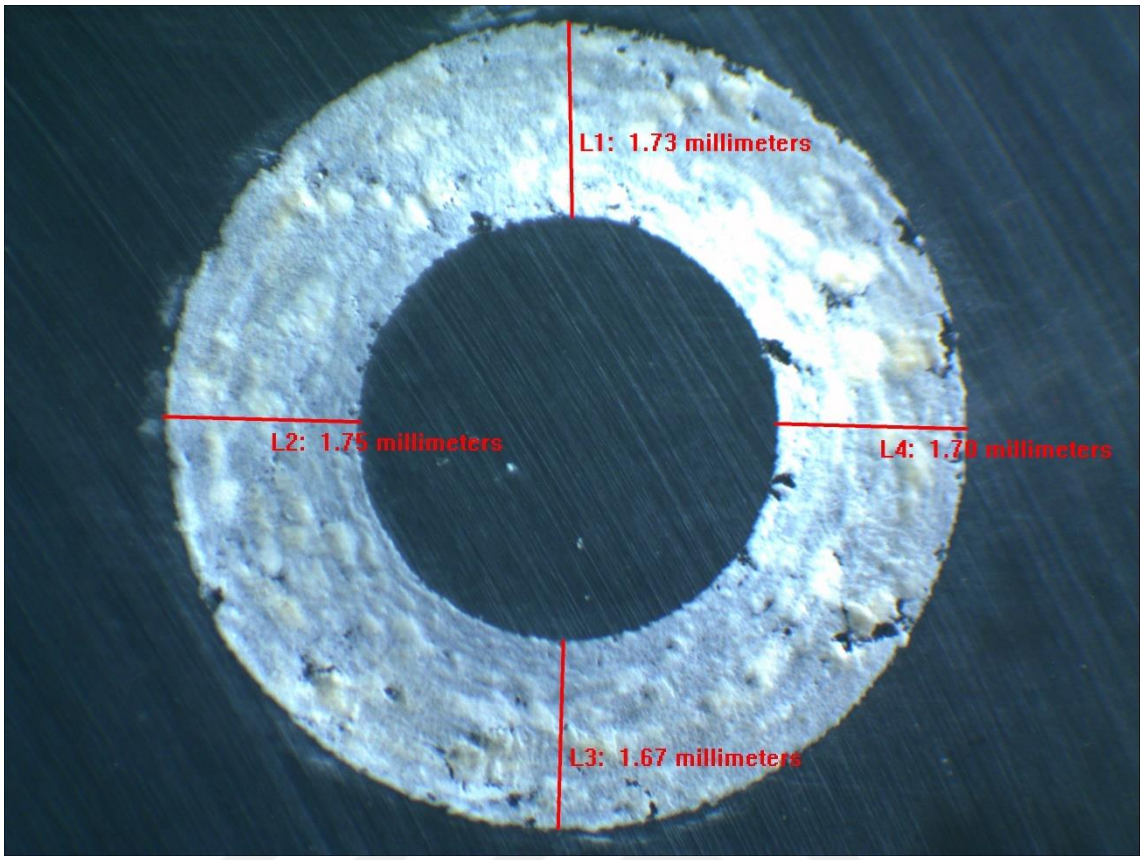

Figure B.9 Macroscopy image and wear track measurement of S3-3.

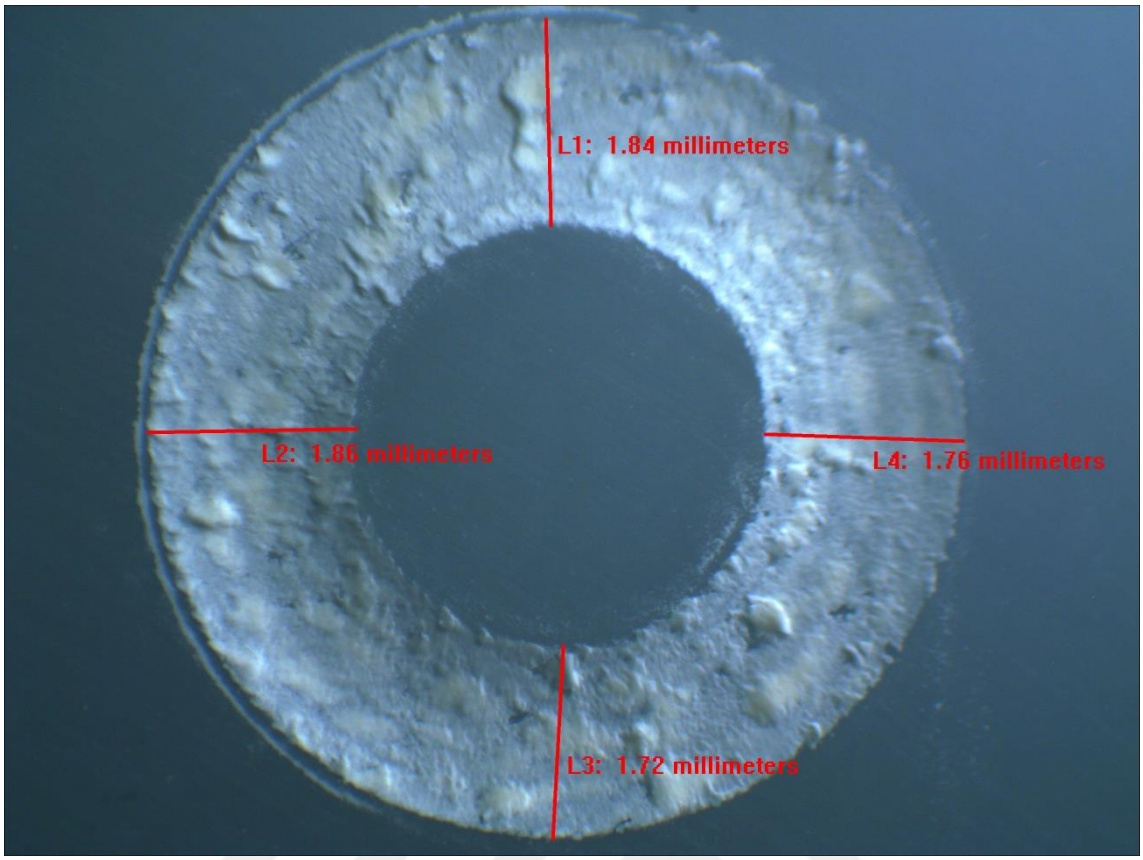

Figure B.10 Macroscopy image and wear track measurement of S4-1.

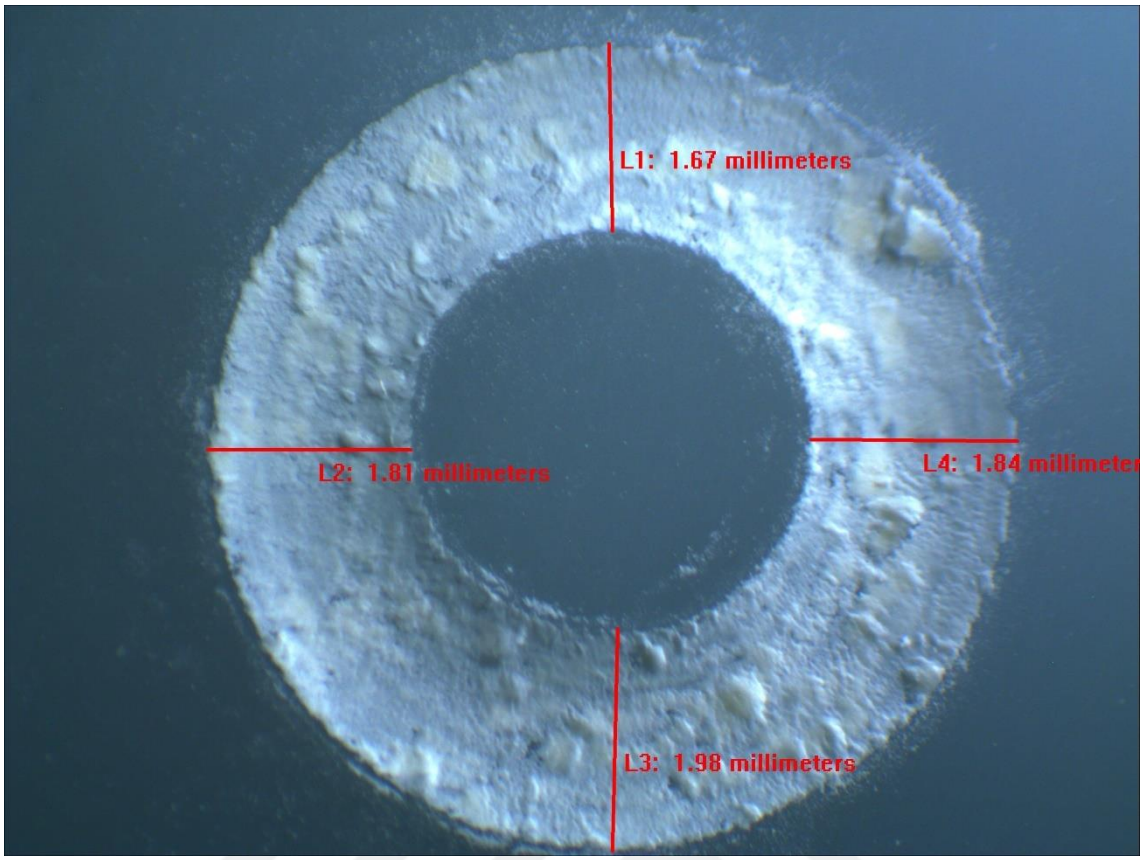

Figure B.11 Macroscopy image and wear track measurement of S4-2.

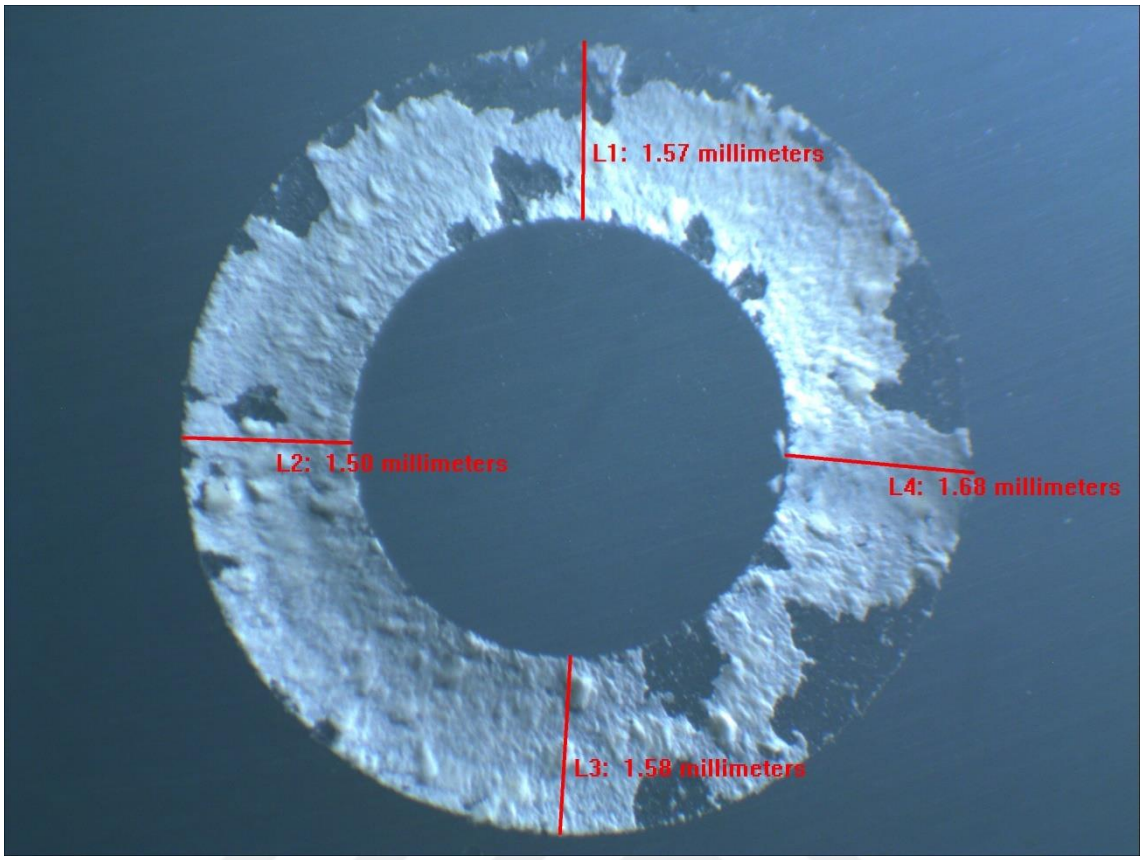

Figure B.12 Macroscopy image and wear track measurement of S4-3.

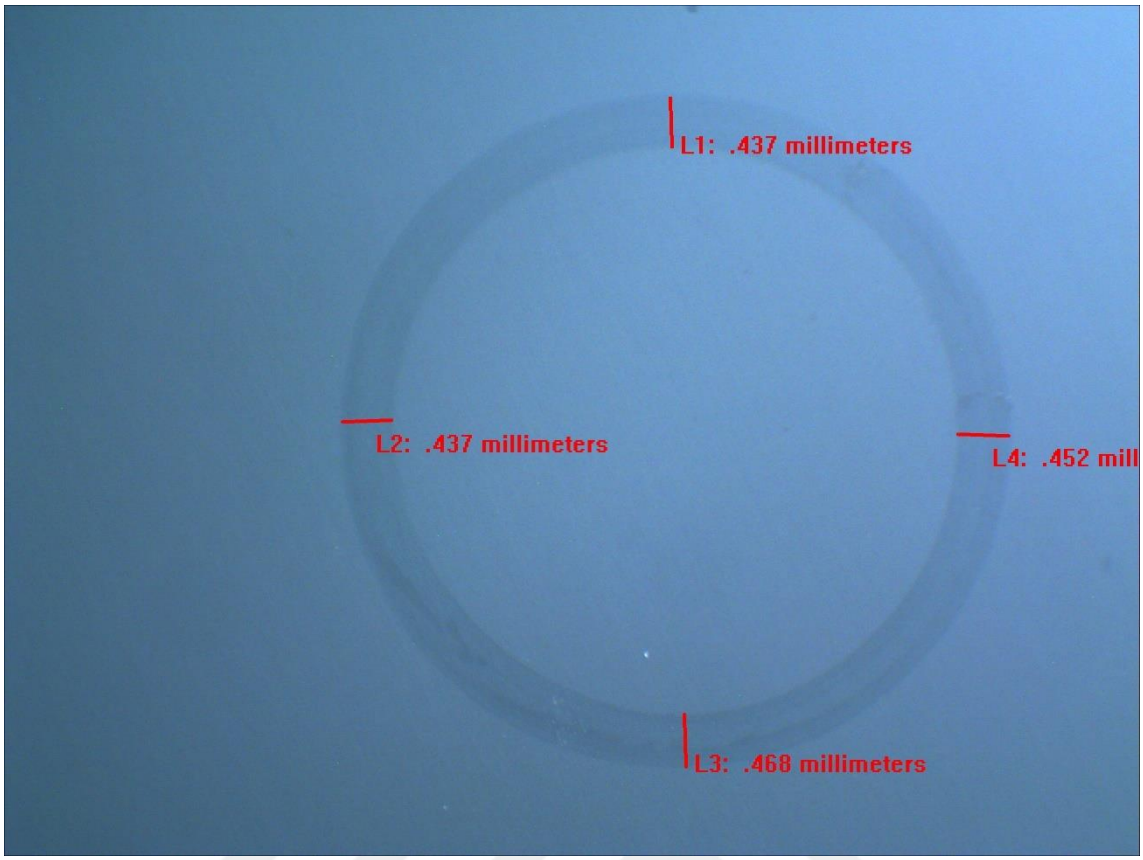

Figure B.13 Macroscopy image and wear track measurement of S5-1.

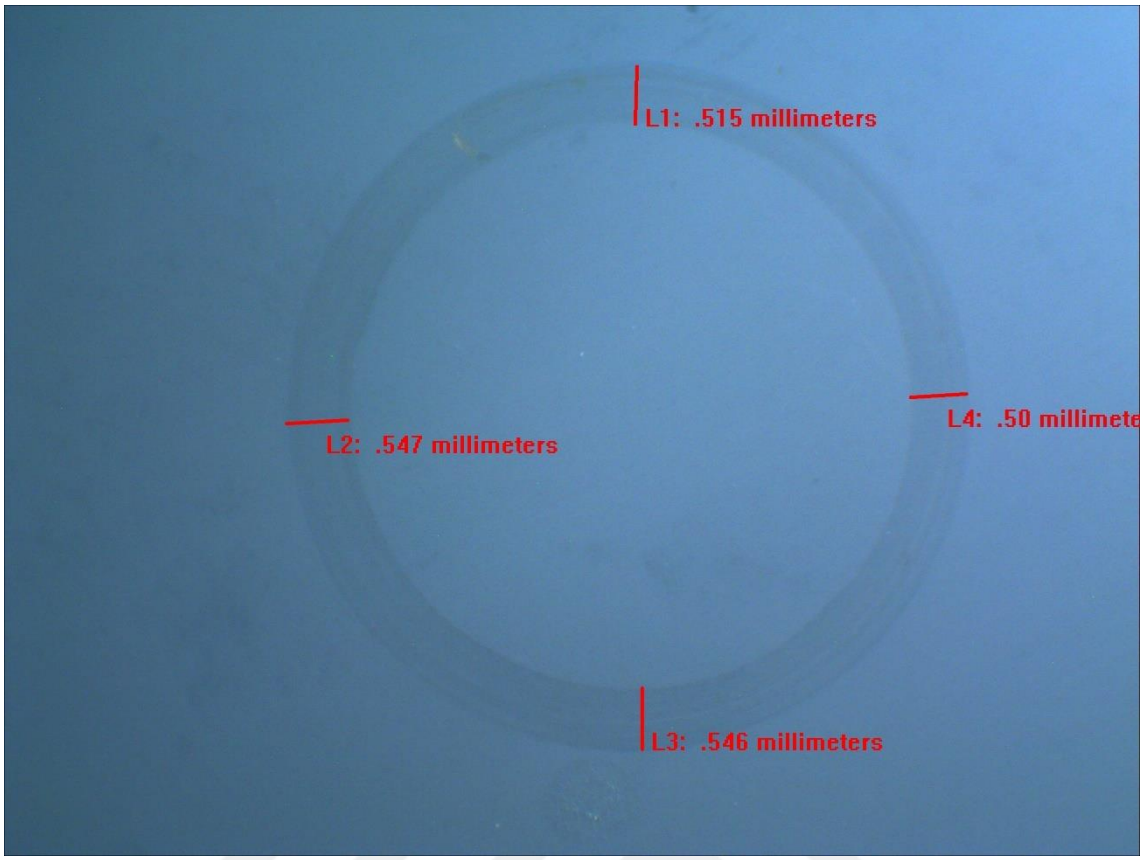

Figure B.14 Macroscopy image and wear track measurement of S5-2.

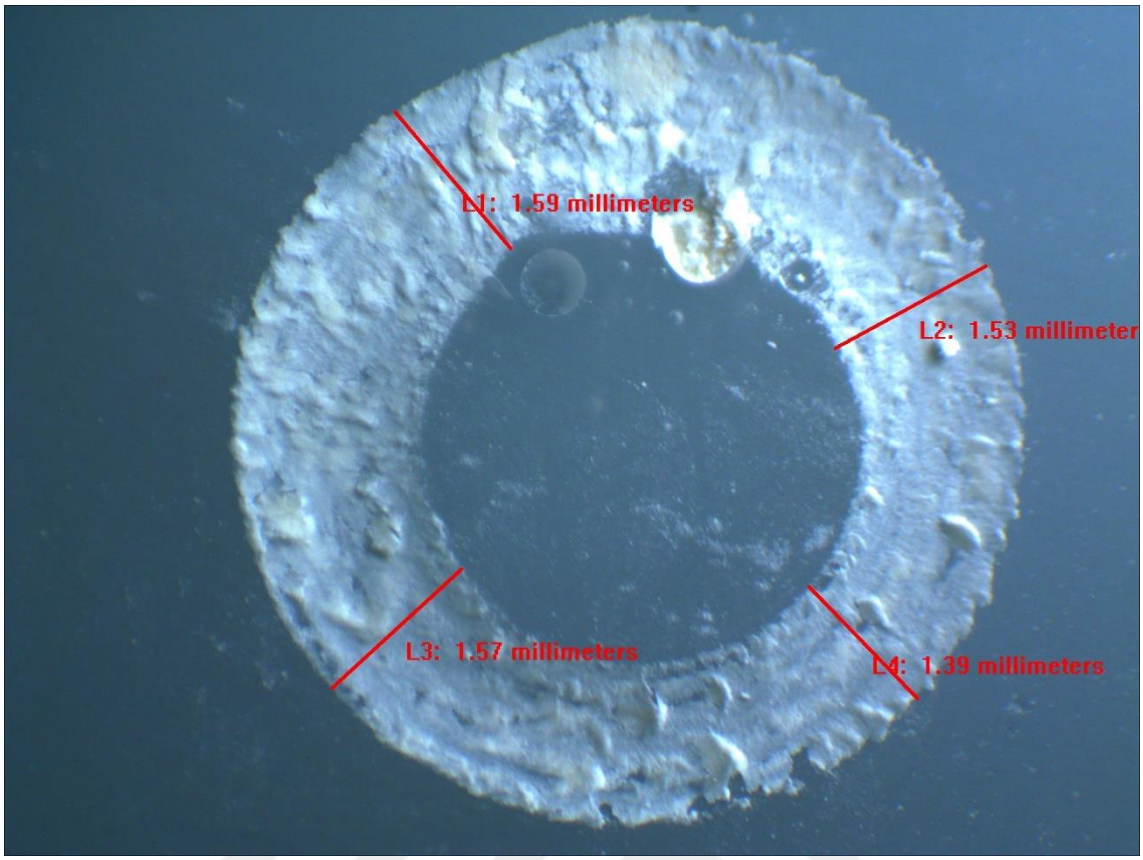

Figure B.15 Macroscopy image and wear track measurement of S5-3.

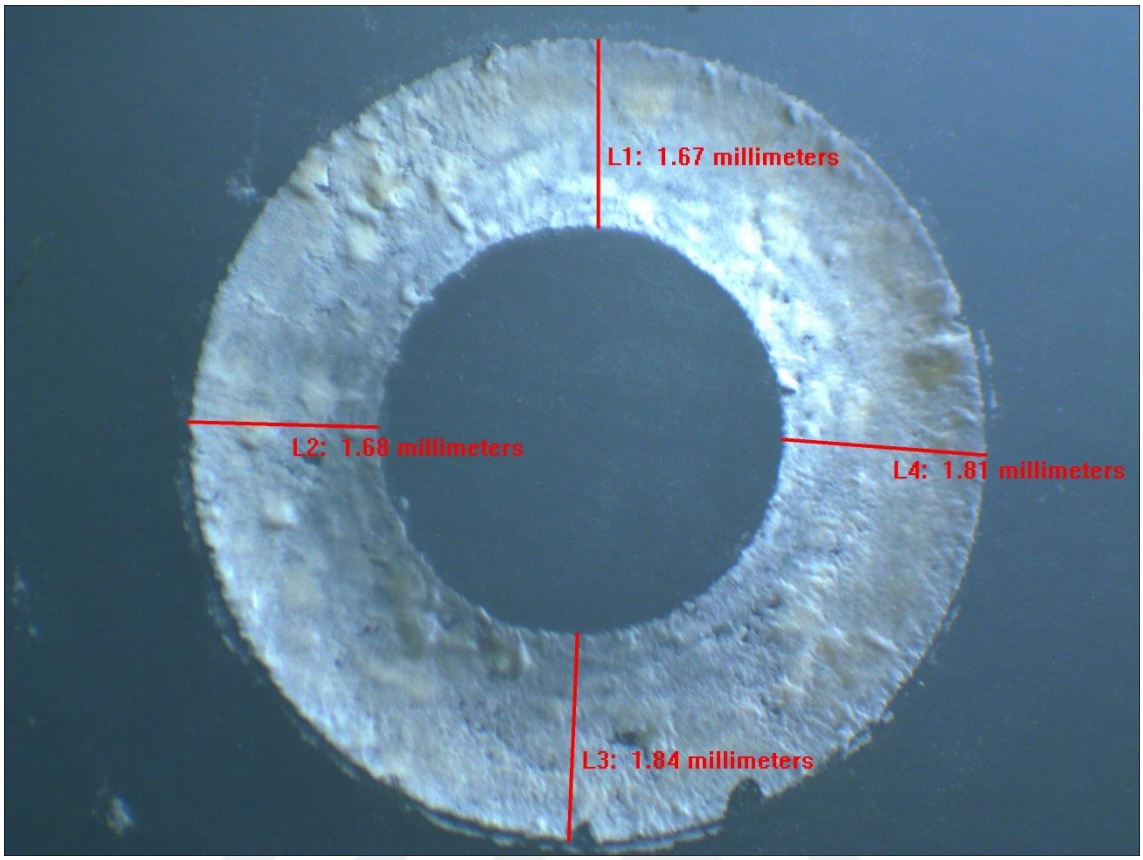

Figure B.16 Macroscopy image and wear track measurement of S6-1.

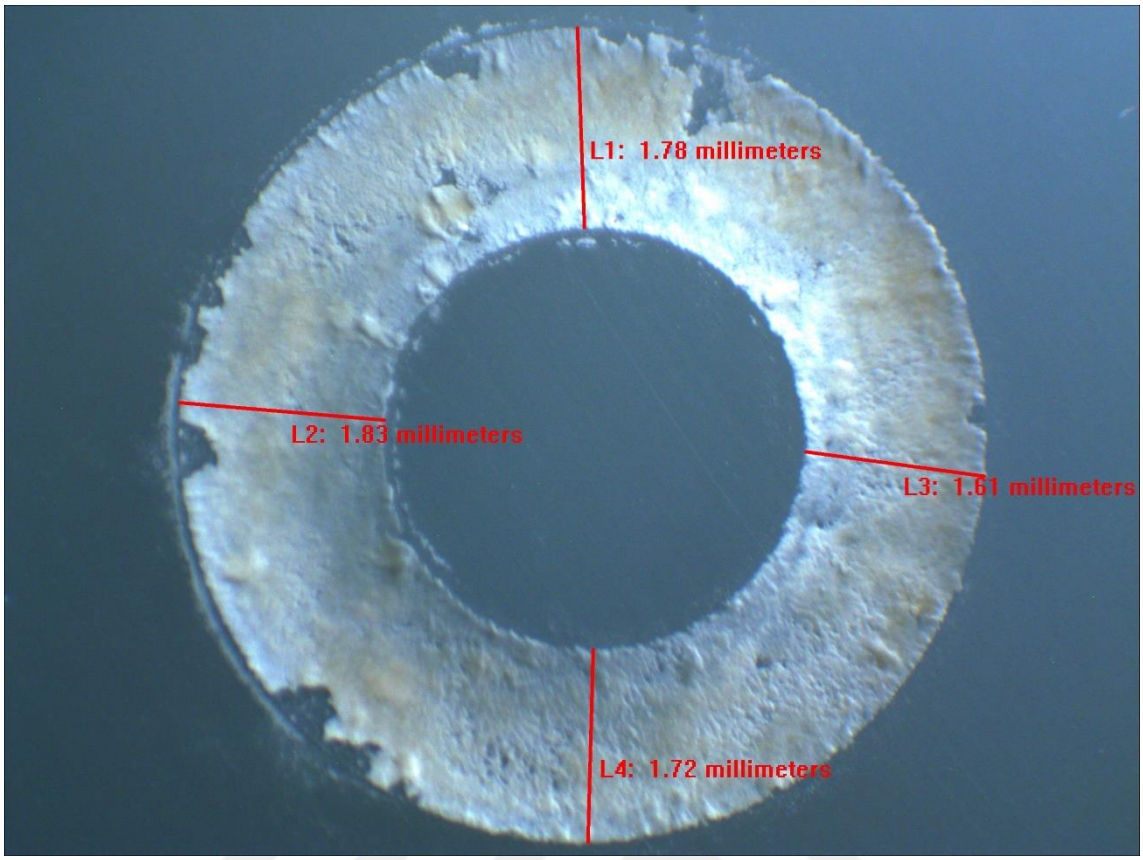

Figure B.17 Macroscopy image and wear track measurement of S6-2.

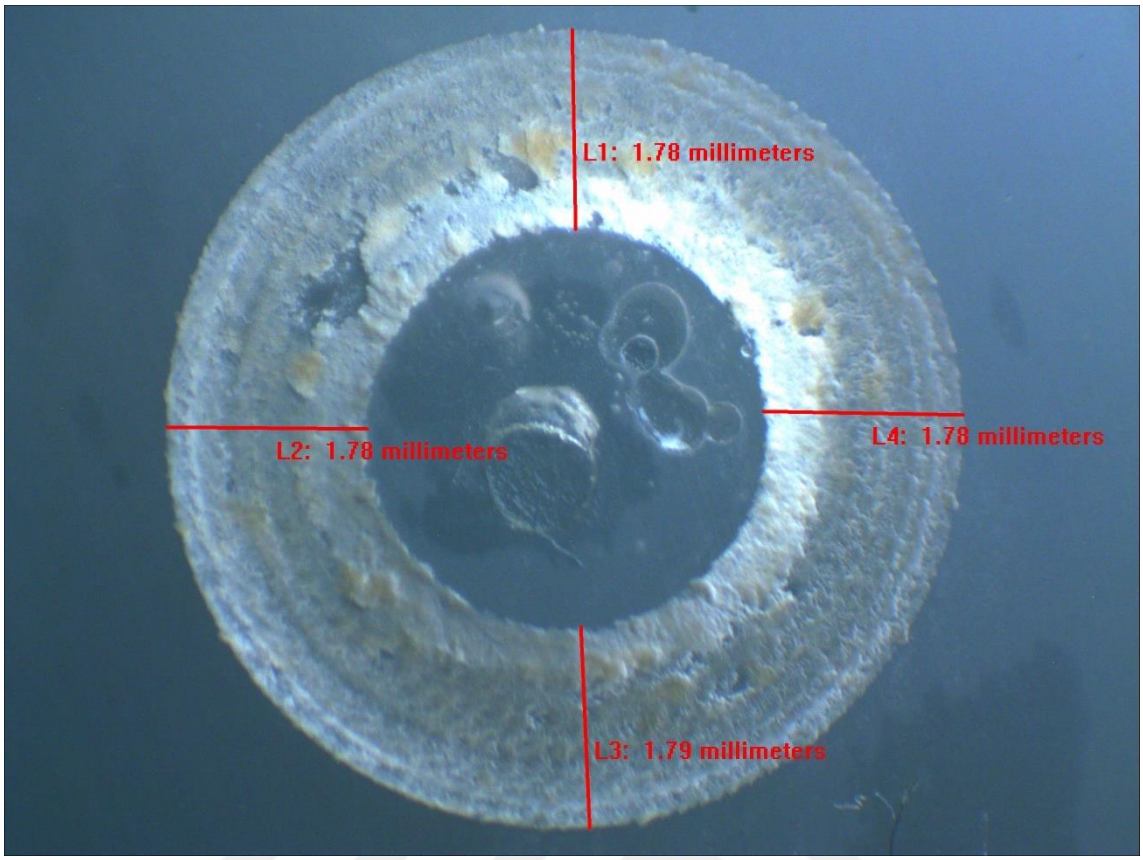

Figure B.18 Macroscopy image and wear track measurement of S6-3.

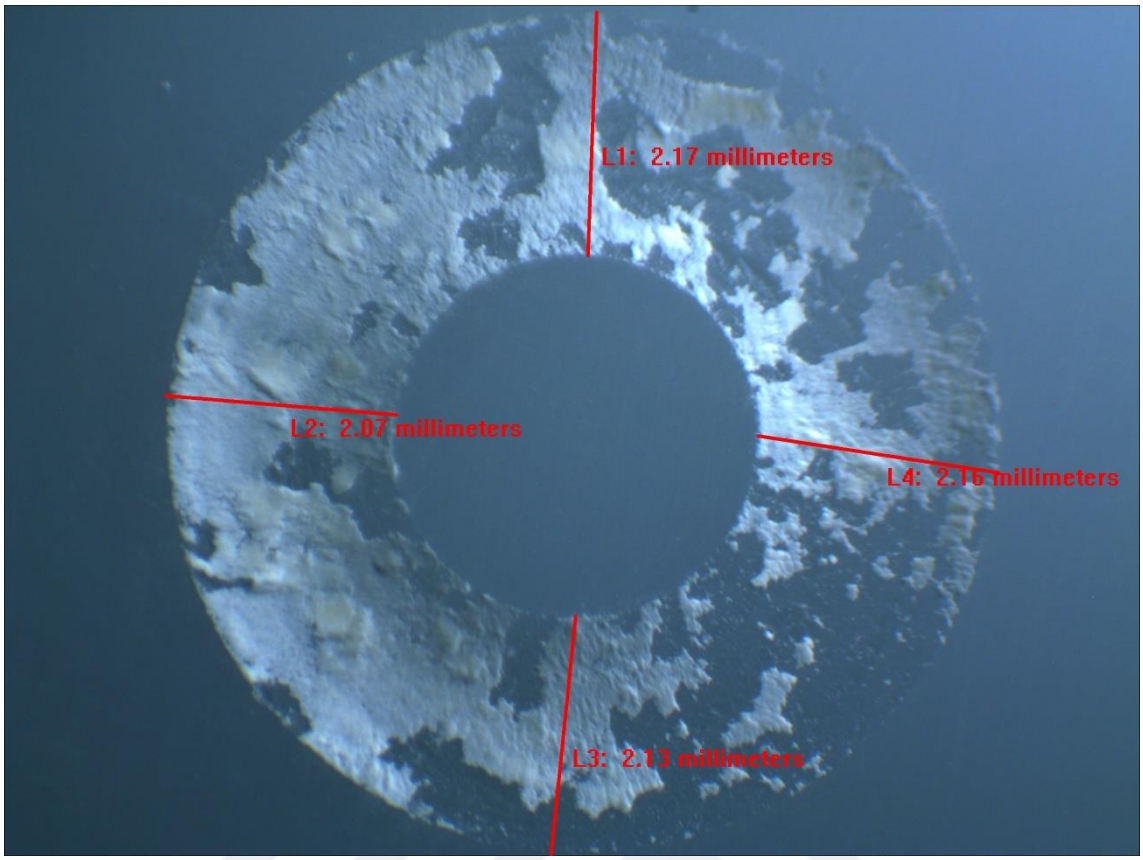

Figure B.19 Macroscopy image and wear track measurement of S7-1.

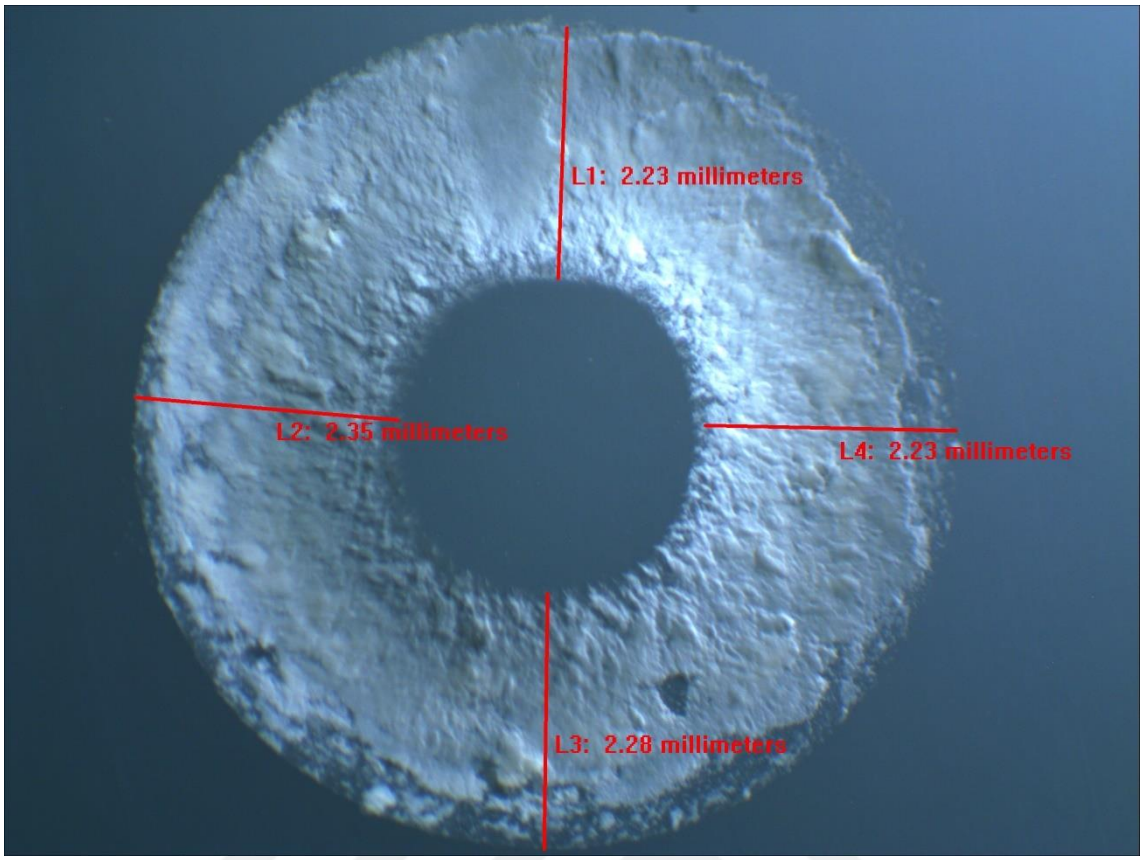

Figure B.20 Macroscopy image and wear track measurement of S7-2.

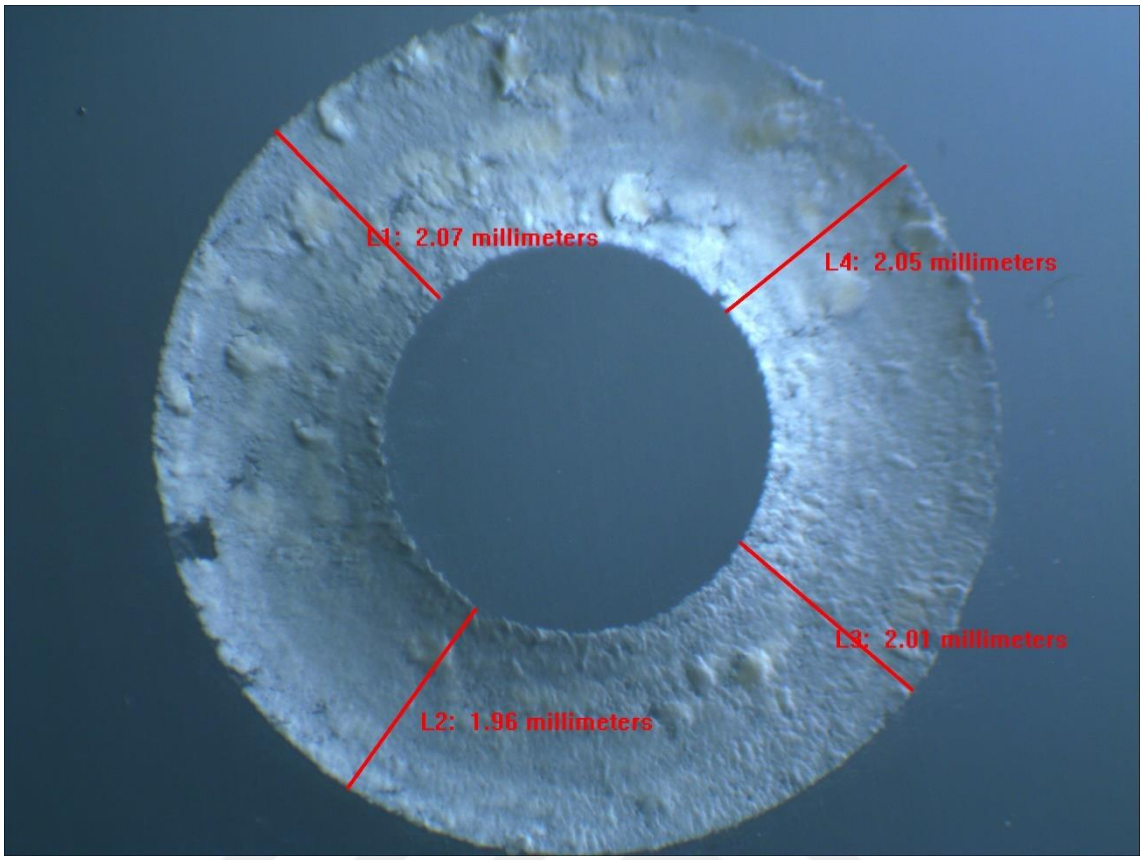

Figure B.21 Macroscopy image and wear track measurement of S7-3.

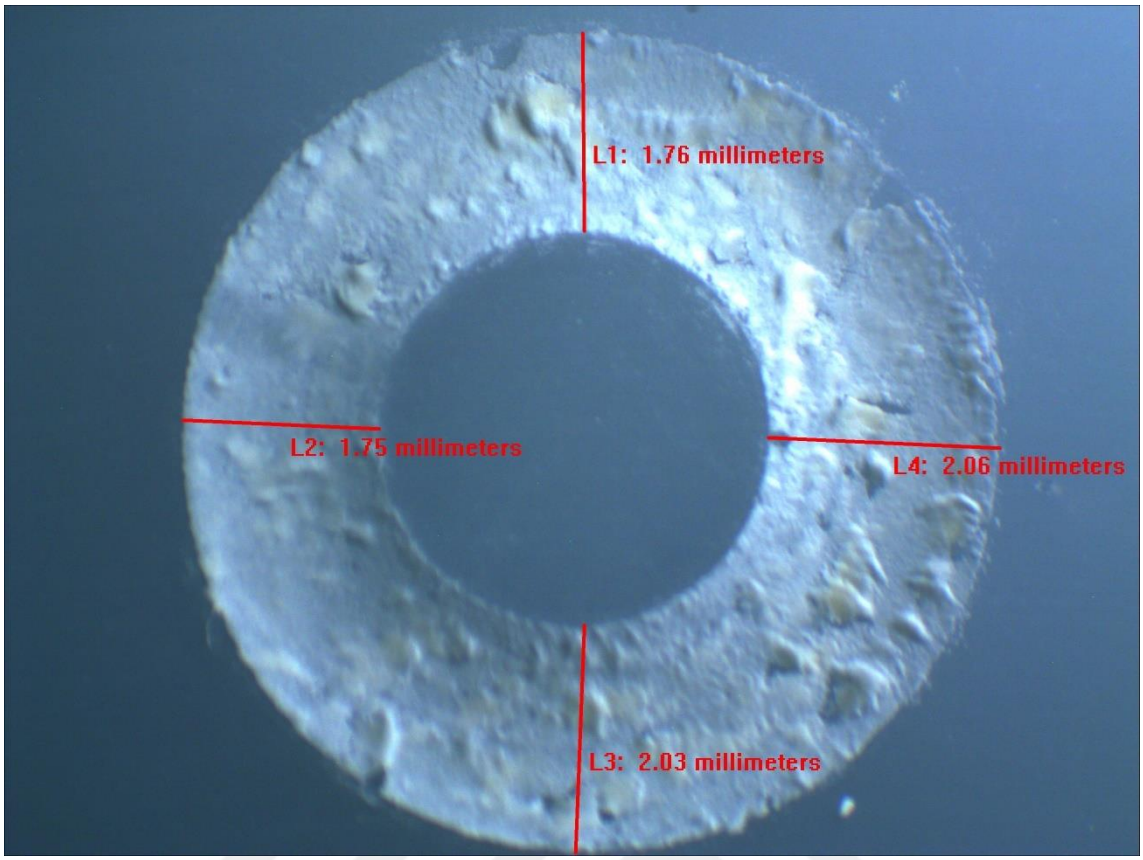

Figure B.22 Macroscopy image and wear track measurement of S8-1.

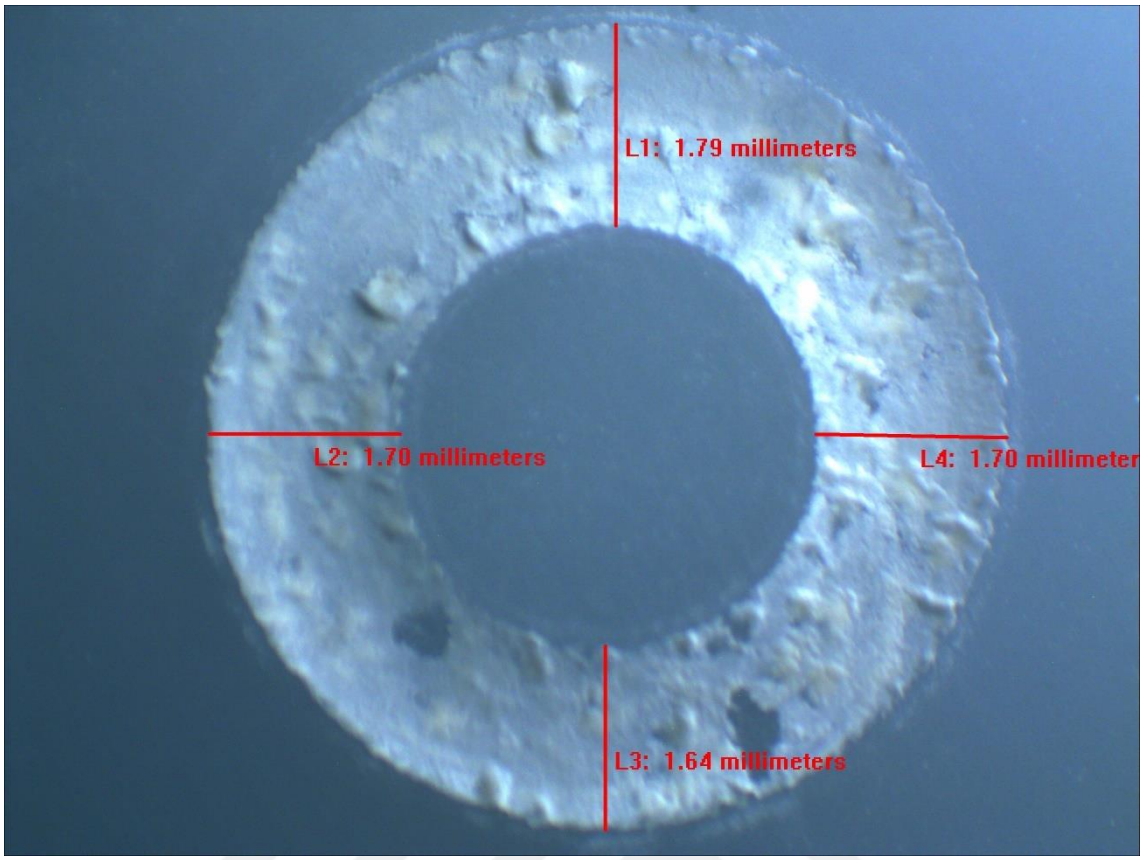

Figure B.23 Macroscopy image and wear track measurement of S8-2.

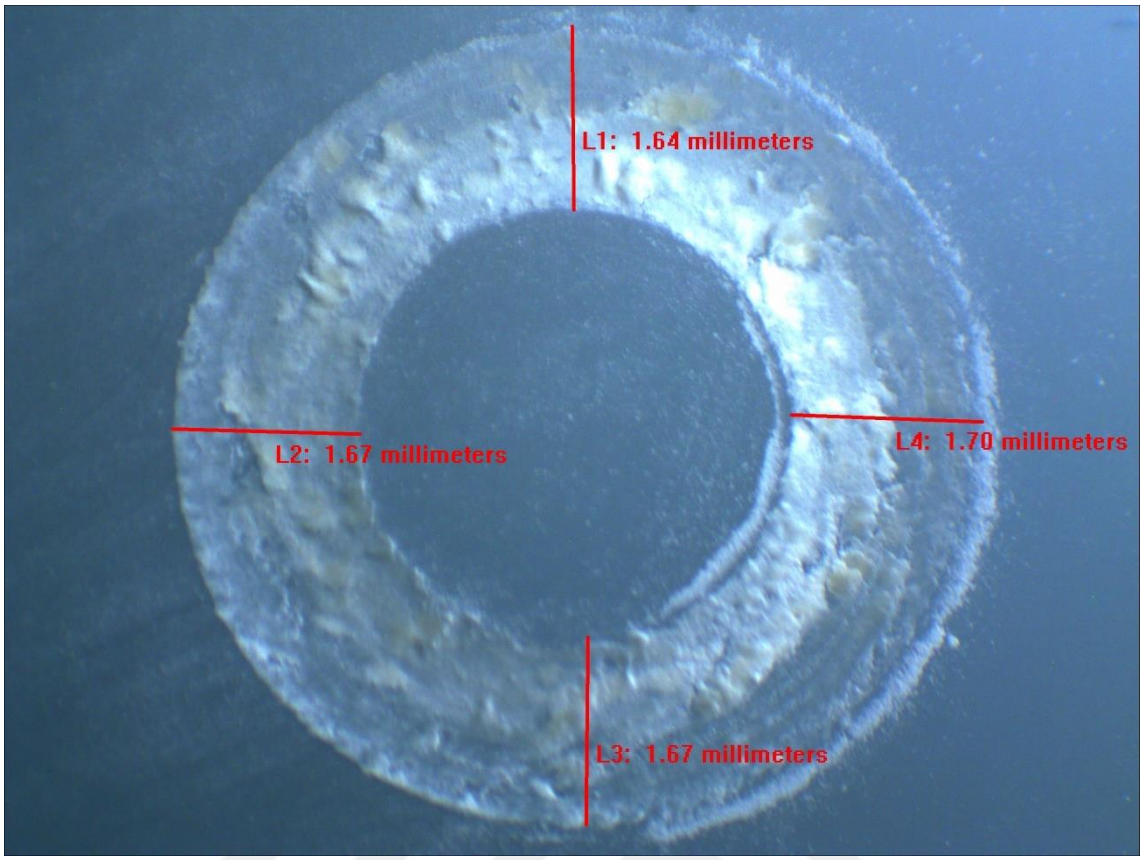

Figure B.24 Macroscopy image and wear track measurement of S8-3.

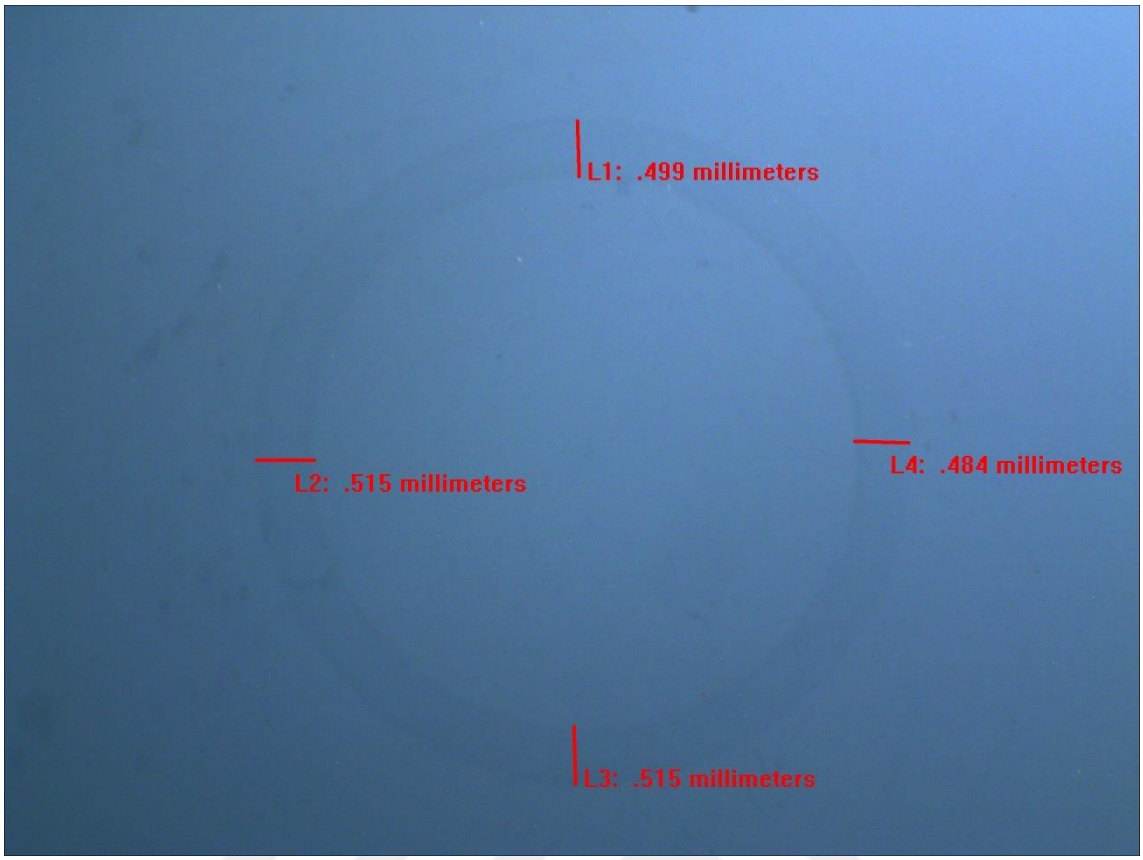

Figure B.25 Macroscopy image and wear track measurement of S9-1.

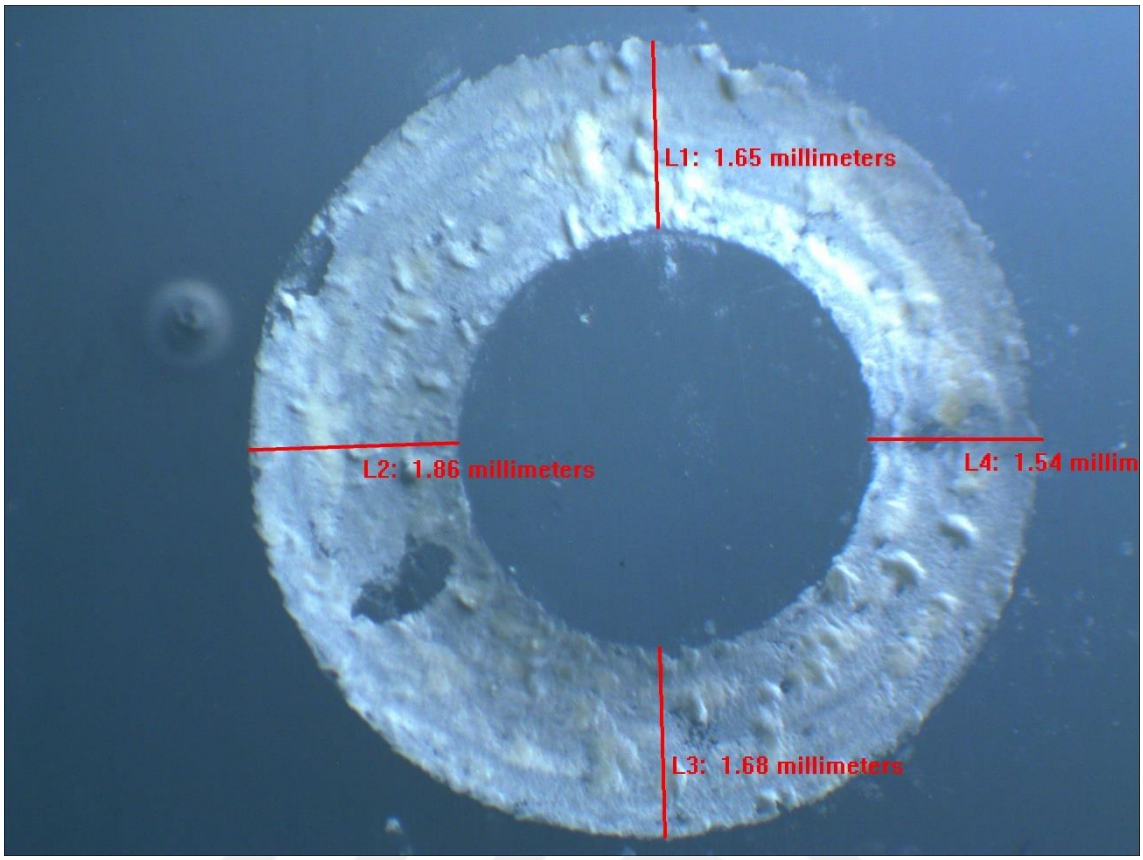

Figure B.26 Macroscopy image and wear track measurement of S9-2.

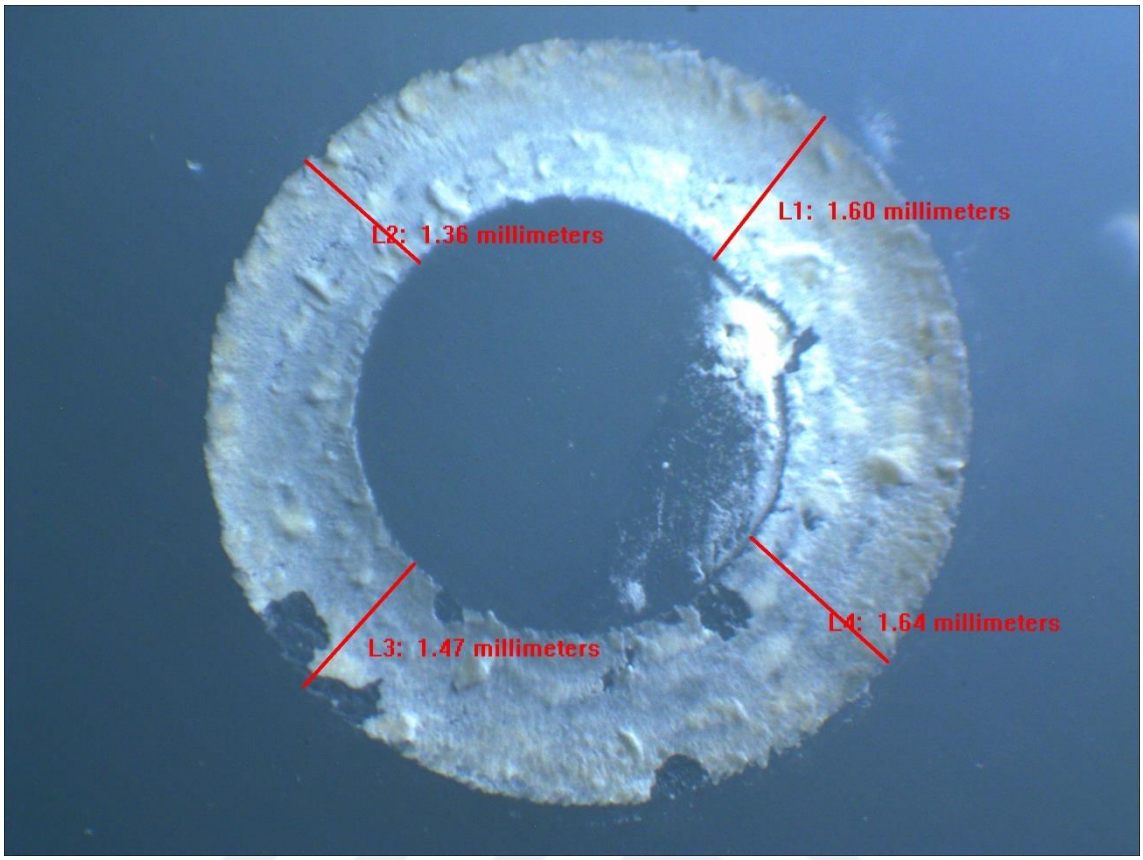

Figure B.27 Macroscopy image and wear track measurement of S9-3.

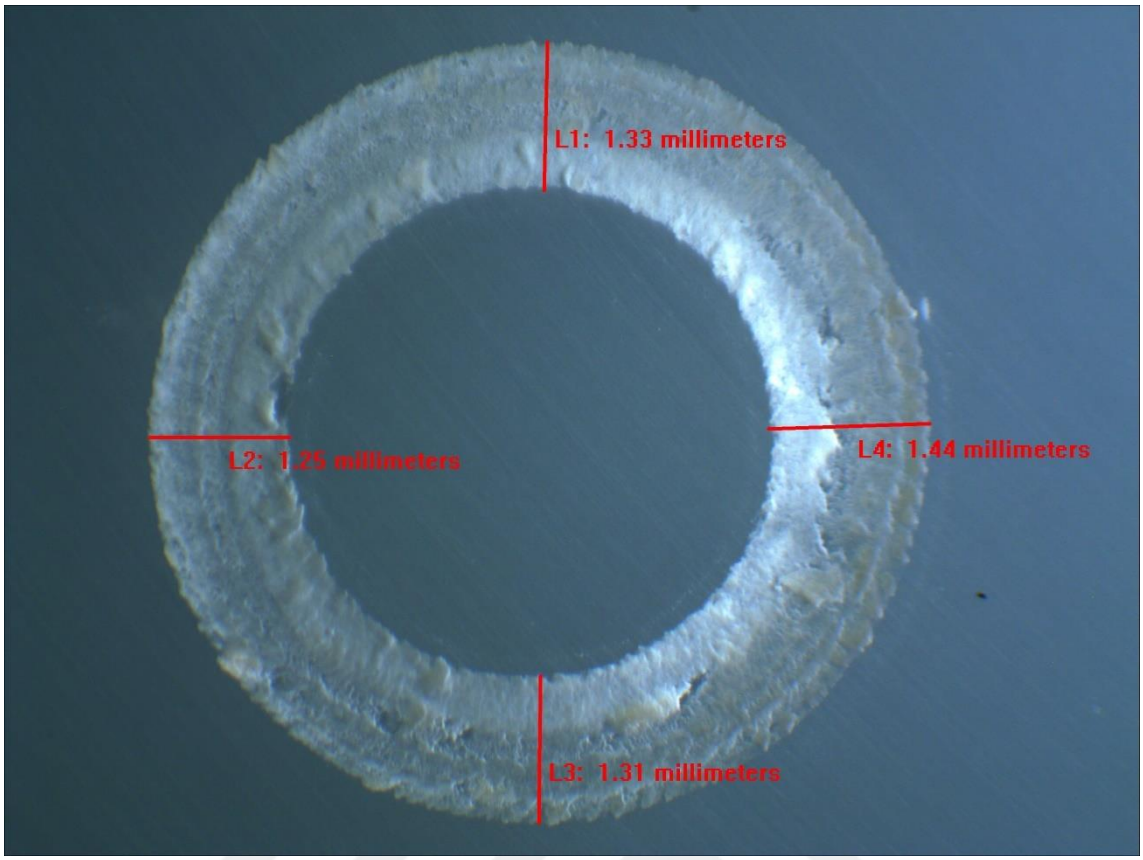

Figure B.28 Macroscopy image and wear track measurement of Verification-1.

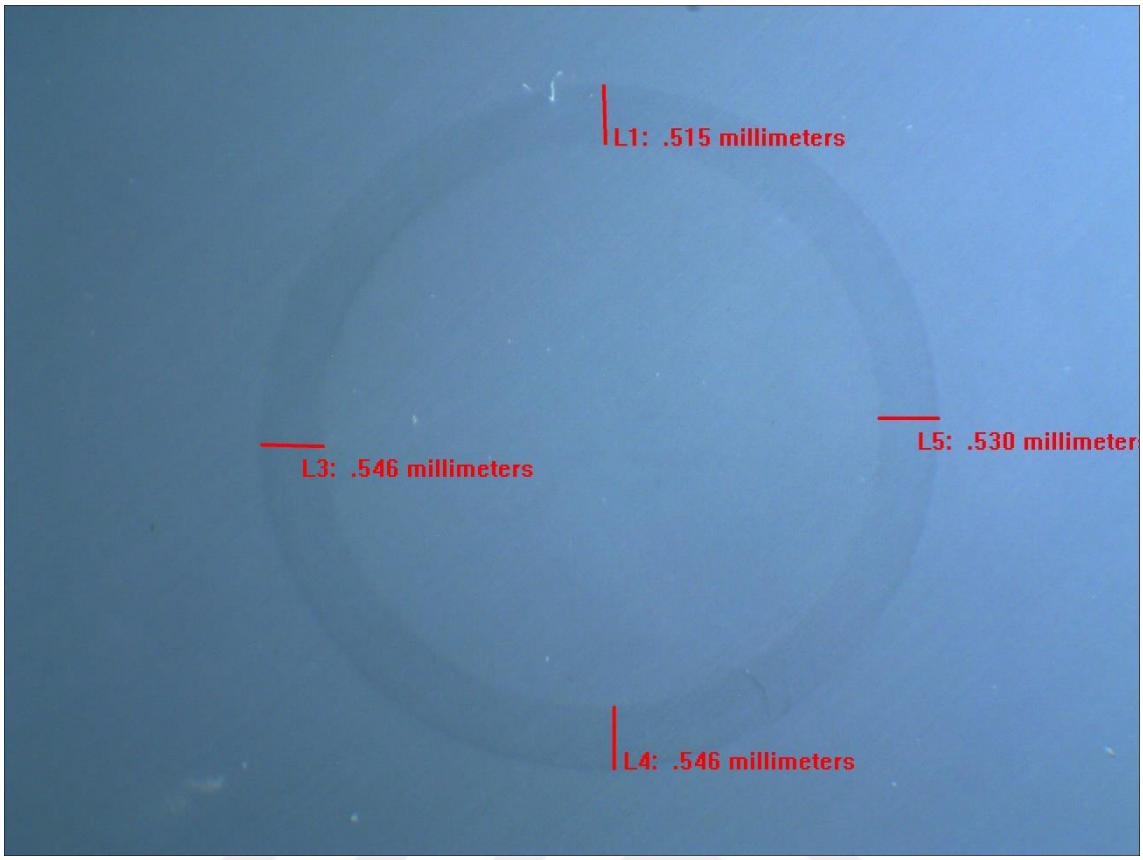

Figure B.29 Macroscopy image and wear track measurement of Verification-2.

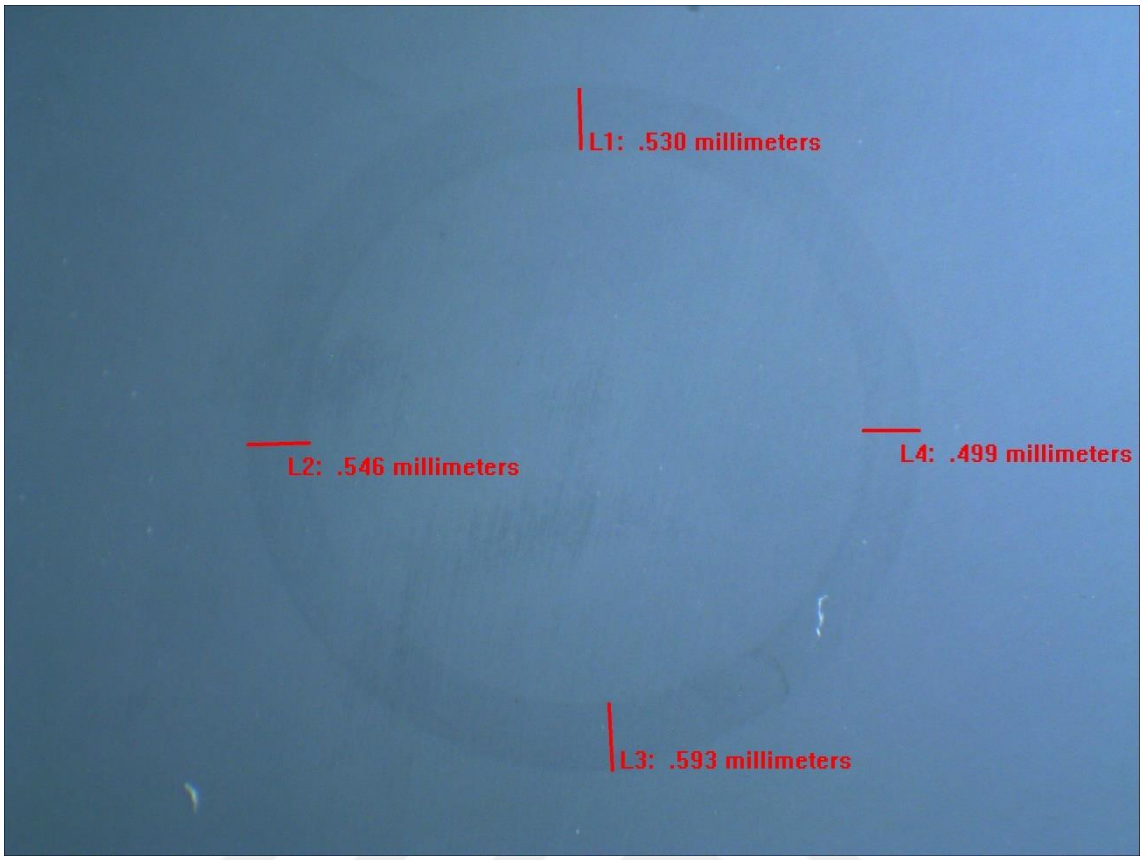

Figure B.30 Macroscopy image and wear track measurement of Verification-3.

PUBLICATIONS FROM THE THESIS

Conference Papers

1. M. Demirkol, M. Heydarpoor, B. O. Kucukyildirim, “Effects of titanium dioxide nanoparticle reinforcement to the hardness and wear rate of photocatalytic PMMA composites”, 5th International Conference on Advances In Mechanical Engineering, Istanbul, Türkiye.